Title
From Spliceosome Assembly to Catalysis: Multiple Roles for DEAD-box ATPase Prp28 and Master Regulator Prp8

Author
Price, Argenta Margaret

Publication Date
2014

Peer reviewed|Thesis/dissertation

From Spliceosome Assembly to Catalysis: Multiple Roles for DEAD-box ATPase Prp28 and Master Regulator Prp8

by

Argenta M. Price

DISSERTATION

Submitted in partial satisfaction of the requirements for the degree of

DOCTOR OF PHILOSOPHY

in

Biochemistry and Molecular Biology

in the

GRADUATE DIVISION

of the

UNIVERSITY OF CALIFORNIA, SAN FRANCISCO

Acknowledgements

I would first like to thank my advisor, Christine Guthrie, for her continual support and mentorship throughout graduate school. She created a wonderful environment for me to grow as a scientist and never tired of asking "What is the question?" when helping me write or talk about my research. I particularly appreciate the support that Christine gave me for non-research interests: from encouraging me to take a scientific writing course and teach through SEP to allowing me to take a leave of absence to do a science policy fellowship in DC, Christine always cared that I got the experiences that were best for me.

The Guthrie lab has been a great place to be a graduate student. I learned from every person in the lab and enjoyed many scientific and non-scientific conversations. Current lab members Anne de Bruyn Kops, Jaclyn Greimann, Yangzi He, Sarah Ledoux, Michael Marvin, Megan Mayerle, Kelly Nissen, and Kristin Patrick are great to work with. They, along with former lab members, Megan Bergkessel, Haralambos Hadjivassiliou, Rebecca Holmes, Tracy Kress, Corina Maeder, Quinn Mitrovich, Erica Moehle, Gregg Whitworth, and Gwen Wilmes, have been great colleagues, friends, and advisors. My summer students Diana Velazquez and Senen Mendoza were fun to work with - they brought a lot of enthusiasm and fresh ideas. I have worked particularly closely with Sarah Ledoux and Megan Mayerle on Team Toggle and really enjoyed our conversations and collaboration. Finally, the lab would not be the same without the excitement of John Abelson, who still gets excited when PCR works and comes up with amazing ideas for how everything in the spliceosome works together.

It has been a privilege to have David Morgan and Jonathan Weissman on my thesis committee. They provided excellent guidance and valuable insights on all of my projects, and happily came to my thesis committee meetings that we always seemed to schedule for holidays.

Thanks to my collaborators David Brow and Janina Gornemann for years back-and-forth as our project took twists and turns.

Thanks to Matthew Kahlscheuer, Mario Blanco, and Nils Walter for teaching me about single molecule FRET during my visit to Michigan, and thanks to Ramya Krishnan for additional FRET conversations about our collaboration.

My classmates have been comrades through the ups and downs of graduate school. In particular, my roommates for several years, Beth Cimini and Stacey Hanlon, were the best possible roommates. I am very thankful to a group of ladies, Beth Cimini, Erin Currie, Ellen Edenberg, Heather Eshleman, and Erica Moehle Urnov, whose conversations, affirmations, and action items helped me get through even the most stressful times.

Finally, I would like to thank my family. My parents Jon and Beth Price taught me to love science and always be curious, supported all of my decisions, and challenged me to think about my research in different ways by asking unexpected questions. I have had many fun and challenging conversations with my brother, Alex Price. My new Hoffmann family is also wonderfully supportive. Love and many thanks to my husband, Tom Hoffmann, who gives me statistical advice, helps me enjoy time outside of lab, understands when I need to be in lab at midnight, and always supports me no matter what.

Published and Collaborative work

Chapter 1 is reproduced from work that is published in *RNA*, in collaboration with Janina Gornemann and David Brow:

Price AM, Görnemann J, Guthrie C, Brow DA. (2014) An unanticipated early function of DEAD-box ATPase Prp28 during commitment to splicing is modulated by U5 snRNP protein Prp8. RNA. 2014 Jan;20(1):46-60. doi: 10.1261/rna.041970.113. Epub 2013 Nov 14. PMID: 24231520

Chapter 2 is an unpublished collaboration with Matthew Kahlscheuer, Ramya Krishnan, and Nils Walter at the University of Michigan.

Chapter 3 is a work in progress in collaboration with other members of the Guthrie lab: Megan Mayerle, Sarah Ledoux, Erica Moehle, Haralambos Hadjivassiliou, Yangzi He, Senen Mendoza, Diana Velazquez, John Abelson, and Christine Guthrie.

From spliceosome assembly to catalysis: multiple roles for DEAD-box ATPase Prp28 and master regulator Prp8

Argenta M. Price

Abstract

The spliceosome is a dynamic ribonucleoprotein machine that identifies and removes introns from pre-mRNA molecules. It is composed of five small RNAs and over 100 proteins that assemble de-novo on each intron, through an ordered cascade of recognition, rearrangement, and re-recognition events. At its catalytic core, the spliceosome is thought to be a ribozyme, like the ribosome and group II introns. What then are the functions of the many protein components of the spliceosome? One group of proteins, the family of DExD/H-box ATPase, catalyzes conformational rearrangements to enhance fidelity and drive the ordered cascade of splicing events. Regulation of these events is critical for proper spliceosome function. One particularly interesting protein, Prp8, is thought to affect the structure of the catalytic core of the spliceosome and also serve as a master regulator of spliceosome assembly and activity. Yet how Prp8 interacts with other components of the spliceosome, to regulate their activity or to affect the structure of the catalytic core, is poorly understood.

We began by exploring how Prp8 regulates Prp28, the DEAD-box ATPase that promotes U1 release from and U6 association with the 5' splice site during spliceosome assembly. We found that a cluster of mutations in the N-terminus of Prp8 suppressed the growth defect of the cold-sensitive prp28-1 allele. Surprisingly, Prp28 was required not only for U1 release but also for earlier steps including ATP-independent formation of commitment complex 2. The prp28-1 suppressors in Prp8 also suppressed defects in early this ATP-independent step, suggesting that Prp8 and the U5 snRNP also participate in the very earliest steps of spliceosome assembly (Chapter 1). Next we explored the dynamics of commitment complex 2 formation and its

dependence on Prp28 using single molecule FRET to probe pre-mRNA conformations (Chapter 2).

Prp8 is critical for splicing catalysis as well as assembly, and it sits at the catalytic core of the spliceosome. Two classes of Prp8 alleles have been characterized that bias the spliceosome toward two opposing conformations. We propose a model, based on comparisons to the group II ribozyme, that these conformations represent catalytic and transitional (rearrangement) conformations of the spliceosome. We used a cluster of mutations that stabilize two different structures in Prp8 to investigate how a structural toggle in Prp8 affects the catalytic and transitional conformations of the spliceosome. Supporting our model, we found that Prp8 alleles predicted to stabilize the catalytic conformation were error prone and catalyzed in the 1st step of splicing efficiently in vitro, while alleles predicted to stabilize the transitional conformation were hyper-accurate and inefficient at the 1st step of splicing (Chapter 3).

Both spliceosome assembly and catalysis are points at which the fidelity or activity of the spliceosome could be regulated. My goal in this research has been to understand how individual steps are controlled by proteins such as Prp28 and Prp8 in hopes that this will give us a better context in which to study how cells could regulate these components to regulate splicing. New structural studies are giving the field the power to generate more informed hypotheses, based on structure, as a starting point for future genetic and biochemical studies.

Table of Contents

List of Tables

List of Figures

Chapter 1 continued

Chapter 2

Chapter 3

Chapter 3, continued

Epilogue

Appendix

Prologue

Prologue

Living organisms continually make new materials such as proteins and RNAs to do the work necessary for staying alive. The instructions for making all these materials are stored as DNA in the nucleus of eukaryotic cells. According to the central dogma of molecular biology, DNA is transcribed into RNA which then carries the information to ribosomes to be translated into protein. However, in most eukaryotes, genes (the DNA sequences that code for proteins) are often broken up by extra chunks of information that need to be removed from the transcribed RNA before the correct protein can be made. These extra chunks of information, called introns, are recognized and removed by a fascinating ribonucleoprotein (RNP) machine, the spliceosome. The spliceosome is highly dynamic - it assembles de-novo on each new intron. This makes the spliceosome particularly fascinating, but also particularly difficult, to study. The splicing field has been built on innovative genetic and biochemical studies to elucidate how each of its components interact and function, and recently has begun to benefit from high resolution crystal structures of some of its components (for reviews see Will and Lührmann 2011; Galej et al. 2014). There is a lot of potential for structures of the catalytic core of the spliceosome and its assembling subunits (once they are solved) to allow us to more fully understand how the decades of genetic and biochemical information fit together, and to serve as a starting point for asking new questions and designing more guided experiments.

One motivation for studying the mechanism of splicing is to better understand regulation of splicing. Regulation of splicing provides eukaryotic cells with an opportunity for an extra layer of regulation in gene expression (for example, Roy et al. 2013; Pleiss et al. 2007), and the possibility of alternative splicing to create different proteins with different combinations of exons from the same original DNA sequence. Budding yeast, *Saccharomyces cerevisiae*, only has a couple of genes with multiple introns so does not alternatively splice the way metazoans do.

Even yeast, however, differentially regulates the efficiency of splicing of particular subsets of genes in order to respond to environmental stress (for example, Pleiss et al. 2007) or to express meiotic genes (Munding et al. 2010). Before we can fully understand how splicing is regulated for these purposes, we need to understand the basic mechanism of splicing. How does the spliceosome rapidly and accurately identify the correct sequences to remove - with single nucleotide precision, but do so with enough flexibility to make alternative or regulated splicing possible?

The spliceosome is a dynamic RNP machine that assembles de-novo on each new intron. It recognizes short sequences in the intron (and at the intron/exon boundaries) through an ordered series of recognition/binding, rearrangement, and re-recognition events (Figure 1 reviewed in Brow 2002). Based on 35 years of research, we know a considerable amount about the components and assembly of the spliceosome. The spliceosome is composed of five small nuclear RNAs (snRNAs) and over 100 proteins in yeast (for reviews see Staley and Guthrie 1998; Wahl et al. 2009; Will and Lührmann 2011), many of which pre-assemble into snRNP complexes that are named for the snRNA they contain: U1, U2, U4, U5, or U6. The 5' splice site (5'ss) is initially recognized by the U1 snRNP, which base pairs with a consensus sequence at the 5' end of the intron. This forms a complex called Commitment Complex 1 (CC1), because labeled pre-mRNA that has formed this complex is now committed to the process of splicing - commitment complexes are resistant to challenge with unlabeled pre-mRNAs (Seraphin and Rosbash 1989; Legrain et al. 1988). Next, a dimer of Branchpoint Binding Protein and U2 bind to the conserved branch sequence, forming Commitment Complex 2 (CC2) (Liao et al. 1992). CC1 and CC2 do not require energy from ATP hydrolysis to form and are thought to be in equilibrium with one another; it is unclear if one necessarily forms before the other. Next, the U2 snRNP joins the assembling spliceosome. Two ATPases, Prp5 and Sub2, hydrolyze ATP to cause rearrangements at this step - Prp5 catalyzes a rearrangement in U2 that allows U2 to join (Perriman et al. 2003), while Sub2 promotes the release of BBP and Mud2 so that U2 can base-

pair with the branch sequence (Kistler and Guthrie 2001; Zhang and Green 2001). This forms the pre-spliceosome. Prp5 and Sub2 have also been shown to have ATP-independent functions involving protein-protein interactions that affect this and previous steps (Xu et al. 2004; Perriman et al. 2003; Kosowski et al. 2009; Zhang and Green 2001). The branch sequence has now been recognized twice by separate components of the spliceosome. This is one way the spliceosome insures that only the correct sequences are spliced. Interestingly, Shcherbakova et al. (2013) found, using single molecule methods to monitor spliceosome assembly, that U2 can sometimes bind the pre-mRNA before U1, depending on which pre-mRNA was used. Therefore, the functional relevance of the commitment complexes which contain U1 but not U2 may depend on the pre-mRNA and the environmental context.

The subsequent steps of spliceosome assembly have been shown to occur in an ordered sequence (Görnemann et al. 2005; Tardiff and Rosbash 2006; Hoskins et al. 2011). A pre-formed triple-snRNP complex composed of U4, U5, and U6 joins the pre-spliceosome, forming the B complex. The U6 snRNA is capable of base-pairing with both the 5'ss and the U2 snRNA, but two more ATPases are required at this step in order for that to happen. DEAD-box ATPase Prp28 promotes the release of U1 from the 5'ss, allowing U6 to base-pair with the same sequence instead (Staley and Guthrie 1999; Chen et al. 2001). In coordination with Prp28, the Brr2 helicase unwinds the extensive base-pairing between U4 and U6 (Raghunathan and Guthrie 1998), which rearranges U6 so that it base-pairs with U2 and also forms an internal stem loop that is important for the catalytic steps of splicing (Sashital et al. 2004; Fica et al. 2013). Both the U1 and U4 snRNPs are released at this point. The fully assembled and activated U2/U6-U5 spliceosome, the B-act complex (Fabrizio et al. 2009), is formed after an additional protein complex, the NineTeen Complex also binds (Hogg et al. 2010) (not shown in Figure 1; the exact timing and which components bind when is a topic of study). However, even the fully assembled spliceosome is not yet able to catalyze the chemical steps of splicing.

The chemical steps of splicing are two sequential trans-esterification reactions (Figure 2; reviewed in Will and Lührmann 2011). The spliceosome catalyzes these reactions by positioning the pre-mRNA and coordinating magnesium ions for catalysis. For the first reaction, the spliceosome positions the pre-mRNA such that its branch site adenosine bulges out, positioning its 2' hydroxyl to attack the 5' ss. This first chemical step forms a branched lariat intermediate structure and a free 5' exon, which the spliceosome holds onto. Next, the spliceosome positions the 5' exon so that its newly formed 3' hydroxyl is properly oriented to attack the 3' splice site (3'ss) at the start of the 3' exon. The second chemical step of splicing occurs, yielding the ligated pre-mRNA and releasing the branched lariat intron.

The catalytically competent spliceosome is formed from the Bact complex, composed of the U2, U5, and U6 snRNPs, several accessory proteins, and components of the NTC (Fabrizio et al. 2009; Will and Lührmann 2011; Bessonov et al. 2010). Warkocki et al. (2009) showed that the Bact complex can be purified from stalled prp2-1 splicing reactions. The first chemical step of splicing can then be reconstituted in vitro by adding ATP and three additional proteins: the ATPase Prp2, its cofactor Spp2, and an accessory factor Cwc25 (Warkocki et al. 2009). The activity of Prp2 rearranges several proteins, including destabilizing the SF3a/3b components of the U2 snRNP to activate the spliceosome (Kim and Lin 1996; Lardelli et al. 2010; Ohrt et al. 2012), and Cwc25 finally kicks the spliceosome into its catalytic conformation allowing the first chemical step to occur (Chiu et al. 2009; Krishnan et al. 2013). After the first catalytic step with this purified system, the second chemical step can also be reconstituted by addition of ATP plus the ATPase Prp16, and accessory factors Prp17, Prp18, and Slu7 (Ansari and Schwer 1995; Ohrt et al. 2013). Prp16 promotes rearrangements of the catalytic core to release Cwc25 and reposition the pre-mRNA for the second step of splicing (Tseng et al. 2011), and one of the accessory factors must serve a role in the 2nd step similar to that of Cwc25. Two more ATPase and their accessory proteins finish the splicing cycle. Prp22, which is also a 2nd step factor that improves the 2nd step for certain introns, hydrolyzes ATP to promote release of the mRNA

(Schwer and Gross 1998; Wagner et al. 1998; Ohrt et al. 2013). Finally, Prp43 with its cofactors Ntr1/2 catalyzes disassembly of the spliceosome from the lariat intron (Tsai et al. 2007). The spliceosome can now be recycled and reassembled on a new intron.

Each ATP-dependent rearrangement step, catalyzed by an ATPase of the DExD/H box family, is used by the spliceosome to check for errors by kinetic proofreading (reviewed in Burgess and Guthrie 1993b; Semlow and Staley 2012; Koodathingal and Staley 2013). Kinetic proofreading in the spliceosome uses each ATPase as a molecular clock that allows the spliceosome a limited amount of time to complete its previous step before the ATPase catalyzes the next rearrangement. If the spliceosome has successfully completed its previous step (as it would do quickly if it interacts with optimal splice sites) before the ATPase acts, the rearrangement catalyzed by the ATPase will drive the splicing reaction forward to the next step. If the spliceosome is slow, such as because it has encountered a suboptimal substrate, the ATPase will act before the spliceosome has properly lined up the previous step, and the rearrangement promoted by the ATPase will instead lead to discard. For example, Prp22, the ATPase that promotes mRNA release, has been shown to proofread the second step of splicing - exon ligation (Mayas et al. 2006). If the spliceosome is slow to complete the second step of splicing because it has a suboptimal pre-mRNA substrate, Prp22 will act on the spliceosome at hand, promoting discard of the incomplete splicing intermediate instead. Mutations in Prp22 that slow down the rate of ATP hydrolysis create spliceosomes that are error prone - more likely to splice pre-mRNAs with incorrect 3'ss sequences because mutated Prp22 allows more time for the spliceosome to complete the reaction on the incorrect substrate. This general principle of kinetic proofreading has also been shown for most of the other ATPases in the splicing cycle, including Prp5, Prp28, Prp2, and Prp16 (Yang et al. 2013; Wlodaver and Staley 2014; Koodathingal et al. 2010; Burgess and Guthrie 1993a; Xu and Query 2007). The fidelity of splicing can also be modulated by other factors that affect the conformation of catalytic core of the spliceosome or that control the activity of the ATPases. Interesting questions remain in the

splicing field about how cells modulate the fidelity of splicing to alternatively splice different sequences or modulate expression of specific genes in response to environmental signals.

When I joined the Guthrie lab, I was fascinated with the DEAD-box ATPase Prp28, which catalyzes the exchange of U1 for U6 at the 5'ss and promotes release of the U1 snRNP (Staley and Guthrie 1999; Chen et al. 2001). During this step, the spliceosome confirms the identity of the 5'ss a second time, connecting it with U6 which ultimately positions it properly for catalysis. Prp28 also provided a logical opportunity for the spliceosome to proofread the 5'ss, which was later shown to be true (Yang et al. 2013).

Prp28 was particularly intriguing because its activity appeared to be coordinated with that of Brr2, the helicase that unwinds U4 from U6. Mutations that prevent U4/U6 unwinding block U1 release and are synthetic lethal with prp28-1, a cold-sensitive mutation between RNA binding motifs in Prp28 (Kuhn et al. 1999; Strauss and Guthrie 1991), and in turn the *prp28-1* mutation blocks U4 release in vitro (Staley and Guthrie 1999). These reciprocal phenotypes suggested that Prp28 and Brr2 must be co-regulated so that their activities could be coordinated. I set out to investigate how Prp28 and Brr2 are coordinated.

A massive U5 snRNP protein, Prp8, is the logical protein to coordinate Prp28 and Brr2 activities. Yeast Prp8 is 280 kDa and is extremely highly conserved between yeast and humans: 61% identity (for review, see Grainger and Beggs 2005). Because of its extensive genetic and physical interactions with multiple components of the spliceosome and with all three splicing sequences in the pre-mRNA itself, Prp8 has been proposed to be a master regulator of spliceosome assembly and activity (Kuhn et al. 2002; Grainger and Beggs 2005). It, along with Brr2, is an integral component of the U5 and triple-snRNPs (Stevens et al. 2001), and Prp28 is also a component of the U5 snRNP and is associated with the triple-snRNP at least in some contexts (Stevens et al. 2001; Small et al. 2006; Mathew et al. 2008). So these proteins are in the appropriate complexes to be regulated by Prp8. Indeed, the Jab/MPN domain at the C-terminus of Prp8 regulates Brr2's ATPase activity (Maeder et al. 2008; Mozaffari-Jovin et al.

2012). Furthermore, mutations in Prp8 suppress mutations in Brr2, Prp28, and the U4 snRNA (Kuhn et al. 2002; Kuhn and Brow 2000). When I began my work, one allele near the N-terminus of Prp8 had been previously found that suppressed the cold-sensitivity of *prp28-1*. Our collaborators David Brow and Janina Gornemann at the University of Wisconsin, Madison, had just completed a screen looking for additional prp28-1 suppressors, so we joined forces. Our collaboration took a surprising turn when we noticed that the prp28-1 allele blocked not only U1 and U4 release, but also reduced the association of U2, U5, and U6 by two independent assays. Thus, our collaboration (Chapter 1) turned to understanding the roles of Prp28 and Prp8 in the earliest steps of spliceosome assembly. Chapter 2 follows up on the ATP-independent role of Prp28 in commitment complex formation.

Prp8 is critical not only for regulating spliceosome assembly, but for forming the catalytic center of the spliceosome. Recent crystal structures of Prp8 have given us a structural context in which to reinterpret previous genetic and biochemical information, plus the ability to ask more structured questions. The crystal structures of Prp8 revealed an RNaseH fold, a reverse-transcriptase-like domain, and an endonuclease-like fold, all of which are missing catalytic residues (Yang et al. 2008; Pena et al. 2008; Ritchie et al. 2008; Schellenberg et al. 2013; Galej et al. 2013). These domains suggest that Prp8 probably evolved from a transposon and lost catalytic activities but maintained domains important for interacting with RNA. The RNaseH domain is particularly fascinating because it cross-links to the 5'ss of the pre-mRNA (Siatecka et al. 1999) and houses a number of interesting alleles. The most complete Prp8 structure, of 2/3 of the protein, shows the RNaseH domain on one side of a large cavity and the RT and Endo domains on the other (Galej et al. 2013). Based on where the pre-mRNA cross-links to the RNaseH domain, the pre-mRNA would probably sit in this cavity. So Prp8 at a minimum provides a structural scaffold on which the snRNAs (U6 in particular because it coordinates two magnesium ions for catalysis - Fica et al. 2013, 2014) form the catalytic core of the spliceosome. A recent paper found that Prp8's RNaseH domain, while lacking catalytic residues,

does bind a magnesium ion in a conformation-dependent manner (Schellenberg et al. 2013). Mutations that prevent Mg++ binding also inhibit in vitro splicing, suggesting that the Mg++ ion plays an important structural role or possibly even contributes to catalysis (Schellenberg et al. 2013). In addition to changing the ability to bind Mg++, the two conformations of the RNaseH domain change the structure of a 17aa insertion from a hairpin to a loop. This insertion has previously been proposed to interact with RNA (Yang et al. 2008). Amazingly, at least 14 individual mutations have been identified in this 17aa insertion that have genetic interactions with other components of the spliceosome and/or affect the fidelity of splicing. Several of these mutations stabilize either the hairpin or loop structure (Schellenberg et al. 2013), suggesting that both structures (and the ability to toggle between them) are important for different aspects of the function of the spliceosome.

Chapter 3 describes my efforts, along with the rest of "Team Toggle," to explore the functional significance that the hairpin and loop structures in Prp8's RNaseH domain have on the catalytic conformation of the spliceosome. Based on analogy to the group II ribozyme, for which structures of the catalytic states have been solved (see Marcia et al. 2013 for a review), the spliceosome must form a catalytic conformation for the first step of catalysis, rearrange into a transitional state between catalytic steps, and re-form a catalytic conformation for the second step of catalysis. Existing genetic data (Query and Konarska 2004; Liu et al. 2007; Yang et al. 2008; Schellenberg et al. 2013) supports a model in which the two Prp8 structures bias the spliceosome toward two different conformations. Previously, these conformations were proposed to be the 1st step catalytic conformation and the 2nd step catalytic conformation (Query and Konarska 2004). However, when this 1st step/2nd step model was proposed, the idea that the spliceosome must undergo a transitional state between catalytic steps had not yet been discussed. In chapter 3, we create an expanded genetic dataset so that we have comparable information about all 14 previously identified RNaseH insertion alleles. We test specifically whether the "2nd step" alleles actually bias the spliceosome toward a generally catalytic

conformation for both steps of splicing while the "1st step" alleles instead promote the transitional conformation.

My journey with Prp8 and Prp28 from the earliest steps of spliceosome assembly to the heart of the catalytic spliceosome has been motivated by a desire to learn how the spliceosome accurately and precisely removes introns while remaining flexible enough for its activity and fidelity to be regulated by the cell. The specific steps that I've studied are points at which the fidelity or activity of the spliceosome could be modulated. My hope is that by learning about how spliceosomal proteins such as Prp8 and Prp28 control these individual steps, we will be able to later interrogate more effectively how the cell regulates these proteins to regulate splicing. It would be particularly interesting to study whether and how Prp8 is regulated, since it affects everything from assembly to catalysis and may itself be the master regulator of spliceosome activity. Like the splicing field as a whole, my research has moved from genetics and biochemistry toward using high resolution structures as a way to provide context for previous data and generate new questions - a starting point for future biochemical and genetic investigation.

References

Ansari A, Schwer B. 1995. SLU7 and a novel activity, SSF1, act during the PRP16-dependent step of yeast pre-mRNA splicing. *EMBO J* **14**: 4001–4009.

Bessonov S, Anokhina M, Krasauskas A, Golas MM, Sander B, Will CL, Urlaub H, Stark H, Lührmann R. 2010. Characterization of purified human Bact spliceosomal complexes reveals compositional and morphological changes during spliceosome activation and first step catalysis. *RNA New York N* **16**: 2384–2403.

Brow DA. 2002. Allosteric cascade of spliceosome activation. *Annu Rev Genet* **36**: 333–360.

Burgess SM, Guthrie C. 1993a. A mechanism to enhance mRNA splicing fidelity: The RNA-dependent ATPase Prp16 governs usage of a discard pathway for aberrant lariat intermediates. *Cell* **73**: 1377–1391.

Burgess SM, Guthrie C. 1993b. Beat the clock: paradigms for NTPases in the maintenance of biological fidelity. *Trends Biochem Sci* **18**: 381–384.

Chen JY-F, Stands L, Staley JP, Jackups Jr. RR, Latus LJ, Chang T-H. 2001. Specific alterations of U1-C protein or U1 small nuclear RNA can eliminate the requirement of Prp28p, an essential DEAD box splicing factor. *Mol Cell* **7**: 227–232.

Chiu Y-F, Liu Y-C, Chiang T-W, Yeh T-C, Tseng C-K, Wu N-Y, Cheng S-C. 2009. Cwc25 Is a Novel Splicing Factor Required after Prp2 and Yju2 To Facilitate the First Catalytic Reaction. *Mol Cell Biol* **29**: 5671–5678.

Fabrizio P, Dannenberg J, Dube P, Kastner B, Stark H, Urlaub H, Lührmann R. 2009. The evolutionarily conserved core design of the catalytic activation step of the yeast spliceosome. *Mol Cell* **36**: 593–608.

Fica SM, Mefford MA, Piccirilli JA, Staley JP. 2014. Evidence for a group II intron-like catalytic triplex in the spliceosome. *Nat Struct Mol Biol* **21**: 464–471.

Fica SM, Tuttle N, Novak T, Li N-S, Lu J, Koodathingal P, Dai Q, Staley JP, Piccirilli JA. 2013. RNA catalyses nuclear pre-mRNA splicing. *Nature* **503**: 229–234.

Galej WP, Nguyen THD, Newman AJ, Nagai K. 2014. Structural studies of the spliceosome: zooming into the heart of the machine. *Curr Opin Struct Biol* **25**: 57–66.

Galej WP, Oubridge C, Newman AJ, Nagai K. 2013. Crystal structure of Prp8 reveals active site cavity of the spliceosome. *Nature* **493**: 638–643.

Görnemann J, Kotovic KM, Hujer K, Neugebauer KM. 2005. Cotranscriptional spliceosome assembly occurs in a stepwise fashion and requires the cap binding complex. *Mol Cell* **19**: 53–63.

Grainger RJ, Beggs JD. 2005. Prp8 protein: at the heart of the spliceosome. *RNA* **11**: 533–557.

Hogg R, McGrail JC, O'Keefe RT. 2010. The function of the NineTeen Complex (NTC) in regulating spliceosome conformations and fidelity during pre-mRNA splicing. *Biochem Soc Trans* **38**: 1110–1115.

Hoskins AA, Friedman LJ, Gallagher SS, Crawford DJ, Anderson EG, Wombacher R, Ramirez N, Cornish VW, Gelles J, Moore MJ. 2011. Ordered and dynamic assembly of single spliceosomes. *Science* **331**: 1289–1295.

Kim SH, Lin RJ. 1996. Spliceosome activation by PRP2 ATPase prior to the first transesterification reaction of pre-mRNA splicing. *Mol Cell Biol* **16**: 6810–6819.

Kistler AL, Guthrie C. 2001. Deletion of MUD2, the yeast homolog of U2AF65, can bypass the requirement for Sub2, an essential spliceosomal ATPase. *Genes Dev* **15**: 42–49.

Koodathingal P, Novak T, Piccirilli JA, Staley JP. 2010. The DEAH box ATPases Prp16 and Prp43 cooperate to proofread 5' splice site cleavage during pre-mRNA splicing. *Mol Cell* **39**: 385–395.

Koodathingal P, Staley JP. 2013. Splicing fidelity: DEAD/H-box ATPases as molecular clocks. *RNA Biol* **10**: 1073–1079.

Kosowski TR, Keys HR, Quan TK, Ruby SW. 2009. DExD/H-box Prp5 protein is in the spliceosome during most of the splicing cycle. *RNA* **15**: 1345–1362.

Krishnan R, Blanco MR, Kahlscheuer ML, Abelson J, Guthrie C, Walter NG. 2013. Biased Brownian ratcheting leads to pre-mRNA remodeling and capture prior to first-step splicing. *Nat Struct Mol Biol* **20**: 1450–1457.

Kuhn AN, Brow DA. 2000. Suppressors of a cold-sensitive mutation in yeast U4 RNA define five domains in the splicing factor Prp8 that influence spliceosome activation. *Genetics* **155**: 1667–1682.

Kuhn AN, Li Z, Brow DA. 1999. Splicing factor Prp8 governs U4/U6 RNA unwinding during activation of the spliceosome. *Mol Cell* **3**: 65–75.

Kuhn AN, Reichl EM, Brow DA. 2002. Distinct domains of splicing factor Prp8 mediate different aspects of spliceosome activation. *Proc Natl Acad Sci* **99**: 9145–9149.

Lardelli RM, Thompson JX, Yates JR 3rd, Stevens SW. 2010. Release of SF3 from the intron branchpoint activates the first step of pre-mRNA splicing. *RNA New York N* **16**: 516–528.

Legrain P, Seraphin B, Rosbash M. 1988. Early commitment of yeast pre-mRNA to the spliceosome pathway. *Mol Cell Biol* **8**: 3755–3760.

Liao XC, Colot HV, Wang Y, Rosbash M. 1992. Requirements for U2 snRNP Addition to Yeast Pre-mRNA. *Nucleic Acids Res* **20**: 4237–4245.

Liu L, Query CC, Konarska MM. 2007. Opposing classes of prp8 alleles modulate the transition between the catalytic steps of pre-mRNA splicing. *Nat Struct Mol Biol* **14**: 519–526.

Maeder C, Kutach AK, Guthrie C. 2008. ATP-dependent unwinding of U4/U6 snRNAs by the Brr2 helicase requires the C terminus of Prp8. *Nat Struct Mol Biol* **16**: 42–48.

Marcia M, Somarowthu S, Pyle AM. 2013. Now on display: a gallery of group II intron structures at different stages of catalysis. *Mob DNA* **4**: 14.

Mathew R, Hartmuth K, Möhlmann S, Urlaub H, Ficner R, Lührmann R. 2008. Phosphorylation of human PRP28 by SRPK2 is required for integration of the U4/U6-U5 tri-snRNP into the spliceosome. *Nat Struct Mol Biol* **15**: 435–443.

Mayas RM, Maita H, Staley JP. 2006. Exon ligation is proofread by the DExD/H-box ATPase Prp22p. *Nat Struct Mol Biol* **13**: 482–490.

Mozaffari-Jovin S, Santos KF, Hsiao H-H, Will CL, Urlaub H, Wahl MC, Lührmann R. 2012. The Prp8 RNase H-like domain inhibits Brr2-mediated U4/U6 snRNA unwinding by blocking Brr2 loading onto the U4 snRNA. *Genes Dev* **26**: 2422–2434.

Munding EM, Igel AH, Shiue L, Dorighi KM, Treviño LR, Ares M. 2010. Integration of a splicing regulatory network within the meiotic gene expression program of Saccharomyces cerevisiae. *Genes Dev* **24**: 2693–2704.

Ohrt T, Odenwälder P, Dannenberg J, Prior M, Warkocki Z, Schmitzová J, Karaduman R, Gregor I, Enderlein J, Fabrizio P, et al. 2013. Molecular dissection of step 2 catalysis of yeast pre-mRNA splicing investigated in a purified system. *RNA New York N* **19**: 902–915.

Ohrt T, Prior M, Dannenberg J, Odenwälder P, Dybkov O, Rasche N, Schmitzová J, Gregor I, Fabrizio P, Enderlein J, et al. 2012. Prp2-mediated protein rearrangements at the catalytic core of the spliceosome as revealed by dcFCCS. *RNA New York N* **18**: 1244–1256.

Pena V, Rozov A, Fabrizio P, Lührmann R, Wahl MC. 2008. Structure and function of an RNase H domain at the heart of the spliceosome. *EMBO J* **27**: 2929–2940.

Perriman R, Barta I, Voeltz GK, Abelson J, Ares M. 2003. ATP requirement for Prp5p function is determined by Cus2p and the structure of U2 small nuclear RNA. *Proc Natl Acad Sci* **100**: 13857–13862.

Pleiss JA, Whitworth GB, Bergkessel M, Guthrie C. 2007. Rapid, transcript-specific changes in splicing in response to environmental stress. *Mol Cell* **27**: 928–937.

Query CC, Konarska MM. 2004. Suppression of multiple substrate mutations by spliceosomal prp8 alleles suggests functional correlations with ribosomal ambiguity mutants. *Mol Cell* **14**: 343–354.

Raghunathan PL, Guthrie C. 1998. RNA unwinding in U4/U6 snRNPs requires ATP hydrolysis and the DEIH-box splicing factor Brr2. *Curr Biol* **8**: 847–855.

Ritchie DB, Schellenberg MJ, Gesner EM, Raithatha SA, Stuart DT, MacMillan AM. 2008. Structural elucidation of a PRP8 core domain from the heart of the spliceosome. *Nat Struct Mol Biol* **15**: 1199–1205.

Roy B, Haupt LM, Griffiths LR. 2013. Review: Alternative Splicing (AS) of Genes As An Approach for Generating Protein Complexity. *Curr Genomics* **14**: 182–194.

Sashital DG, Cornilescu G, McManus CJ, Brow DA, Butcher SE. 2004. U2-U6 RNA folding reveals a group II intron-like domain and a four-helix junction. *Nat Struct Mol Biol* **11**: 1237–1242.

Schellenberg MJ, Wu T, Ritchie DB, Fica S, Staley JP, Atta KA, LaPointe P, MacMillan AM. 2013. A conformational switch in PRP8 mediates metal ion coordination that promotes pre-mRNA exon ligation. *Nat Struct Mol Biol* **20**: 728–734.

Schwer B, Gross CH. 1998. Prp22, a DExH-box RNA helicase, plays two distinct roles in yeast pre-mRNA splicing. *EMBO J* **17**: 2086–2094.

Semlow DR, Staley JP. 2012. Staying on message: ensuring fidelity in pre-mRNA splicing. *Trends Biochem Sci* **37**: 263–273.

Seraphin B, Rosbash M. 1989. Identification of functional U1 snRNA-pre-mRNA complexes committed to spliceosome assembly and splicing. *Cell* **59**: 349–358.

Shcherbakova I, Hoskins AA, Friedman LJ, Serebrov V, Corrêa IR, Xu M-Q, Gelles J, Moore MJ. 2013. Alternative spliceosome assembly pathways revealed by single-molecule fluorescence microscopy. *Cell Rep* **5**: 151–165.

Siatecka M, Reyes JL, Konarska MM. 1999. Functional interactions of Prp8 with both splice sites at the spliceosomal catalytic center. *Genes Dev* **13**: 1983–1993.

Small EC, Leggett SR, Winans AA, Staley JP. 2006. The EF-G-like GTPase Snu114p regulates spliceosome dynamics mediated by Brr2p, a DExD/H box ATPase. *Mol Cell* **23**: 389–399.

Staley JP, Guthrie C. 1999. An RNA switch at the 5’ splice site requires ATP and the DEAD box protein Prp28p. *Mol Cell* **3**: 55–64.

Staley JP, Guthrie C. 1998. Mechanical devices of the spliceosome: motors, clocks, springs, and things. *Cell* **92**: 315–326.

Stevens SW, Barta I, Ge HY, Moore RE, Young MK, Lee TD, Abelson J. 2001. Biochemical and genetic analyses of the U5, U6, and U4/U6 x U5 small nuclear ribonucleoproteins from Saccharomyces cerevisiae. *RNA New York N* **7**: 1543–1553.

Strauss EJ, Guthrie C. 1991. A cold-sensitive mRNA splicing mutant is a member of the RNA helicase gene family. *Genes Dev* **5**: 629–641.

Tardiff DF, Rosbash M. 2006. Arrested yeast splicing complexes indicate stepwise snRNP recruitment during in vivo spliceosome assembly. *RNA* **12**: 968–979.

Tsai R-T, Tseng C-K, Lee P-J, Chen H-C, Fu R-H, Chang K, Yeh F-L, Cheng S-C. 2007. Dynamic interactions of Ntr1-Ntr2 with Prp43 and with U5 govern the recruitment of Prp43 to mediate spliceosome disassembly. *Mol Cell Biol* **27**: 8027–8037.

Tseng C-K, Liu H-L, Cheng S-C. 2011. DEAH-Box ATPase Prp16 has dual roles in remodeling of the spliceosome in catalytic steps. *RNA* **17**: 145–154.

Wagner JD, Jankowsky E, Company M, Pyle AM, Abelson JN. 1998. The DEAH-box protein PRP22 is an ATPase that mediates ATP-dependent mRNA release from the spliceosome and unwinds RNA duplexes. *EMBO J* **17**: 2926–2937.

Wahl MC, Will CL, Lührmann R. 2009. The spliceosome: design principles of a dynamic RNP machine. *Cell* **136**: 701–718.

Warkocki Z, Odenwälder P, Schmitzová J, Platzmann F, Stark H, Urlaub H, Ficner R, Fabrizio P, Lührmann R. 2009. Reconstitution of both steps of Saccharomyces cerevisiae splicing with purified spliceosomal components. *Nat Struct Mol Biol* **16**: 1237–1243.

Will CL, Lührmann R. 2011. Spliceosome structure and function. *Cold Spring Harb Perspect Biol* **3**: a003707.

Wlodaver AM, Staley JP. 2014. The DExD/H-box ATPase Prp2p destabilizes and proofreads the catalytic RNA core of the spliceosome. *RNA New York N* **20**: 282–294.

Xu Y-Z, Newnham CM, Kameoka S, Huang T, Konarska MM, Query CC. 2004. Prp5 bridges U1 and U2 snRNPs and enables stable U2 snRNP association with intron RNA. *EMBO J* **23**: 376–385.

Xu Y-Z, Query CC. 2007. Competition between the ATPase Prp5 and branch region-U2 snRNA pairing modulates the fidelity of spliceosome assembly. *Mol Cell* **28**: 838–849.

Yang F, Wang X-Y, Zhang Z-M, Pu J, Fan Y-J, Zhou J, Query CC, Xu Y-Z. 2013. Splicing proofreading at 5′ splice sites by ATPase Prp28p. *Nucleic Acids Res* **41**: 4660–4670.

Yang K, Zhang L, Xu T, Heroux A, Zhao R. 2008. Crystal structure of the B-finger domain of Prp8 reveals analogy to ribosomal proteins. *Proc Natl Acad Sci* **105**: 13817–13822.

Zhang M, Green MR. 2001. Identification and characterization of yUAP/Sub2p, a yeast homolog of the essential human pre-mRNA splicing factor hUAP56. *Genes Dev* **15**: 30–35.

Figures

Figure 1: Diagram of the splicing cycle from assembly through catalysis and disassembly. See text for full description. Names spliceosome assembly complexes are indicated in bold. DExD/H-box ATPases have "ATP" next to them.

Figure 1

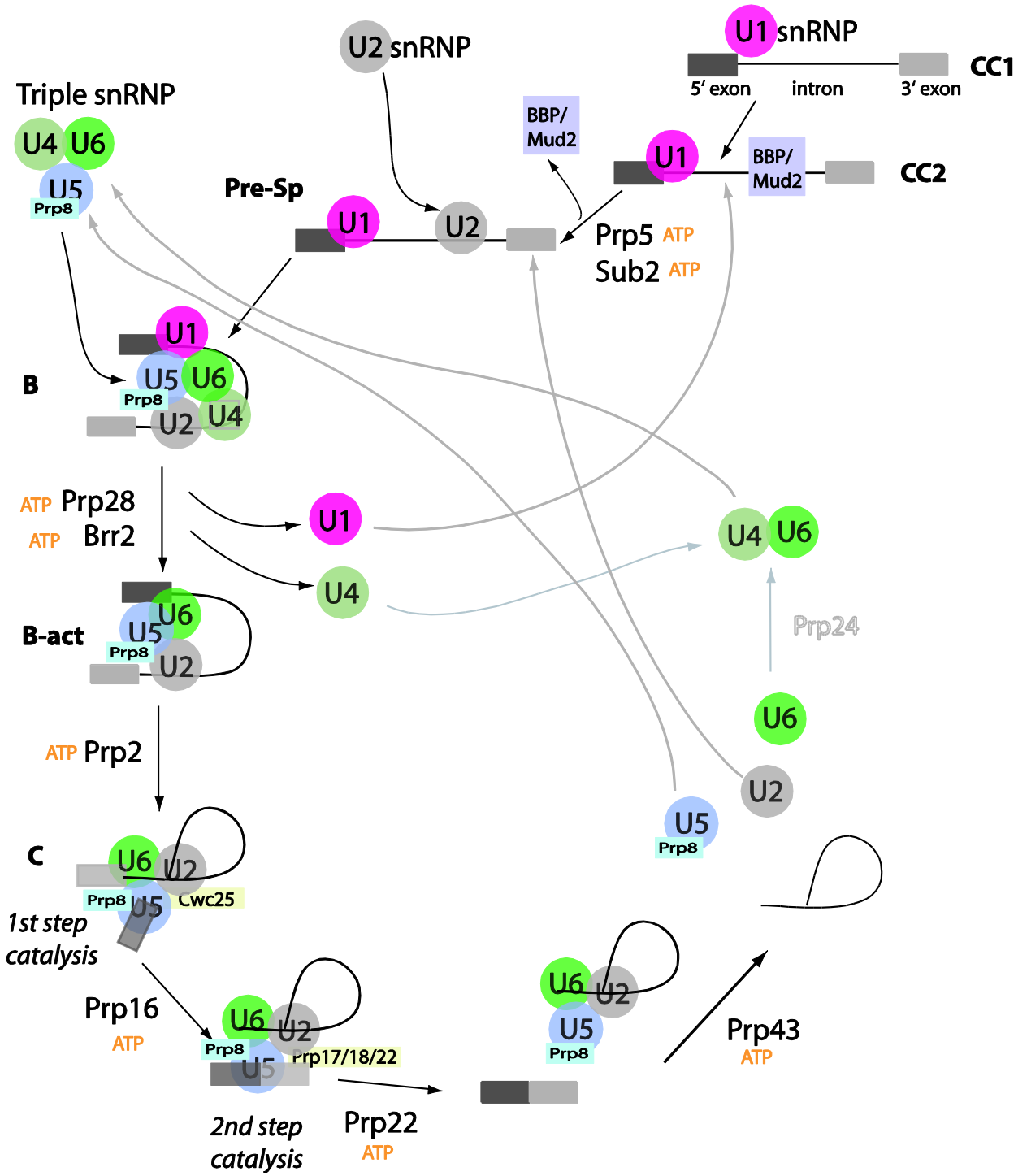
U2 snRNP
U1 snRNP
CC1
5′ exon
intron
3′ exon
Triple snRNP
U4 U6
U5
Prp8
BBP/
Mud2
U1
BBP/
Mud2
CC2
Pre-Sp
U1
U2
Prp5 ATP
Sub2 ATP
U1
B
U5 U6
Prp8
U2 U4
ATP Prp28
ATP Brr2
U1
U4 U6
U4
B-act
U6
U5
Prp8
U2
Prp24
U6
ATP Prp2
U2
U5
Prp8
C
U6 U2
Prp8 U5
Cwc25
1st step
catalysis
Prp16
ATP
U6 U2
Prp8
U5
Prp17/18/22
U6 U2
U5
Prp8
Prp43
ATP
2nd step
catalysis
Prp22
ATP

Figure 2: Diagram of the two chemical steps of splicing. In the first step, the 2' hydroxyl of the branch-site adenosine attacks the 5' splice site, forming free 5' exon and lariat intermediate. In the second step, the 3' hydroxyl of the freed 5' exon attacks the 3' splice site, forming ligated exon1 + exon2 mRNA and free lariat intron.

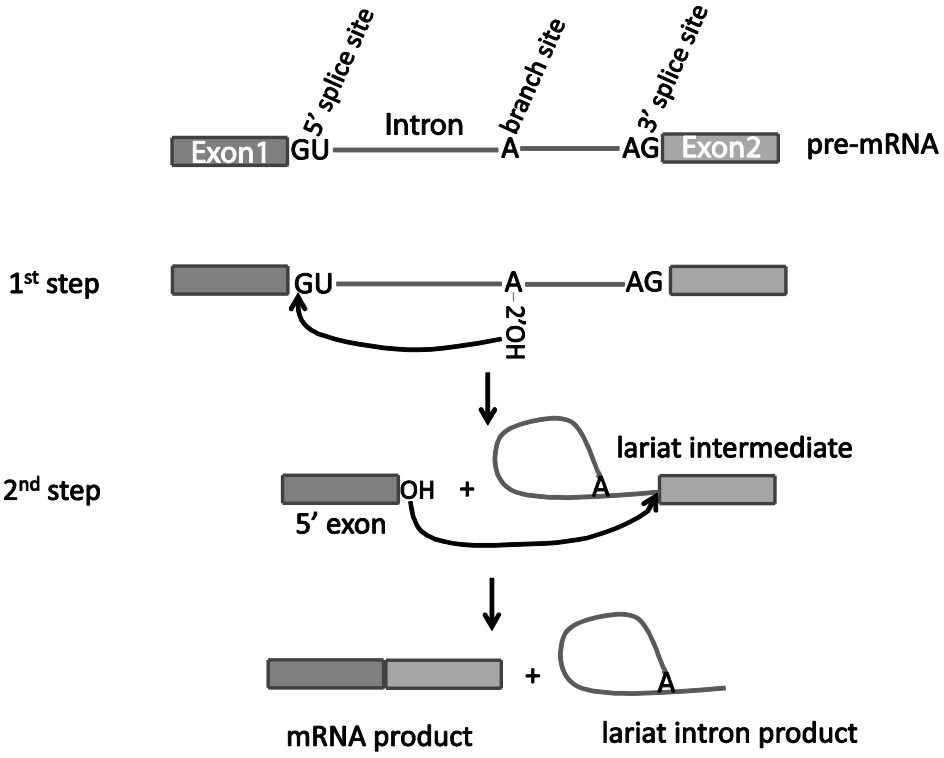

Chapter 1

An unanticipated early function of DEAD-box ATPase Prp28 during commitment to splicing is modulated by U5 snRNP protein Prp8

An unanticipated early function of DEAD-box ATPase Prp28 during commitment to splicing is modulated by U5 snRNP protein Prp8

Argenta M. Price[1], Janina Görnemann[2,3*], Christine Guthrie[1,4], and David A. Brow[2,4]

[1]Department of Biochemistry and Biophysics, University of California, San Francisco, California 94143, USA

[2]Department of Biomolecular Chemistry, School of Medicine and Public Health, University of Wisconsin, Madison, Wisconsin 53706, USA

[3]Max Planck Institute of Molecular Cell Biology and Genetics, Pfotenhauerstrasse 108, 01307 Dresden, Germany

[4]Co-corresponding authors: christineguthrie@gmail.com, dabrow@wisc.edu

*current address: Department of Cellular and Molecular Medicine, KU Leuven, Belgium

Running title: Early functions of Prp28 and Prp8 in splicing

Keywords: pre-mRNA splicing, Prp28, Prp8, commitment complex, pre-spliceosome

Abstract

The stepwise assembly of the highly dynamic spliceosome is guided by RNA-dependent ATPases of the DEAD-box family, whose regulation is poorly understood. In the canonical assembly model, the U4/U6.U5 triple snRNP binds only after joining of the U1 and, subsequently, U2 snRNPs to the intron-containing pre-mRNA. Catalytic activation requires the exchange of U6 for U1 snRNA at the 5' splice site, which is promoted by the DEAD-box protein Prp28. Because Prp8, an integral U5 snRNP protein, is thought to be a central regulator of DEAD-box proteins, we conducted a targeted search in Prp8 for cold-insensitive suppressors of a cold-sensitive Prp28 mutant, *prp28-1*. We identified a cluster of suppressor mutations in an N-terminal bromodomain-like sequence of Prp8. To identify the precise defect in *prp28-1* strains that is suppressed by the Prp8 alleles, we analyzed spliceosome assembly *in vivo* and *in vitro*. Surprisingly, in the *prp28-1* strain, we observed a block not only to spliceosome activation but also to one of the earliest steps of assembly, formation of the ATP-independent Commitment Complex 2 (CC2). The Prp8 suppressor partially corrected both the early assembly and later activation defects of *prp28-1*, supporting a role for this U5 snRNP protein in both the ATP-independent and ATP-dependent functions of Prp28. We conclude that the U5 snRNP has a role in the earliest events of assembly, prior to its stable incorporation into the spliceosome.

Introduction

The spliceosome is a macromolecular machine that locates and excises introns with single-nucleotide precision. To accurately identify and remove introns, the spliceosome undergoes a stepwise series of binding events and conformational rearrangements, guided by proteins of the DEXD/H-box family of RNA-dependent ATPases. In the canonical model of spliceosome assembly (reviewed in Will and Lührmann 2011) the U1 snRNP first recognizes the 5' splice site (5'ss), forming commitment complex 1 (CC1). The branch site and 3' end of the intron are then recognized by two proteins, BBP and Mud2 in yeast, forming commitment complex 2 (CC2). Next, the first ATP-dependent step of splicing occurs: DEAD/DECD-box proteins Prp5 and Sub2 promote rearrangements that replace BBP and Mud2 with the U2 snRNP at the branch site, forming the pre-spliceosome or A complex. The U4/U6.U5 triple-snRNP (tri-snRNP) then joins to form the assembled spliceosome or B complex.

Once assembled, the spliceosome undergoes activation for catalysis. DEAD-box protein Prp28 promotes release of the U1 snRNP, allowing U6 to base-pair with the 5'ss. In coordination with Prp28, DEIH-box helicase Brr2 (a stable component of the U5 snRNP) unwinds U4 from U6, allowing U6 to base-pair with U2. Together, these ATP-dependent activities of Prp28 and Brr2 form the U2/U6.U5 spliceosome (B^{act} complex) competent for the final steps of activation, which include binding of the Nineteen Complex (NTC) and additional rearrangements catalyzed by the DEAH-box protein Prp2. While this general sequence of events is well supported, several studies have also implicated the U5 snRNP in very early steps of spliceosome assembly, before stable incorporation of the tri-snRNP (Wyatt et al. 1992; Wassarman and Steitz 1992; Newman et al. 1995; Ast and Weiner 1997; Maroney et al. 2000). In addition, the mechanisms underlying the timing and coordination of each assembly step remain poorly understood. In this study, we focus on Prp28 and its interactions with Prp8, an integral component of the U5 and tri-snRNPs, thought to be a central regulator of spliceosome activity (Kuhn et al. 2002; Grainger and Beggs 2005; Galej et al. 2013).

Several studies have provided evidence that Prp28 promotes U1 snRNP release and is involved in stable tri-snRNP incorporation into the spliceosome. The cold-sensitive *prp28-1* mutation, G279E, is in motif 1b of the DEAD-box domain (Strauss and Guthrie 1991, 1994), which likely contacts an as yet unknown RNA substrate (Fairman-Williams et al. 2010). It causes a broad splicing defect (Pleiss et al. 2007) and exacerbates mutations that hyperstabilize the base-pairing between U1 and the 5'ss (Staley and Guthrie 1999). Other mutations in Prp28 reduce fidelity of U6/5'ss base-pairing, the interaction that replaces U1/5'ss pairing (Yang et al. 2013). Further supporting a role in U1 snRNP release, Prp28 is nonessential in strains with mutations that are predicted to destabilize the U1/5'ss interaction (Chen et al. 2001; Hage et al. 2009; Schwer et al. 2013). Finally, U1/5'ss hyperstabilization and *prp28-1* cause similar in vitro spliceosome assembly defects, which include inhibition of U4/U6 unwinding and reduced stability of tri-snRNP association (Staley and Guthrie 1999). In mammalian cells, Prp28 is a stable component of the tri-snRNP (Teigelkamp et al. 1997) and is directly involved in its recruitment to the spliceosome (Ismaili et al. 2001; Mathew et al. 2008). However, yeast Prp28 appears to be less stably associated with tri-snRNP (Strauss and Guthrie 1994; Gottschalk et al. 1999; Stevens et al. 2001; Small et al. 2006), so it is unclear whether the defect in tri-snRNP incorporation in the *prp28-1* strain is direct, or is an indirect consequence of the block to U1 snRNP release.

The Prp28- and Brr2-catalyzed releases of the U1 and U4 snRNPs appear to be coordinated: mutations that inhibit either step also block the other (Kuhn et al. 1999; Staley and Guthrie 1999). Prp8 is a good candidate for regulating Prp28 and coordinating its activity with that of Brr2. The Jab1/MPN domain at the C-terminus of Prp8 is known to regulate Brr2 activity (Maeder et al. 2008; Mozaffari-Jovin et al. 2012, 2013). Furthermore, the N-terminal domain (NTD) of Prp8 harbors a mutation that suppresses the cold-sensitivity of the *prp28-1* mutation (Kuhn et al. 2002), and also physically interacts with two U1 snRNP proteins (Abovich and Rosbash 1997; van Nues and Beggs 2001). A recent study found that Prp8 cross-links to the U1

snRNA, and mutations in U1 that reduce this cross-link also reduce triple-snRNP association with the pre-mRNA (Li et al. 2013). Therefore, Prp8 is perfectly positioned to promote tri-snRNP joining through interactions with U1 and then regulate Prp28-directed-U1 release.

To define Prp28's interaction with Prp8, we conducted a targeted selection for cold-insensitive suppressors of *prp28-1* in the Prp8-NTD. We identified 15 suppressor substitutions that cluster in a proposed bromodomain (Dlakić and Mushegian 2011). To determine the precise order of spliceosome assembly defects caused by *prp28-1* and to identify which defects are suppressed by the Prp8 alleles, we monitored the kinetics of co-transcriptional spliceosome assembly *in vivo* and posttranscriptional spliceosome assembly *in vitro*. As expected, *prp28-1* blocks U1 and U4 release and reduces stable tri-snRNP association. Surprisingly, however, *prp28-1* also inhibits formation of the pre-spliceosome and ATP-independent CC2. Therefore, we propose that Prp28 has at least two distinct roles in spliceosome assembly and activation: an ATP-independent role in CC2 formation and a subsequent ATP-dependent role in U1 release. A *prp28-1*-suppressor mutation in the *PRP8-NTD* partially alleviates all of the spliceosome assembly and activation defects caused by *prp28-1*, including the early CC2 formation defect. Our results provide evidence that Prp8 and the U5 snRNP have a role in the earliest events of spliceosome assembly, prior to the stable incorporation of the tri-snRNP into the spliceosome.

Results

prp8-tes alleles: substitutions in the N-terminal quarter of Prp8 that suppress *prp28-1*

In order to characterize the interactions between Prp28 and its potential regulator, Prp8, we screened the NTD of Prp8 for suppressors of *prp28-1.* Prp8 is a 280 kDa protein that is an integral component of the U5 and tri-snRNPs. Substitutions in distinct regions of Prp8 suppress mutations in a variety of spliceosomal proteins as well as mutations in snRNAs and conserved splice signals in the pre-mRNA itself (Grainger and Beggs 2005). Recent studies have provided

deep insight into the structure of the C-terminal two-thirds of Prp8 (Galej et al. 2013). The C-terminal domains of Prp8 contact the 5'ss with an RNase-H like fold (Pena et al. 2008; Ritchie et al. 2008; Yang et al. 2008; Schellenberg et al. 2013) and regulate Brr2 through a Jab/MPN domain (Pena et al. 2007; Maeder et al. 2008; Mozaffari-Jovin et al. 2012, 2013). The N-terminal portion of Prp8 remains structurally elusive, but is particularly interesting in connection with Prp28. In a prior selection for suppressors of a cold-sensitive mutation in U4 RNA (U4-cs1) that blocks U4 and U1 release at 16˚C, we isolated an N-terminal Prp8 substitution (L280P) that suppressed both U4-cs1 and *prp28-1* (Kuhn et al. 2002). This substitution was the only U4-cs1-suppressor of 13 tested that also suppressed *prp28-1,* implying that suppression of *prp28-1* is due to alteration of a specific interaction rather than a general effect of decreased Prp8 activity.

Therefore, we sought to map this interaction surface in the N-terminal quarter of Prp8 by mutagenizing codons 1-660 of *PRP8* by error-prone PCR and selecting alleles that allow a *prp28-1* strain to grow at 16˚C (Figs. 1A and B, Table 1). Thirty-seven cold-resistant clones were isolated, 16 of which contained the substitution D273G, either as the sole substitution (8 clones) or as one of two or more substitutions. Three additional suppressors contained a D273N substitution, once as the sole mutation. Seven clones had an R226G substitution, in two cases as the sole mutation, and another clone had the R226S substitution. Of the remaining 10 clones, 3 had at least one substitution between residues 222 and 229, 6 had at least one change between residues 263 to 281, and one had the substitution L314S. Silent (synonymous) and secondary mutations spanned codons 20 to 595 in the mutagenized region, indicating that the tight clustering of the suppressor mutations is not an artifact of the PCR mutagenesis or *in vivo* recombination. Furthermore, the most common suppressor mutations were isolated in three independent selections; therefore it is unlikely that they were overrepresented in the mutant pool by chance.

Working from the collection of suppressor alleles, we generated *PRP8* alleles containing 15 different single amino acid substitutions at 12 positions between residues 222 and 314. We

refer to these collectively as "*prp8-tes*" alleles, for *twenty-eight-1 suppression*. The *prp8-tes* alleles were scored for their strength of suppression of *prp28-1* (Fig. 1B and Table 1). P263L and W279G gave stronger suppression when present in combination, as isolated in the selection, than when present individually. The previously isolated L280P substitution conferred a level of cold-resistant growth similar to that of the newly selected suppressors of *prp28-1*.

To assess the general effects of the suppressor substitutions on Prp8 function, we also tested the *prp8-tes* alleles for growth phenotypes in the presence of wild-type *PRP28*. The R226S substitution conferred a strong heat-sensitive growth defect at 37˚C, but supported normal growth at 16 and 30˚C (Fig. 1C). All other substitutions exhibited no qualitative growth defect at 16, 30, or 37˚C. Importantly, the *prp8-R226S*, *prp28-1* double mutant strain was not heat-sensitive (Fig. 1C), indicating that these two mutations mutually suppress one another.

Of the 12 residues altered by *prp8-tes* mutations, 9 are invariant in yeast, rice, fruit fly, worm, and human Prp8 (Fig. 1A), consistent with an important function. Intriguingly, the region encompassing the *prp8-tes* substitutions corresponds to a recently proposed bromodomain (BRD) in Prp8 (Dlakić and Mushegian 2011). Bromodomains bind acetylated lysine residues in histones and other proteins (Filippakopoulos and Knapp 2012). The putative Prp8 bromodomain lacks several residues important for acetylated-lysine binding (Dlakić and Mushegian 2011), and so may serve as a general protein-protein interaction domain instead. Strikingly, when the suppressor residues are mapped on the structural model of the bromodomain from Dlakić and Mushegian (2011) , the residues cluster tightly in the four alpha-helices of a helical bundle (Fig. 1D), in contrast to their dispersal in the primary structure. All but three of the 15 substitutions substantially alter the side chain structure, and thus are likely to destabilize the putative four-helix bundle itself and/or its interaction with another protein or RNA.

Substitutions in Prp8 that suppress *prp28-1* do not generally suppress U4-cs1

Since the original *prp28-1* suppressor, Prp8-L280P, was isolated in a selection for suppressors of the cold-sensitivity of U4-cs1, we hypothesized that mutations in the Prp8-NTD

that decrease reliance of the spliceosome on Prp28 may also counteract the effects of U4-cs1. To test this hypothesis, we assessed the ability of *prp8-tes* alleles to suppress U4-cs1. None other than L280P suppressed U4-cs1, nor did any suppress the cold-sensitive growth phenotype conferred by *brr2-1*, which blocks U4 release (Raghunathan and Guthrie 1998) (Fig 1E and data not shown). This result indicates that suppression of the growth defect of *prp28-1* is not sufficient for suppression of U4-cs1, and suggests that L280P is unusual in its ability to suppress both mutations.

prp8-tes substitutions do not promote U1/5'ss destabilization or alter the interaction of Prp8-NTD with Prp39, Prp40, or Prp28 _in vitro_

We next tested the hypothesis that disruption of Prp8-U1 snRNP interactions by the *prp8-tes* alleles could bypass the growth requirement for Prp28 function. The *prp8-tes* mutations cluster in a potential protein-protein interaction interface, and the Prp8-NTD is known to interact with U1 snRNP proteins Prp39 and Prp40 (Abovich and Rosbash 1997; van Nues and Beggs 2001). Further, Prp28 is nonessential in the presence of mutations in U1 snRNP proteins or the U1 snRNA that are expected to destabilize the U1/5'ss interaction (Chen et al. 2001; Hage et al. 2009; Schwer et al. 2013). Therefore, if loss of Prp8-U1 interactions similarly leads to destabilization of U1 snRNP from the 5'ss, they might bypass the requirement for Prp28. However, we found that a *prp8-tes* allele did not rescue the lethality caused by a complete absence of Prp28 protein or by a substitution predicted to destroy the catalytic activity of Prp28 (*prp28-D341N*; Fig. 2A). Nor did a *prp8-tes* allele suppress the low-temperature growth defect caused by hyperstabilization of U1/5'ss base-pairing (Fig. 2B). These results indicate that *prp8-tes* alleles do not significantly destabilize the U1/5'ss interaction.

To more directly test the effect of *prp8-tes* alleles on binding of the Prp8-NTD to Prp39 or Prp40, we used in vitro binding assays. An N-terminal fragment of Prp8 (Prp8 residues 1-330) with an N-terminal glutathione S-transferase (GST) tag and either wild-type sequence or one of three *prp8-tes* substitutions was expressed in *E. coli*. Full-length Prp39 and Prp40 with

C-terminal His_6 tags were also expressed in *E. coli*. Using a standard GST pull-down method, we reproduced the known interactions of the Prp8-NTD with Prp39 and Prp40. However, wild-type Prp8-NTD and the three *prp8-tes* alleles all pulled down similar amounts of both Prp39 and Prp40 (Fig. 2C). Taken together, our results indicate that *prp8-tes* alleles suppress *prp28-1* by a means other than altering interactions between Prp8 and Prp39 or Prp40, or by directly promoting destabilization of the U1/5'ss interaction.

If the *prp8-tes* mutations are not suppressing *prp28-1* indirectly by destabilizing the U1 snRNP-5' splice site interaction, they may be acting directly by altering a Prp8-Prp28 interaction. Although a direct interaction between Prp28 and the Prp8-NTD has not been reported, we were able to detect binding by GST pull-down using moderately stringent wash conditions (200 mM KOAc at room temperature). However, the *prp8-tes* substitutions did not alter that interaction under the conditions of our assay (Figure 2D). These results do not exclude the possibility that the *prp8-tes* substitutions alter Prp8-Prp28 interactions in a way that alters regulation of Prp28 activity by Prp8.

A *prp8-tes* allele partially suppresses the *prp28-1* global splicing defect

To measure the effect of a *prp8-tes* mutation on the global splicing defect caused by *prp28-1 in vivo*, we used splicing-specific DNA microarrays (Pleiss et al. 2007). The *prp8-tes* strain *P263L/W279G* was chosen for this and subsequent assays, as it displays strong suppression of the *prp28-1* growth defect. Cy3- or Cy5-labeled cDNA was made from total cellular RNA isolated from wild-type, *prp28-1*, *prp8-tes*, or *prp28-1/prp8*-tes double-mutant strains, then was competitively hybridized to DNA microarrays as indicated in Figure 3.

Genome-wide splicing improved in the *prp28-1/prp8-tes* strain relative to *prp28-1* alone. The *prp28-1* strain exhibited a broad splicing defect at 16˚C, characterized by increases in intron levels and decreases in spliced RNA levels relative to wild-type, consistent with our previous report (Pleiss et al. 2007) (Fig. 3, lanes 6 and 10). The *prp8-tes* strain by itself behaved similarly to wild-type (lanes 1, 5 and 9), as expected given its lack of growth defect. Suppression

of the *prp28-1* splicing defect can be seen by comparing the *prp28-1* vs. wild-type pattern to the *prp28-1*/*prp8-tes* vs. wild-type pattern (compare lanes 6 and 7), or by directly testing suppression on the array by competitively hybridizing cDNA from *prp28-1* against cDNA from *prp28-1*/*prp8-tes* (lanes 4, 8 and 12). Intron-containing RNA accumulated to some extent in the suppressed double mutant relative to wild-type (lane 7). A mild level of suppression is consistent with the incomplete suppression of the *prp28-1* growth defect (Fig. 1B).

U2 snRNP joining and subsequent steps of spliceosome assembly are inhibited by *prp28-1 in vivo*

In order to determine the precise defect in the *prp28-1* strain that is suppressed by *prp8-P263L/W279G*, we monitored the kinetics of co-transcriptional spliceosome assembly in *prp28-1* and *prp28-1/prp8-tes* strains using chromatin immunoprecipitation (ChIP). We measured the occupancy of several HA-tagged splicing factors (representatives of the U1, U2, and U5 snRNPs and of the NTC) at five positions along an intron containing gene, *ECM33*. As pre-mRNA is synthesized, splicing factors bind and can be crosslinked to nearby DNA. Thus, the position of crosslinking along a gene can be used as a readout for splicing factor association with the nascent pre-mRNA (Kotovic et al. 2003; Görnemann et al. 2005; Lacadie and Rosbash 2005) (Fig. 4A). To compare spliceosome assembly at permissive and non-permissive temperatures, cultures were grown at 30˚C, then divided and incubated at either 30˚C or 16˚C for 45 minutes.

Our results for a wild-type strain at 30˚C are consistent with previous reports (Görnemann et al. 2005; Lacadie and Rosbash 2005). U1 snRNP association peaked near the region of *ECM33* DNA that corresponds to the 3'ss, then decreased by 500 bp downstream to a level similar to that at the 5'ss, consistent with release of the U1 snRNP upon activation of the spliceosome (Fig. 4B, black). U2 snRNP occupancy was highest near the 3'ss, then slowly decreased over the next 1000 bp (Fig. 4C). U5 and NTC associations were similar: they peaked over the second exon, consistent with tri-snRNP and NTC addition following U2 snRNP binding

(Figs. 4D and 4E). When wild-type cultures were shifted to 16˚C prior to crosslinking for ChIP, the patterns of U1 snRNP and NTC binding were similar to those at 30˚C (Suppl. Fig. 1). U2 and U5 snRNP associations were slightly delayed compared to 30˚C but reached similar maximum levels (Suppl. Fig. 1).

The *prp28-1* strain shifted to restrictive temperature (16˚C) yielded a dramatically different ChIP pattern (Fig. 4B-E, orange). In agreement with the function of Prp28 in displacing the U1 snRNP from the 5'ss, we observed persistence of the U1 snRNP signal in the *prp28-1* background up to 1500 bp downstream of the 5'ss (Fig. 4B). This delayed release was most pronounced at 16˚C, but was evident even at permissive temperature (30˚C). U2 snRNP recruitment was predicted to be unaltered by the *prp28-1* mutation because the U2 snRNP is thought to bind the branch point well before Prp28 removes the U1 snRNP from the 5'ss (reviewed in Will and Lührmann 2011). Surprisingly, shifting the *prp28-1* strain to 16˚C caused a pronounced delay in U2 snRNP recruitment and decreased the maximum U2 snRNP signal (Fig. 4C). We also observed a severe delay in U5 snRNP binding at 16˚C: the highest signal was at the end of the gene and was well below the peak signal observed at 30˚C (Fig. 4D). This finding was confirmed by analyzing the U5 snRNP pattern along *SEC27*, a gene with a longer second exon than *ECM33* (Supplemental Fig. 2). We conclude that *prp28-1* causes a delay in recruitment of the U2 and tri-snRNPs to introns *in vivo*.

The *prp28-1* strain exhibited even more dramatically delayed/reduced association of NTC, even at permissive temperature (Fig. 4E). The NTC joins the spliceosome soon after the tri-snRNP (Hoskins et al. 2011), and appears to be more stably associated after the U4 snRNP is released from the tri-snRNP (Fabrizio et al. 2009). Thus, the result that the NTC is even more sensitive to *prp28-1* is consistent with the allosteric cascade model, which posits that later binding events are dependent on conformational changes induced by earlier binding events (Brow 2002). Similarly, the inhibition of U2 snRNP joining by *prp28-1* may be a consequence of decreased commitment complex 2 formation (see below).

The *prp8-tes* allele partially suppressed all of the co-transcriptional assembly defects caused by *prp28-1* at the non-permissive temperature. U1 snRNP release was still somewhat delayed in the *prp28-1/prp8-tes* strain, but substantially less so than in the absence of the suppressor mutation (Fig. 4B). A corresponding increase in the rate and magnitude of recruitment of U2 snRNP, U5 snRNP, and NTC was observed at 16˚C (Fig. 4C-E). The ability of *prp8-tes* to suppress the U2 association defect suggests that Prp8, a component of the tri-snRNP, can influence a step of splicing that occurs prior to tri-snRNP incorporation into the spliceosome.

U2 and tri-snRNP association are inhibited by *prp28-1 in vitro*, and inhibition is suppressed by *prp8-tes*

To determine whether the effects of *prp28-1* and *prp8-tes* on U2 snRNP and U5 snRNP association also occur in the absence of chromatin and transcription, we monitored the kinetics of spliceosome assembly *in vitro* at 16˚C (Fig. 5). snRNP association with biotinylated pre-mRNA as a function of time was determined by streptavidin affinity purification followed by RT-qPCR for each snRNA. All five snRNPs associated rapidly with pre-mRNA in wild-type splicing reactions, reaching maximum accumulation at 5-15 minutes. Using a pull-down procedure with low stringency washes to maintain U1 snRNP association, we were able to see that *prp28-1* blocks release of U1 snRNP in vitro (Fig. 5A), as proposed but not directly observed previously (Staley and Guthrie 1999). At most time points, about 2-fold more U1 was pulled down from reactions containing *prp28-1* extract than from reactions containing wild-type extract (Fig. 5A). We also confirmed the previous report that U4 is released in wild-type reactions but retained in *prp28-1* reactions at late time points (Fig. 5B, Staley and Guthrie 1999). Consistent with our *in vivo* ChIP results, we found that association of U2, as well as U5 and U6, was inhibited in reactions containing *prp28-1* relative to wild-type (Fig 5C-E). The accumulation of excess U4 RNA in spliceosomes assembled in *prp28-1* extract, despite the decreased level of U5 and U6 RNAs, implies that decreased tri-snRNP recruitment is accompanied by decreased Brr2 activity

and thus increased U4 snRNP retention, as observed previously (Staley and Guthrie 1999). Our *in vivo* and *in vitro* results suggest that Prp28 has at least two functions: one important for early spliceosome assembly, affecting U2 and subsequent tri-snRNP association with pre-mRNA, and one required for U1 and U4 release after spliceosome assembly.

The *prp8-tes* allele was able to suppress most of the in vitro spliceosome assembly defects (Fig. 5A-E, green). Importantly, the reduction in U2 snRNA pull-down was completely suppressed, which indicates that the functional role of Prp8 early in spliceosome assembly is not specific to co-transcriptional spliceosome assembly. The defects in U5 and U6 binding and U4 release were also partially suppressed. However, U1 release was not improved in the *prp28-1*/*prp8-tes* double-mutant extract (see Discussion).

***prp28-1* inhibits ATP-independent CC2 formation**

The surprising *in vivo* and *in vitro* defect in U2 snRNP recruitment caused by *prp28-1* could result from inhibition of an even earlier assembly step, so we investigated commitment complex and pre-spliceosome formation directly. Splicing reactions with radiolabled RP51A pre-mRNA were incubated at non-permissive temperature (16˚C) and run on native gels that resolve CC1 from CC2 (Seraphin and Rosbash 1989, 1991). Wild-type splicing reactions depleted of ATP formed roughly equal amounts of CC1 and CC2, and very little pre-spliceosome or spliceosome (P/SP – these complexes co-migrate) (Fig. 6, lane 1). Addition of ATP and incubation for an additional 20 minutes converted most of the CC2 into P/SP (Fig. 6, lane 5). In contrast, *prp28-1* splicing reactions without ATP accumulated the majority of pre-mRNA in CC1 (Fig. 6, lane 3), and the CC1 band appeared more diffuse. Upon addition of ATP to the *prp28-1* splicing reaction, only about half as much pre-mRNA was converted to P/SP than was with wild-type extract, and most of the pre-mRNA that remained in commitment complexes remained in CC1 (Fig. 6, lane 7). Thus *prp28-1* not only inhibits U2 snRNP joining but also reduces BBP and Mud2 association with CC1 (see Fig. 4A). The decrease in U2 joining, seen in this assay and in Figures 4 and 5, is thus likely a downstream result of inefficient CC2 formation.

Splicing is not completely blocked at 16˚C by the *prp28-1* mutation (Strauss and Guthrie 1991 and data not shown), so we repeated the commitment complex gels with extracts from a strain in which Prp28 expression can be turned off by growth in glucose-containing media (P. Raghunathan and C. Guthrie, unpublished). After 3.5-5 hours of growth in the presence of glucose, splicing extract made from these cells no longer contained HA-tagged Prp28 detectable by Western blot for HA and failed to splice at 16˚C (data not shown). This extract formed even less CC2 (-ATP) and subsequent splicing complexes (+ATP) than *prp28-1* extract (Fig 6, lanes 9-10). This result confirms that Prp28 contributes to the ATP-independent formation of CC2, and shows that the defect in CC2 formation is not specific to the *prp28-1* allele.

We also assayed the ability of *prp8-tes* to suppress the *prp28-1* defects in CC2 and pre-spliceosome formation (Fig. 6, lanes 4 and 8). Only partial suppression was observed, but *prp8-tes/prp28-1* extract reproducibly formed CC2 and pre-spliceosome better than *PRP8/prp28-1* extract. Therefore, Prp8, in addition to Prp28, influences this ATP-independent step of spliceosome assembly.

Discussion

A novel, ATP-independent function of Prp28 in CC2 formation

Here we have shown that the DEAD-box ATPase Prp28 has an unanticipated function early in spliceosome assembly. Specifically, we found that Prp28 promotes formation of CC2 prior to the first ATP-dependent step of splicing, since ATP-depleted splicing reactions containing *prp28-1* or depleted of Prp28 accumulated CC1 instead of CC2 (Fig 6). We also observed *prp28-1*-dependent decreases in U2 and tri-snRNP association *in vitro* and *in vivo*, which are likely downstream effects of the failure to efficiently or stably form CC2 (Figs. 4 and 5). Previous studies on Prp28 indicated that it acts during spliceosome activation to promote U1 snRNP release (Staley and Guthrie 1999; Chen et al. 2001; Ismaili et al. 2001), and our current

results confirm this conclusion. Therefore, we propose a model in which Prp28 has at least two roles during spliceosome assembly and activation: one ATP-independent role in which Prp28 helps stabilize U1, BBP, and Mud2 on the pre-mRNA during CC2 formation, and a subsequent ATP-dependent role in which Prp28 facilitates the release of U1 following tri-snRNP association (Fig. 7).

Prp28 is an essential gene, but becomes non-essential in the presence of mutations predicted to destabilize the U1/5'ss interaction and facilitate U1 release independent of Prp28 (Chen et al. 2001; Hage et al. 2009; Schwer et al. 2013). Therefore, while Prp28 strongly stimulates CC2 formation on the gene we tested, it is likely not absolutely required for this assembly step. Indeed, cells that have lost *PRP28* in the presence of the *yhc1-1* bypass mutant grow very slowly (Fig. 2B), consistent with the low level of CC2 formation we observed in extract depleted of Prp28 (Fig. 6).

It is not surprising that a substitution in a conserved helicase motif of Prp28 inhibits its ATP-dependent function in U1 snRNP displacement, but why would this substitution affect an ATP-independent role in CC2 formation? Motif Ib, in which the *prp28-1* substitution lies, is implicated in RNA-binding (Fairman-Williams et al., 2010), and so may influence the ATP-independent interaction with an RNA substrate.

The DEXD/H-box splicing factors Prp5 and Sub2 also have both ATP-dependent and ATP-independent roles in spliceosome assembly. Prp5 uses ATP hydrolysis to promote rearrangements in the U2 snRNP that allow U2 RNA to base-pair with the branchsite, but it first helps recruit U2 to the pre-mRNA in an ATP-independent manner (Perriman et al. 2003; Xu et al. 2004; Kosowski et al. 2009). In addition, extracts depleted of Prp5 are less able to form commitment complexes (Kosowski et al. 2009). Sub2 uses ATP hydrolysis to release BBP and Mud2 during pre-spliceosome formation (Kistler and Guthrie 2001; Libri et al. 2001), but is also required for CC2 formation: depletion of Sub2 results in spliceosomes that are stalled at CC1 (Zhang and Green 2001). Our finding that Prp28 promotes CC2 formation suggests that Prp28,

Sub2, and Prp5 all collaborate to promote formation of CC2, whose components they later destabilize.

Substitutions in the U5 snRNP protein Prp8 promote formation of early spliceosomal complexes

Our finding that substitutions in the N-terminus of Prp8, an integral U5 snRNP and tri-snRNP protein, suppress the early assembly defects caused by *prp28-1*, supports the hypothesis that the U5 snRNP functions in the earliest steps of spliceosome assembly, prior to its stable incorporation into the spliceosome. We identified 15 "*prp8-tes*" substitutions spanning a recently proposed bromodomain in the N-terminus of Prp8, each of which partially suppressed the cold-sensitive growth defect of a *prp28-1* strain. We tested one of the strongest *prp8-tes* alleles in subsequent assays, and it was able to partially suppress every *prp28-1* splicing defect discussed above, including the CC2 and pre-spliceosome formation defects (Figs. 4-6), except the in vitro U1 snRNP release defect (Fig. 5A). Suppression of the U1 snRNP release defect could be substrate dependent, or could require that additional factors specific to co-transcriptional splicing collaborate with Prp8 and Prp28 to promote U1 release *in vivo*. The strongest *prp8-tes* allele did not bypass the growth requirement for Prp28 nor did it physically interact differently with two U1 snRNP proteins or suppress the growth defect caused by hyperstabilizing U1/5'ss base-pairing (Fig. 2). Together, our results indicate that *prp8-tes* suppresses *prp28-1* by promoting formation of early splicing complexes, not by destabilizing U1 from the spliceosome.

The finding that substitutions in Prp8 suppress the earliest spliceosome assembly defects caused by *prp28-1* raises the intriguing possibility that both Prp28 and Prp8 act on CC1 in the context of the U5 snRNP. Yeast Prp28 is associated only weakly with U5 snRNP (Gottschalk et al. 1999; Stevens et al. 2001; Small et al. 2006), and our results do not determine whether it promotes CC2 formation as a component of the U5 snRNP or tri-snRNP or as a free protein. Prp8, however, is an integral component of both the U5 snRNP and tri-snRNP and is

unlikely to exist as free protein, so it presumably acts as part of the U5 snRNP or tri-snRNP when influencing CC2 formation. Whether the U5 snRNP or the tri-snRNP interact with the pre-mRNA early in spliceosome assembly has been a controversial topic in the splicing field. Several prior observations are consistent with an early, transient, role for Prp8 and the U5 snRNP. In vitro crosslinking data place the U5 snRNA and Prp8 at the 5'ss at early timepoints in the splicing cycle, both in human (Wassarman and Steitz 1992; Wyatt et al. 1992; Ast and Weiner 1997) and yeast (Newman et al. 1995) cell extracts. Also, affinity-purified human pre-spliceosomes contain U5 snRNP proteins, including Prp28 (Hartmuth et al. 2002). Further characterization of an early interaction between Prp8 and the 5'ss showed that it required intact U4 and U6 RNAs and ATP, but was independent of U2 snRNP binding to the branch point (Maroney et al. 2000). Therefore, tri-snRNP/pre-mRNA interactions apparently occur prior to U2 binding. However, more recent ChIP and single-molecule studies found that, in wild-type yeast cells or yeast cell extract, spliceosome assembly usually takes place in a step-wise sequence according to the canonical assembly pathway (Kotovic et al. 2003; Görnemann et al. 2005; Lacadie and Rosbash 2005; Lacadie et al. 2006; Hoskins et al. 2011). These latter studies showed that the spliceosome is unlikely to bind an intron as a pre-formed penta-snRNP, but they do not rule out the transient U5-U1-pre-mRNA interactions that are suggested by our results and others.

While our results implicate the U5 snRNP in early spliceosome assembly events, we cannot rule out the possibility that Prp28 promotes CC2 formation as a free protein and the *prp8-tes* substitutions destabilize Prp28-U5 snRNP interactions, thereby increasing the pool of free Prp28 and compensating for reduced Prp28 function. We found that the N-terminal domain of Prp8 binds Prp28 *in vitro*, and the *prp8-tes* alleles do not alter the pull-down of Prp28 with Prp8-NTD (Fig. 2D). However, *prp8-tes* alleles could interact differently with Prp28 in the context of full length Prp8 and the U5 snRNP. Alternatively, the *prp8-tes* mutations may alter interactions in the Aar2-U5 snRNP, which is a precursor of the U5 snRNP that lacks Brr2 and

co-purifies with the U1 snRNP (Gottschalk et al. 2001; Weber et al. 2011). If the U1 snRNP's interaction with the Aar2-U5 snRNP competes with stable CC2 formation, weakening this interaction via substitutions in Prp8 could promote CC2 formation.

Prp8 as a master regulator of spliceosome assembly

Prp8 sits at the heart of the spliceosome starting from the time the tri-snRNP binds until after the second step of catalysis, has an extensive set of physical and genetic interactions with other spliceosome components, and has been shown to regulate Brr2 for U4/U6 unwinding (Maeder et al. 2008; Mozaffari-Jovin et al. 2012, 2013). Because of these many interactions, Prp8 is perfectly situated to be a master regulator of spliceosome assembly, activation, and disassembly. Here, we have shown that substitutions in the N-terminus of Prp8 promote CC2 and pre-spliceosome formation in a *prp28-1* background. Thus, Prp8 may also regulate the earliest steps of spliceosome assembly, even before stable tri-snRNP joining. This regulation could be through physical contacts that Prp8 makes with U1 snRNP proteins or the U1 snRNA (Li et al. 2013), although the Prp8/U1 protein interactions tested here were not affected by *prp8-tes* alleles (Fig. 2). Prp8 may also exert its influence on this step by regulating the activity of Prp28, for example by switching Prp28 between two states: one that promotes a U1 conformation that is favorable for CC2 formation, and one in which Prp28's ATPase activity is activated to promote U1 release after tri-snRNP joining. Additional structural and biochemical studies will be required to discriminate between such possibilities.

Materials and Methods

Yeast strains

Yeast strains used in this study are listed in Supplementary Table 1. For strains JG111-JG116 and JG121-JG126, a C-terminal HA_6 tag was added to splicing factors by one-step gene replacement using *K. lactis TRP1* as a selection marker (Knop et al. 1999). Wild-type strains for ChIP are as described (Görnemann et al. 2011). Strains JG110/AMP27 and JG120/AMP28

were generated by replacing YCp50-PRP8 in ANK828 with pRS313-PRP8 (Kuhn and Brow 2000) or pRS313-prp8-P263L/W279G by plasmid shuffle. AMP25 and AMP26 were generated by crossing ANK828 to EJS54 (a gift from E. Strauss: wild-type sister spore of the parent strain of ANK828, EJS51 (Strauss and Guthrie 1991)) and selecting for *prp8Δ::ADE2 PRP28* spores, then replacing YCp50-PRP8 with pRS313-PRP8 or -*prp8-P263L/W279G* by plasmid shuffle.

Selection for suppressors of *prp28-1* in *PRP8*

We used error-prone PCR and gap repair as described previously (Umen and Guthrie 1996) to introduce mutations into the first quarter of the *PRP8* gene. A region of pRS313-*PRP8* including 233 bp of vector sequence as well as 719 bp upstream of the *PRP8* open reading frame and the first 1980 bp of the open reading frame were amplified with Taq DNA polymerase and co-transformed into ANK828 with pRS313-*PRP8* that was gapped by restriction digest with *Xho*I and *Sal*I between bp (-717) and bp 1715 relative to the start codon. Functional *PRP8* alleles were selected by their ability to lose the wild-type copy of *PRP8* on medium containing 5-FOA, then suppressors of *prp28-1* were selected by replica plating to YEPD and incubating at 16˚C. Colonies present after 14 days were transferred to fresh medium. Plasmids were isolated from clones that had grown at 16˚C within 10 days, their suppression capacity confirmed by re-transforming ANK828, and then sequenced from 50 bp upstream of the Prp8 open reading frame to codon 660 to identify mutated residues. Three independent selections were performed. The *Apa*I/*Sal*I fragments (bp -726 to +1715) were subcloned into pRS313-*PRP8* to ensure that suppression was due to mutations within this region. Selected mutations from clones with more than one amino acid substitution were introduced into pRS313-*PRP8* as single substitutions using the QuikChange technique (Stratagene) and analyzed for their ability to suppress the cold-sensitivity of *prp28-1*. All suppressor alleles were also introduced into ANK800 (wild-type), ZRL102 (U4-cs1) and ANK821 (brr2-1) and the wild-type allele of *PRP8* was shuffled out to test for genetic interactions. Growth at different temperatures was assayed by spotting 10-fold serial dilutions of OD_{600} = 0.25 cultures on solid YEPD medium, followed by incubation as indicated.

Test for bypass suppression of *prp28-1*

Strain JG140 was constructed by one-step gene disruption of the *PRP28* locus in strain JG120, using the PCR amplified kanMX6 cassette of pYM1 (Knop et al. 1999) adding 45 bp homologous overhangs to delete bp -2 to +1650 of the *PRP28* locus. The PCR product was co-transformed with *YCp50-PRP28*. Resulting strains were transformed with *pRS317-PRP28, pRS317-prp28-D341N* or *pRS317-yhc1-1* to create strains JG141, JG142, and JG144. Ten-fold serial dilutions of OD_{600} = 0.25 cultures were then plated onto YEPD or YEPD + 5-FOA to select for loss of *YCp50-PRP28* and grown at 30°C.

Test for suppression of U1/5'ss hyperstabilization

A *prp8Δ::LYS2* strain, TB72 (a gift from T. Brenner), was crossed to a *cup1Δ::ura3-52* strain, YS72 (Burgess and Guthrie 1993), and a *prp8Δ, cup1Δ* spore was selected. This strain, AMP24, was transformed with pRS313-PRP8 or -*prp8-P263L/W279G*, and with Act1-Cup1 splicing reporters (Lesser and Guthrie 1993) pCG90 (wild-type)or pCG91 (5'ss modified to extend U1/5'ss base-pairing to 10 bp) (Staley and Guthrie 1999), generating AMP39-42. Cultures were grown to OD_{600} 0.6, diluted back to OD_{600} 0.1, and 5-fold serial dilutions were plated onto SD -Ura medium with varying concentrations of copper and were grown for 6 days at 16 °C.

GST pull-down assay to test *in vitro* protein-protein interactions

Prp28 protein was expressed in *E. coli* BL21(DE3) RIPL (Agilent) from plasmid pRSetA-Prp28 (a gift from Nils Walter), in which Prp28 has a C-terminal His_6 tag. 3 L of bacteria containing the Prp28 plasmid were grown to OD_{600} 0.6 and induced with 1 mM IPTG at 18˚C for 15 hours. Cells were harvested and frozen at -80˚C. Cells were then resuspended in 50 mM NaH_2P0_4 (pH 8.0), 300 mM NaCl, 5 mM β-mercaptoethanol, 10 mM imidazole and sonicated in five 30 second bursts at 10% intensity with 30 second rests. Lysate was clarified for 30 minutes at 20,000 RPM in a JA25.5 rotor, then the supernatant was passed through a 0.22 μM filter and flowed over a column of Ni-NTA Agarose (Qiagen). Beads were washed with 50 mM NaH_2PO_4,

300 mM NaCl, 5 mM β-mercaptoethanol, and 20 mM imidazole (pH 8), then a second wash with imidazole increased to 36 mM. Prp28 protein was eluted with 50 mM NaH_2PO_4, 300 mM NaCl, 5 mM β-mercaptoethanol, and 250 mM imidazole (pH 8.0), then dialyzed into 20% glycerol, 100 mM KCl, 20 mM HEPES (pH 7.9), 0.2 mM EDTA, 0.5 mM DTT and stored at -80°C.

Full length Prp39 and Prp40 were tagged with His_g by cloning into pET21b (Novagen) at the *Bam*HI and *Xho*I restriction sites. Prp39 and Prp40 proteins were expressed in *E. coli* Rosetta strain (Novagen) by growing 100 ml LB cultures to OD_{600} 0.8 and then inducing with 400 µM IPTG for 3 hr at 30˚C. Cells were harvested, washed once with 1x PBS pH 7.2, resuspended in 1.5 ml lysis buffer (according to Qiagen protocol for native conditions) and frozen at -20˚C. After thawing, lysozyme was added to 1 mg/ml and cells were sonicated in two 15 sec bursts at 25% intensity, with a 30 sec break. His_6-fusion Prp39 and Prp40 were batch purified with Ni-NTA Agarose (Qiagen), following the manufacturer's protocol for native conditions, and stored at 4°C.

Prp8-NTD (1-330) was GST-tagged by cloning into pGEX-KG (Guan and Dixon 1991) at the *Xma*I and *Xho*I restriction sites. GST-Prp8-NTD was expressed as described for Prp39 and Prp40, except 100 µM IPTG was used for induction and the cell pellet was resuspended in pull-down buffer (20 mM Hepes pH 7.2, 200 mM potassium acetate, 2 mM magnesium acetate, 0.5% Tween 20, 1 mM DTT). After two clearing spins at 4°C (10 min each at 10,000 rcf), GST-Prp8-NTD lysate was frozen in liquid nitrogen and stored at -80°C for up to 3 months. For pull-downs, 100 µl of GST fusion protein lysate per sample was added to 25 µl of a 50% slurry of glutathione-Sepharose 4 fast flow (GE Healthcare). For Prp28 pull-downs, 25 µl of GST fusion protein plus 75 µl pull-down buffer was used. GST fusion protein was shown to be in saturating amounts by checking the supernatant by Western blot for residual GST-tagged protein after incubation (data not shown). Following 1 hr incubation at 4˚C, supernatants were removed, the beads were washed twice with pull-down buffer and used for the pull-down assay. Purified His_6-fusion proteins were added in 350 µl pull-down buffer and incubated for 3 hr at 4°C with rotation.

Beads were then washed 4x with pull-down buffer (4°C for Prp39 and Prp40, room temperature for Prp28), spun for 1 minute at 750 rcf), and boiled with 30 µl 2x SDS sample buffer. Samples were analyzed by Western blot, detecting bound His_6-fusion Prp39 or Prp40 with mouse-anti-His_5 serum (Qiagen) then goat-anti-mouse IgG IR-Dye 680 (LI-COR Biosciences). Bound Prp28 was detected with anti-Prp28 antibody (Strauss and Guthrie 1994) then goat-anti-mouse-HRP secondary antibody (Biorad) and detected by Amersham ECL (GE Healthcare). Equal loading of GST-fusion proteins was checked either by Ponceau stain prior to blocking or detection with goat-anti-GST antiserum (Pharmacia) then donkey anti goat-HRP (Santa Cruz) and ECL.

Microarray analysis of *in vivo* splicing defects

Microarray samples were prepared essentially as in (Pleiss et al. 2007). Briefly, strains AMP25-28 were grown in YEPD at 30°C to OD_{600} 0.4-0.5 then shifted to 16˚C for 50 minutes. Cells from 15 ml of culture were collected by centrifugation. cDNA was prepared from 50 µg of total cell RNA using random 9-mer primers and labeled with Cy3 or Cy5. Labeled cDNA from each mutant was competitively hybridized to the array with cDNA from wild-type or another mutant as indicated in Figure 3. Arrays were analyzed as in (Plocik and Guthrie 2012). The results presented are the average of two biological replicates, each with a dye-flipped technical replicate. Array data are available at GEO (accession # GSE42754).

Chromatin immunoprecipitation and quantitative PCR (ChIP-qPCR)

ChIP-qPCR analysis of the genes *ECM33* and *SEC27* was done essentially as described (Görnemann et al. 2005). To crosslink splicing factors to DNA, 4.0 ml 37% formaldehyde solution was added to 150 ml yeast culture, incubated for 15 min at room temperature, then quenched by addition of 8.1 ml 2.5 M glycine. For parallel analyses at permissive and non-permissive temperatures, cells were grown in 200 ml YPD at 30˚C to an OD_{600} of 0.6 - 0.8. The cultures were divided and 100 ml added to 50 ml 30˚C YPD or 4°C YPD and incubated for 45 min at 30˚C or 16˚C, respectively, before crosslinking. Cells were harvested by centrifugation at 3500xg for 5 min, washed twice with PBS and then frozen. Cell

pellets were thawed on ice, resuspended in 1 ml buffer FA-1 (50 mM HEPES-KOH pH 7.5, 140 mM NaCl, 1 mM EDTA, 1% Triton-X 100, 0.1% sodium deoxycholate) and lysed on a Vortex Disruptor Genie with glass beads for 40 min at 4˚C at maximum speed. Lysates were recovered including 2 washes of the glass beads with 1 ml FA-1 each and subjected to sonication on ice to fragment the chromatin to an average of 500 bp. With the 250D Sonifier Ultrasonic Processor Cell Disruptor (Branson) used, this required 6 min of 15 sec on/off cycles at 30% intensity. Lysates were subsequently cleared by centrifugation at 3500xg for 5 min. Supernatants were cleared prior to immunoprecipitation by addition of 200 µl of a 50% slurry of Sepharose CL-4B beads (Sigma-Aldrich), previously washed with FA-1 buffer, and rotation at 4˚C for 1 h. Eight µg of 12CA5 antibody was then added to 700 µl of lysate, followed by rotation at 4˚C for 2h, then 50 µl of washed GammaBind G beads (GE Healthcare) were added for 1h. Mouse IgG (Sigma) served as a negative control. Beads were washed three times with buffer FA-1, once each with buffer FA-2 (FA-1 with 500 mM NaCl) and FA-3 (20 mM Tris-Cl pH 8.0, 250 mM LiCl, 0.5% NP-40, 0.5% sodium deoxycholate, 1 mM EDTA), and twice with TE buffer (pH 8.0), transferring the beads to a fresh tube. For elution and uncrosslinking, 250 µl TE/1% SDS was added followed by incubation at 65˚C overnight. In parallel, 20 µl of lysate in 200 µl TE/1% SDS was uncrosslinked to serve as input control. Eluates were transferred to a fresh tube, incubated with 10 µl Proteinase K (20 mg/ml) at 55˚C for 2 h and purified with a PCR purification kit according to instructions (Qiagen). The data in Figure 4 represent the average of three independent experiments, except: Prp42 (all strains): n=4; *prp28-1* - Brr2 at 16˚C and 30˚C: n=6; *prp28-1* + *prp8- P263L/W279G* - Brr2 at 16˚C and 30˚C: n=4; Msl1, Brr2, Prp19 in WT: n=4.

Primers used for ChIP-qPCR:

ECM-UP-F: GCAGTATCATCCTTCACGACCC; ECM-UP-R: GCGTCTTTCCCGTTTTTGC; ECM9-31: CAAGAACGCTTTGACTGCTACTG; ECM145-123: GAAGAGGACCACGAATCTACTCG; ECM430-451: ACTTCTGCCACTGCTACTGCTC; ECM562-539: AGGAACCATCAATCTCTTGGATAC; ECM1073-1097:

TTGGTCAATCTTTGTCTATCGTCTC; ECM1173-1150: TGTGTTGTTAGCAATGATGAAACC; ECM1531-1555: TCTAAGAAGTCTAAGGGTGCTGCTC; ECM1582-1561: TGAATGAAGTGGCTGGAACAAG; SEC280-304: GGGTTTTGACTACCTTGTACTCTGG; SEC370-349:GGAGTTTCCGTAACTTGGATGG; SEC931-950: TTTCTGGTTCCGAAGATGGC; SEC1043-1022: TGTTGGATGGGTAGCGATACAC; SEC1309-1330: TTGTTACAGTTGTTGGGGATGG; SEC1395-1372: CAAAGTCTTGACATTTACCGAAGG; SEC1969-1992: GAGAGGTCCATGTTTATGGTTACG; SEC2057-2037: AATGGCTTCTTCAATTTCCCC; SEC2599-2622: CTGTATCAGAAAGAGTTTGTGGGG; SEC2692-2669: GCTGGAGTGGAATCTAAGTCAATG

In vitro splicing extract preparation

2-3 L cultures of strains AMP25-28 were harvested at OD_{600} 1.7-1.9 and splicing extract was prepared as described (Umen and Guthrie 1995), except that frozen cell pellets were ground with a ball mill (Retch MM 301 mixer-mill; 3x 3 min at 11 Hz and 2x 3 min at 12 Hz) and dialyzed twice in 2 L buffer D. Prp28-depleted extract was made from strain PR88 (a gift from P. Raghunathan) in which genomic *PRP28* is deleted and complemented by a plasmid with the *GAL10* promoter controlling a copy of *PRP28* with a 3x HA tag inserted in the ClaI site near the start codon of *PRP28.* The strain was grown to an OD_{600} of 0.5-0.7 in YEP-galactose, then filtered and shifted to YEPD for 3.5-5 hr. Cells were collected and splicing extract prepared as above. Extracts were checked by Western blot with anti-HA antibody to confirm that Prp28 was no longer detectable.

Biotinylated pre-mRNA pull-down experiments

Biotinylated pre-mRNA pull-down experiments were adapted from previous protocols (Kuhn et al. 1999; Ruby et al. 1990; Staley and Guthrie 1999; Brenner and Guthrie 2006). ActinΔ6 pre-mRNA (Vijayraghavan et al. 1986) was synthesized with Megascript T7 RNA polymerase (Ambion) using biotin-11-UTP (Ambion) as 5% of the UTP. Seven pull-down time course experiments were conducted using 4 different extract preparations from each of the four

strains (AMP25-28). 120-140 µl splicing reactions were prepared. 1.9 µl was taken for a “0 minute input” sample, and in 3 experiments a 19 µl “no pre-mRNA” sample was removed to 50 µl stop buffer for background pull-down measurement (shown as “-5 minute” time point). Reactions were started by adding 2.5 fmol pre-mRNA/µl and ATP to 2 mM final concentration, and were incubated at 16°C. Twenty µl aliquots were removed at indicated times, added to 50 µl ice cold stop buffer (20 mM EDTA, 40% Buffer D, 60 mM KPO_4 pH 7, 3% PEG 8000), and incubated on ice until the end of the time course. A 2 µl “input” sample was taken at 30 minutes. 50 µl of streptavidin-agarose beads (Thermo Scientific) (50% slurry in stop buffer, after being blocked in stop buffer plus 10 µg/ml each glycogen, tRNA, and bovine serum albumin) were added to each reaction except inputs, and incubated at 4°C, rocking for 1 hr. For most experiments, 100 µl wash buffer (150 mM NaCl, 60 mM HEPES pH 7.6, 3 mM $MgCl_2$, 15% glycerol, 0.05% NP40, 0.5 mM DTT) was added before supernatant was removed. Beads were then washed 3x with 500 µl wash buffer. snRNAs and pre-mRNA were eluted by adding 50 µl formamide + 40 mM EDTA and incubating at 90°C for ~10 min followed by washing beads with 50 or 100 µl TE + 1% SDS. In two experiments, RNA was instead eluted from beads with Proteinase K as in Kuhn et al. 1999. Input samples were added to 5 µl stop buffer, and were incubated on ice until the elution step, at which point they were treated the same as pull-down samples. RNA was then phenol-chloroform extracted, ethanol precipitated, and resuspended in 20 µl H_2O. Eight µl RNA was reverse transcribed with primers specific to the snRNAs as described in Brenner and Guthrie 2006 and detected with qPCR as described, except the standard curve was generated from serial dilutions of a pool of input samples. qPCR values used are the average of 2-3 qPCR technical replicates.

qPCR values from each individual time course were normalized to the average of the respective 0 and 30 min input samples. All of the values in a single experiment (time courses with all 4 extracts done in parallel) were further normalized to the maximum value for that experiment, which allowed all experiments to be averaged together. In 3 of the experiments, 1

and 2 min time points were taken instead of 1.5 and 3 min. In order to include data from all repeats 1.5 and 3 min values were interpolated assuming a linear trend between 1 and 5 min. Similarly, in one experiment the 30 min value was interpolated from 25 and 50 min time points, and the 50 min measurement was used as an approximation of the 60 minute point. These interpolated values were included in data for Figure 2, but leaving them out did not significantly change the results. Including interpolated values, n=7 for 1.5, 3, 5, 10, 15, and 30 min, and n=6 for 60 min. Exceptions: wt 30 min: n=6, *prp8-tes* 30 min: n=6, *prp28-1* 5, 10, and 30 minute: n=6, *prp28-1/prp8-tes* 1.5 minute: n=6, background (no pre-mRNA added "-5 minute"): n=3. Error: SEM of final values after all described normalization.

Native gel analysis

Commitment complex gels were based on a published protocol (Seraphin and Rosbash 1989). Twenty-two µl standard splicing reactions (Lin et al. 1985) containing 8.8 µl of extract were depleted of ATP by adding glucose to 2 mM and incubating at 25°C for 20 min. 1-2 µl (~15 fmol, or ~30,000 cpm) radiolabeled RP51AΔ2 pre-mRNA (Seraphin and Rosbash 1991) was added to each reaction, and reactions were incubated for 20 min at 16°C. Ten µl was removed to 10 µl ice cold buffer R (2 mM MgOAc, 50 mM Hepes pH 7.5, 1 mg/ml tRNA, 50-fold molar excess cold Ubc4 or Actin pre-mRNA). Then ATP (to 2 mM) was added to the remaining reaction volume, and reactions were incubated for another 20 min at 16°C before the final 10 µl was removed to 10 µl ice cold buffer R. Five µl loading dye (2.5x TBE, 50% glycerol, bromophenol blue and xylene cyanol dyes) was added and the reaction was loaded on a 0.5x TBE, 3% acrylamide, 0.5% agarose, 5% glycerol gel, with a plug of 10% acrylamide gel at the bottom ~3 cm (1x TBE = 89 mM Tris-borate, 2 mM EDTA). The 26 cm gel was run in 0.5x TBE at 120 V for 20-24 hr at 4°C. Bands were detected by phosphorimager (Molecular Dynamics) and quantified with ImageQuant v.5.2 (Molecular Dynamics). Error bars in Figure 6 show SEM from n=5 (-ATP: prp28Δ), n=6 (+ATP: prp28Δ), n=8 (-ATP: wt, prp28-1, prp28-1/prp8-tes), n=9 (-ATP: prp8-tes), n=11 (+ATP: prp28-1/prp8-tes), or n=12 (+ATP: wt, prp8-tes, prp28-1)

replicates. To determine if the CC2:CC1 ratio was different between *prp28-1* and *prp28-1/prp8-tes*, we conducted a paired t-test, pairing reactions that were prepared together and run on the same gel.

Acknowledgements

We thank Karla Neugebauer for supporting the ChIP experiments, Thomas Hoffmann for data analysis advice, Matthew Kahlscheuer and Nils Walter for the Prp28 expression plasmid, members of the Brow and Guthrie labs for helpful suggestions, and Sam Butcher, Tien-Hsien Chang, Charles Query, and Joan Steitz for comments on the manuscript. This study was supported by an NSF GRFP fellowship to A.P., a postdoctoral fellowship from the Deutsche Forschungsgemeinschaft to J.G., and NIH grants to D.A.B and C.G. C.G. is an American Cancer Society Research Professor of Molecular Genetics. This paper is dedicated to the memory of Stephanie W. Ruby, who did pioneering studies on the role of U1 snRNP in spliceosome assembly.

References

Abovich N, Rosbash M. 1997. Cross-intron bridging interactions in the yeast commitment complex are conserved in mammals. *Cell* **89**: 403–412.

Ast G, Weiner AM. 1997. A novel U1/U5 interaction indicates proximity between U1 and U5 snRNAs during an early step of mRNA splicing. *RNA* **3**: 371–381.

Brenner TJ, Guthrie C. 2006. Assembly of Snu114 into U5 snRNP requires Prp8 and a functional GTPase domain. *RNA* **12**: 862–871.

Brow DA. 2002. Allosteric cascade of spliceosome activation. *Annu Rev Genet* **36**: 333–360.

Burgess SM, Guthrie C. 1993. A mechanism to enhance mRNA splicing fidelity: The RNA-dependent ATPase Prp16 governs usage of a discard pathway for aberrant lariat intermediates. *Cell* **73**: 1377–1391.

Chen JY-F, Stands L, Staley JP, Jackups Jr. RR, Latus LJ, Chang T-H. 2001. Specific alterations of U1-C protein or U1 small nuclear RNA can eliminate the requirement of Prp28p, an essential DEAD box splicing factor. *Mol Cell* **7**: 227–232.

Dlakić M, Mushegian A. 2011. Prp8, the pivotal protein of the spliceosomal catalytic center, evolved from a retroelement-encoded reverse transcriptase. *RNA* **17**: 799–808.

Fabrizio P, Dannenberg J, Dube P, Kastner B, Stark H, Urlaub H, Lührmann R. 2009. The evolutionarily conserved core design of the catalytic activation step of the yeast spliceosome. *Mol Cell* **36**: 593–608.

Fairman-Williams ME, Guenther U-P, Jankowsky E. 2010. SF1 and SF2 helicases: family matters. *Curr Opin Struct Biol* **20**: 313–324.

Filippakopoulos P, Knapp S. 2012. The bromodomain interaction module. *Febs Lett* **586**: 2692–2704.

Galej WP, Oubridge C, Newman AJ, Nagai K. 2013. Crystal structure of Prp8 reveals active site cavity of the spliceosome. *Nature* **493**: 638–643.

Görnemann J, Barrandon C, Hujer K, Rutz B, Rigaut G, Kotovic KM, Faux C, Neugebauer KM, Séraphin B. 2011. Cotranscriptional spliceosome assembly and splicing are independent of the Prp40p WW domain. *RNA* **17**: 2119–2129.

Görnemann J, Kotovic KM, Hujer K, Neugebauer KM. 2005. Cotranscriptional spliceosome assembly occurs in a stepwise fashion and requires the cap binding complex. *Mol Cell* **19**: 53–63.

Gottschalk A, Kastner B, Lührmann R, Fabrizio P. 2001. The yeast U5 snRNP coisolated with the U1 snRNP has an unexpected protein composition and includes the splicing factor Aar2p. *RNA* **7**: 1554–1565.

Gottschalk A, Neubauer G, Banroques J, Mann M, Lührmann R, Fabrizio P. 1999. Identification by mass spectrometry and functional analysis of novel proteins of the yeast [U4/U6|U5] tri-snRNP. *Embo J* **18**: 4535–4548.

Grainger RJ, Beggs JD. 2005. Prp8 protein: at the heart of the spliceosome. *RNA* **11**: 533–557.

Guan KL, Dixon JE. 1991. Eukaryotic proteins expressed in Escherichia coli: an improved thrombin cleavage and purification procedure of fusion proteins with glutathione S-transferase. *Anal Biochem* **192**: 262–267.

Hage R, Tung L, Du H, Stands L, Rosbash M, Chang T-H. 2009. A targeted bypass screen identifies Ynl187p, Prp42p, Snu71p, and Cbp80p for stable U1 snRNP/Pre-mRNA interaction. *Mol Cell Biol* **29**: 3941–3952.

Hartmuth K, Urlaub H, Vornlocher H-P, Will CL, Gentzel M, Wilm M, Lührmann R. 2002. Protein composition of human prespliceosomes isolated by a tobramycin affinity-selection method. *Proc Natl Acad Sci U S A* **99**: 16719–16724.

Hoskins AA, Friedman LJ, Gallagher SS, Crawford DJ, Anderson EG, Wombacher R, Ramirez N, Cornish VW, Gelles J, Moore MJ. 2011. Ordered and dynamic assembly of single spliceosomes. *Science* **331**: 1289–1295.

Ismaili N, Sha M, Gustafson EH, Konarska MM. 2001. The 100-kDa U5 snRNP protein (hPrp28p) contacts the 5' splice site through its ATPase site. *RNA* **7**: 182–193.

Kistler AL, Guthrie C. 2001. Deletion of MUD2, the yeast homolog of U2AF65, can bypass the requirement for Sub2, an essential spliceosomal ATPase. *Genes Dev* **15**: 42–49.

Knop M, Siegers K, Pereira G, Zachariae W, Winsor B, Nasmyth K, Schiebel E. 1999. Epitope tagging of yeast genes using a PCR-based strategy: more tags and improved practical routines. *Yeast* **15**: 963–972.

Kosowski TR, Keys HR, Quan TK, Ruby SW. 2009. DExD/H-box Prp5 protein is in the spliceosome during most of the splicing cycle. *RNA* **15**: 1345–1362.

Kotovic KM, Lockshon D, Boric L, Neugebauer KM. 2003. Cotranscriptional recruitment of the U1 snRNP to intron-containing genes in yeast. *Mol Cell Biol* **23**: 5768–5779.

Kuhn AN, Brow DA. 2000. Suppressors of a cold-sensitive mutation in yeast U4 RNA define five domains in the splicing factor Prp8 that influence spliceosome activation. *Genetics* **155**: 1667–1682.

Kuhn AN, Li Z, Brow DA. 1999. Splicing factor Prp8 governs U4/U6 RNA unwinding during activation of the spliceosome. *Mol Cell* **3**: 65–75.

Kuhn AN, Reichl EM, Brow DA. 2002. Distinct domains of splicing factor Prp8 mediate different aspects of spliceosome activation. *Proc Natl Acad Sci* **99**: 9145–9149.

Lacadie SA, Rosbash M. 2005. Cotranscriptional spliceosome assembly dynamics and the role of U1 snRNA:5′ss base pairing in yeast. *Mol Cell* **19**: 65–75.

Lacadie SA, Tardiff DF, Kadener S, Rosbash M. 2006. In vivo commitment to yeast cotranscriptional splicing is sensitive to transcription elongation mutants. *Genes Dev* **20**: 2055–2066.

Lesser CF, Guthrie C. 1993. Mutational analysis of pre-mRNA splicing in Saccharomyces cerevisiae using a sensitive new reporter gene, CUP1. *Genetics* **133**: 851–863.

Li X, Zhang W, Xu T, Ramsey J, Zhang L, Hill R, Hansen KC, Hesselberth JR, Zhao R. 2013. Comprehensive in vivo RNA-binding site analyses reveal a role of Prp8 in spliceosomal assembly. *Nucleic Acids Res* **41**: 3805–3818.

Libri D, Graziani N, Saguez C, Boulay J. 2001. Multiple roles for the yeast SUB2/yUAP56 gene in splicing. *Genes Dev* **15**: 36–41.

Lin RJ, Newman AJ, Cheng SC, Abelson J. 1985. Yeast mRNA splicing in vitro. *J Biol Chem* **260**: 14780–14792.

Maeder C, Kutach AK, Guthrie C. 2008. ATP-dependent unwinding of U4/U6 snRNAs by the Brr2 helicase requires the C terminus of Prp8. *Nat Struct Mol Biol* **16**: 42–48.

Maroney PA, Romfo CM, Nilsen TW. 2000. Functional recognition of the 5′ splice site by U4/U6.U5 tri-snRNP defines a novel ATP-dependent step in early spliceosome assembly. *Mol Cell* **6**: 317–328.

Mathew R, Hartmuth K, Möhlmann S, Urlaub H, Ficner R, Lührmann R. 2008. Phosphorylation of human PRP28 by SRPK2 is required for integration of the U4/U6-U5 tri-snRNP into the spliceosome. *Nat Struct Mol Biol* **15**: 435–443.

Mozaffari-Jovin S, Santos KF, Hsiao H-H, Will CL, Urlaub H, Wahl MC, Lührmann R. 2012. The Prp8 RNase H-like domain inhibits Brr2-mediated U4/U6 snRNA unwinding by blocking Brr2 loading onto the U4 snRNA. *Genes Dev* **26**: 2422–2434.

Mozaffari-Jovin S, Wandersleben T, Santos KF, Will CL, Lührmann R, Wahl MC. 2013. Inhibition of RNA Helicase Brr2 by the C-Terminal Tail of the Spliceosomal Protein Prp8. *Science* **341**: 80–84.

Newman AJ, Teigelkamp S, Beggs JD. 1995. snRNA interactions at 5’ and 3’ splice sites monitored by photoactivated crosslinking in yeast spliceosomes. *RNA* **1**: 968–980.

Pena V, Liu S, Bujnicki JM, Lührmann R, Wahl MC. 2007. Structure of a multipartite protein-protein interaction domain in splicing factor Prp8 and its link to retinitis pigmentosa. *Mol Cell* **25**: 615–624.

Pena V, Rozov A, Fabrizio P, Lührmann R, Wahl MC. 2008. Structure and function of an RNase H domain at the heart of the spliceosome. *Embo J* **27**: 2929–2940.

Perriman R, Barta I, Voeltz GK, Abelson J, Ares M. 2003. ATP requirement for Prp5p function is determined by Cus2p and the structure of U2 small nuclear RNA. *Proc Natl Acad Sci* **100**: 13857–13862.

Pleiss JA, Whitworth GB, Bergkessel M, Guthrie C. 2007. Transcript specificity in yeast pre-mRNA splicing revealed by mutations in core spliceosomal components. *Plos Biol* **5**: e90.

Plocik AM, Guthrie C. 2012. Diverse forms of RPS9 splicing are part of an evolving autoregulatory circuit. *Plos Genet* **8**: e1002620.

Raghunathan PL, Guthrie C. 1998. RNA unwinding in U4/U6 snRNPs requires ATP hydrolysis and the DEIH-box splicing factor Brr2. *Curr Biol* **8**: 847–855.

Ritchie DB, Schellenberg MJ, Gesner EM, Raithatha SA, Stuart DT, MacMillan AM. 2008. Structural elucidation of a PRP8 core domain from the heart of the spliceosome. *Nat Struct Mol Biol* **15**: 1199–1205.

Ruby SW, Goelz SE, Hostomsky Z, Abelson JN. 1990. Affinity chromatography with biotinylated RNAs. *Methods Enzymol* **181**: 97–121.

Schellenberg MJ, Wu T, Ritchie DB, Fica S, Staley JP, Atta KA, LaPointe P, MacMillan AM. 2013. A conformational switch in PRP8 mediates metal ion coordination that promotes pre-mRNA exon ligation. *Nat Struct Mol Biol* **20**: 728–734.

Schwer B, Chang J, Shuman S. 2013. Structure-function analysis of the 5′ end of yeast U1 snRNA highlights genetic interactions with the Msl5•Mud2 branchpoint-binding complex and other spliceosome assembly factors. *Nucleic Acids Res* **41**: 7485–7500.

Seraphin B, Rosbash M. 1989. Identification of functional U1 snRNA-pre-mRNA complexes committed to spliceosome assembly and splicing. *Cell* **59**: 349–358.

Seraphin B, Rosbash M. 1991. The yeast branchpoint sequence is not required for the formation of a stable U1 snRNA-pre-mRNA complex and is recognized in the absence of U2 snRNA. *Embo J* **10**: 1209–1216.

Shcherbakova I, Hoskins AA, Friedman LJ, Serebrov V, Corrêa Jr. IR, Xu M-Q, Gelles J, Moore MJ. Alternative Spliceosome Assembly Pathways Revealed by Single-Molecule Fluorescence Microscopy. *Cell Reports*. http://www.sciencedirect.com/science/article/pii/S2211124713004671 (Accessed October 9, 2013).

Small EC, Leggett SR, Winans AA, Staley JP. 2006. The EF-G-like GTPase Snu114p regulates spliceosome dynamics mediated by Brr2p, a DExD/H box ATPase. *Mol Cell* **23**: 389–399.

Staley JP, Guthrie C. 1999. An RNA switch at the 5′ splice site requires ATP and the DEAD box protein Prp28p. *Mol Cell* **3**: 55–64.

Stevens SW, Barta I, Ge HY, Moore RE, Young MK, Lee TD, Abelson J. 2001. Biochemical and genetic analyses of the U5, U6, and U4/U6 X U5 small nuclear ribonucleoproteins from Saccharomyces cerevisiae. *RNA* **7**: 1543–1553.

Strauss EJ, Guthrie C. 1991. A cold-sensitive mRNA splicing mutant is a member of the RNA helicase gene family. *Genes Dev* **5**: 629–641.

Strauss EJ, Guthrie C. 1994. PRP28, a “DEAD-box” protein, is required for the first step of mRNA splicing in vitro. *Nucleic Acids Res* **22**: 3187–3193.

Teigelkamp S, Mundt C, Achsel T, Will CL, Lührmann R. 1997. The human U5 snRNP-specific 100-kD protein is an RS domain-containing, putative RNA helicase with significant homology to the yeast splicing factor Prp28p. *RNA* **3**: 1313–1326.

Umen JG, Guthrie C. 1995. A novel role for a U5 snRNP protein in 3’ splice site selection. *Genes Dev* **9**: 855–868.

Umen JG, Guthrie C. 1996. Mutagenesis of the yeast gene PRP8 reveals domains governing the specificity and fidelity of 3' splice site selection. *Genetics* **143**: 723–739.

van Nues RW, Beggs JD. 2001. Functional contacts with a range of splicing proteins suggest a central role for Brr2p in the dynamic control of the prder of events in spliceosomes of Saccharomyces cerevisiae. *Genetics* **157**: 1451–1467.

Vijayraghavan U, Parker R, Tamm J, Iimura Y, Rossi J, Abelson J, Guthrie C. 1986. Mutations in conserved intron sequences affect multiple steps in the yeast splicing pathway, particularly assembly of the spliceosome. *Embo J* **5**: 1683–1695.

Wassarman DA, Steitz JA. 1992. Interactions of small nuclear RNA's with precursor messenger RNA during in vitro splicing. *Science* **257**: 1918–1925.

Weber G, Cristão VF, De L. Alves F, Santos KF, Holton N, Rappsilber J, Beggs JD, Wahl MC. 2011. Mechanism for Aar2p function as a U5 snRNP assembly factor. *Genes Dev* **25**: 1601–1612.

Will CL, Lührmann R. 2011. Spliceosome structure and function. *Cold Spring Harb Perspect Biol* **3**: a003707.

Wyatt JR, Sontheimer EJ, Steitz JA. 1992. Site-specific cross-linking of mammalian U5 snRNP to the 5' splice site before the first step of pre-mRNA splicing. *Genes Dev* **6**: 2542–2553.

Xu Y-Z, Newnham CM, Kameoka S, Huang T, Konarska MM, Query CC. 2004. Prp5 bridges U1 and U2 snRNPs and enables stable U2 snRNP association with intron RNA. *Embo J* **23**: 376–385.

Yang F, Wang X-Y, Zhang Z-M, Pu J, Fan Y-J, Zhou J, Query CC, Xu Y-Z. 2013. Splicing proofreading at 5′ splice sites by ATPase Prp28p. *Nucleic Acids Res* **41**: 4660–4670.

Yang K, Zhang L, Xu T, Heroux A, Zhao R. 2008. Crystal structure of the B-finger domain of Prp8 reveals analogy to ribosomal proteins. *Proc Natl Acad Sci* **105**: 13817–13822.

Zhang M, Green MR. 2001. Identification and characterization of yUAP/Sub2p, a yeast homolog of the essential human pre-mRNA splicing factor hUAP56. *Genes Dev* **15**: 30–35.

Table 1. Suppressors of *prp28-1* in the N-terminal quarter of Prp8

substitution	# of independent clones	isolated as single substitution	strength of suppression
I222R	1	1	+++
I222V	1	1	+
R226G	7	2	+++
R226S	1	0	++++
R229Q	1	0	+++
P263L	1	0*	++
I264R	1	0	++++
L266P	1	0	++
L268S	2	2	+++
D273G	16	8	++++
D273N	3	1	++++
W279G	1	0*	+++
L280P**	NA	NA	++
Y281C	1	0	++
L314S	1	0	+++
P263L/W279G	1	n.a.	++++

* P263L/W279G were isolated as double substitution.

** Identified previously (Kuhn et al. 2002)

Figures

Figure 1: Suppressors of *prp28-1* selected in the N-terminal quarter of Prp8. A) Map of Prp8, showing domains identified by sequence or structural homology (Grainger and Beggs 2005; Dlakić and Mushegian 2011; Galej et al. 2013). Numbers indicate amino acid residues. "BRD" refers to bromodomain-like (Dlakić and Mushegian 2011). The region that was screened for *prp28-1*-suppressor mutations and the sub-region in which such mutations were obtained are indicated. Sequences of human (H.s.), fly (D.m.), worm (C.e.), rice (O.s.) and budding yeast (S.c.) Prp8 are shown below, aligned in the region containing suppressor mutations, with the position number of the first residue and selected altered residues indicated. Residues highlighted in blue are identical in all five sequences, while those highlighted in yellow are highly similar. Substitutions that suppress *prp28-1* are shown in red below the alignment, and substitutions that suppress U4-cs1 (Kuhn and Brow 2000) are shown in black. Locations of putative alpha-helices (see panel D) are indicated above the sequences. **B)** *prp8-tes* alleles suppress the cold-sensitive growth defect of *prp28-1*. Ten-fold serial dilutions of wild-type, *prp28-1/PRP8,* and the indicated *prp28-1/prp8-tes* strains were spotted on YEPD medium and incubated at 16˚C for 10 days. **C)** The *prp8-R226S* mutation confers a heat-sensitive growth defect that is suppressed by *prp28-1*. Another substitution at the same position, *prp8-R226G*, is not heat-sensitive. Ten-fold serial dilutions on YEPD are shown. **D)** Location of *prp8-tes* substitutions mapped onto a structural model of the putative Prp8 bromodomain (model from Dlakić and Mushegian 2011). Residues altered by *prp8-tes* mutations are shown in red and selected residues and secondary structure elements are labeled. **E)** *prp8-tes* mutations do not suppress the cold-sensitive phenotype caused by mutations in *BRR2* or the U4 RNA gene. Ten-fold serial dilutions of strains were spotted on YEPD medium and incubated at 16˚C for 10 days, except for U4-cs1 strains (18˚C for 12 days). Controls *prp8-L280P* and *prp8-V1098D* behaved as in (Kuhn et al. 2002).

Figure 1

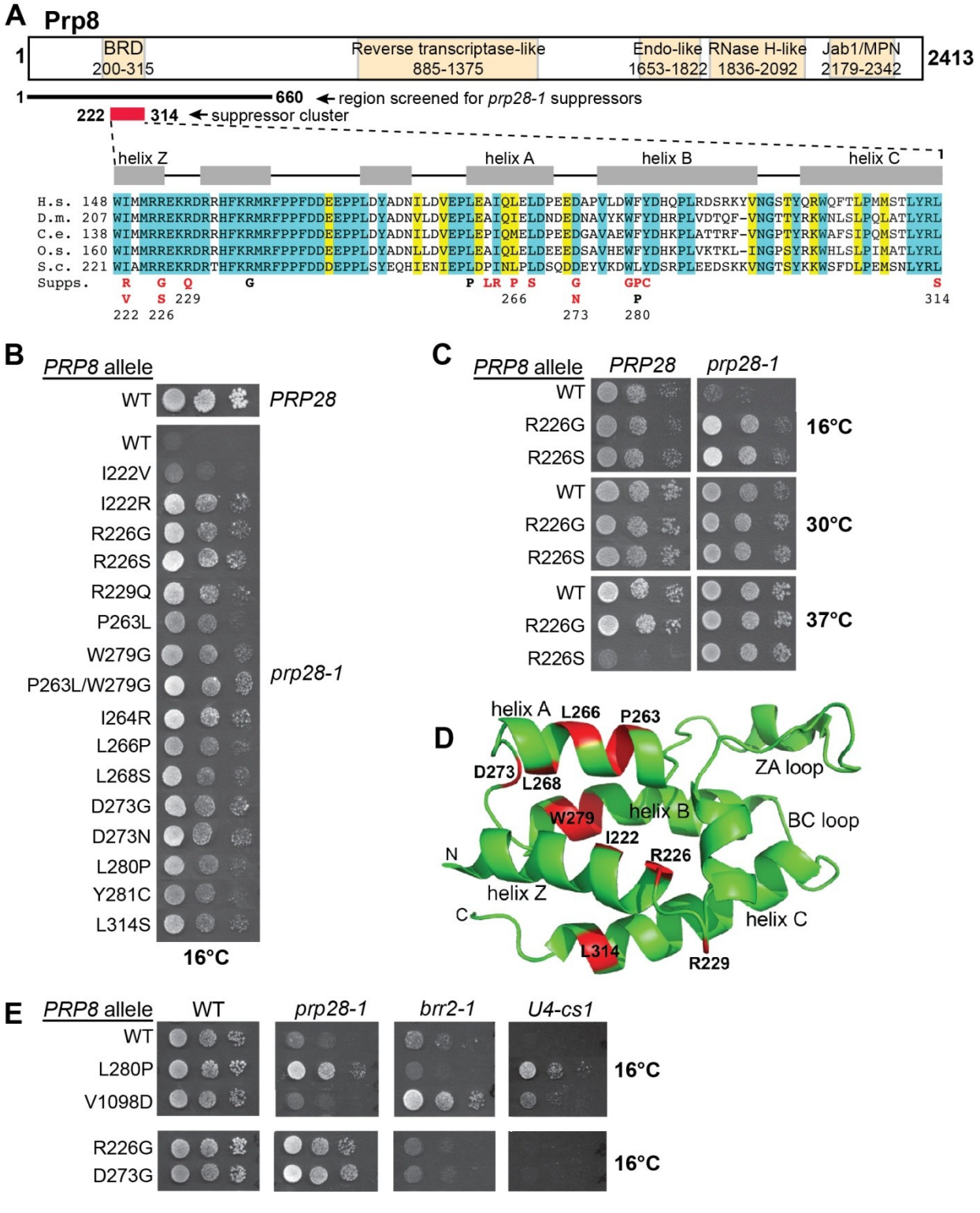
A
Prp8
1
BRD
200-315
Reverse transcriptase-like
885-1375
Endo-like
1653-1822
RNase H-like
1836-2092
Jab1/MPN
2179-2342
2413
1
660
region screened for prp28-1 suppressors
222
314
suppressor cluster
helix Z
helix A
helix B
helix C
H.s. 148 WIMMRREKRDRRHFKRMRFPPFDDEEPPLDYADNILDVEPLEAIQLELDPEEDAPVLDWFYDHQPLRDSRKYVNGSTYQRWQFTLPMMSTLYRL
D.m. 207 WIMMRREKRDRRHFKRMRFPPFDDEEPPLDYADNVLDVEPLEAIQIELDNDEDNAVYKWFYDHRPLVDTQF-VNGTTYRKWNLSLPQLATLYRL
C.e. 138 WIMMRREKRDRRHFKRMRFPPFDDEEPPLDYADNILDVEPLEPIQMELDPEEDGAVAEWFYDHKPLATTRF-VNGPTYRKWAFSIPQMSTLYRL
O.s. 160 WIMMRREKRDRRHFKRMRFPPFDDEEPPLDYADNLLDVEPLEAIQLELDEEEDSAVHEWFYDHKPLVKTKL-INGPSYRKWHLSLPIMATLYRL
S.c. 221 WIAMRREKRDRTHFKRMRFPPFDDDEPPLSYEQHIENIEPLDPINLPLDSQDDEYVKDWLYDSRPLEEDSKKVNGTSYKKWSFDLPEMSNLYRL
Supps. R G Q G P LR P S G GPC S
V S 229 266 N P 314
222 226 273 280
B
PRP8 allele
WT
PRP28
WT
I222V
I222R
R226G
R226S
R229Q
P263L
W279G
P263L/W279G
I264R
L266P
L268S
D273G
D273N
L280P
Y281C
L314S
prp28-1
16°C
C
PRP8 allele
PRP28
prp28-1
WT
R226G
R226S
16°C
WT
R226G
R226S
30°C
WT
R226G
R226S
37°C
D
helix A
L266
P263
D273
L268
ZA loop
W279
helix B
BC loop
I222
N
R226
helix Z
C
helix C
L314
R229
E
PRP8 allele
WT
prp28-1
brr2-1
U4-cs1
WT
L280P
V1098D
16°C
R226G
D273G
16°C

Figure 2: *prp8-tes* does not bypass Prp28, suppress U1/5'ss hyperstabilization, or alter interactions with U1 proteins Prp39 or Prp40 in vitro. A) *prp8-P263L/W279G* does not bypass the requirement for Prp28. A *prp28Δ/prp8Δ* strain (JG140) containing wild-type *PRP28* on a *URA3*-marked plasmid and pRS313-prp8-P263L/W279G was transformed with pRS317 (empty vector), pRS317-PRP28, pRS317-prp28-D341N (should be catalytically inactive), or pRS317-yhc1-1, which is known to bypass Prp28 (Chen et al. 2001). Ten-fold serial dilutions were plated on YEPD or YEPD + 5-FOA and grown at 30˚C for 3 days. Only strains with pRS317-PRP28 or pRS317-yhc1-1 were able to grow in the absence of the *URA3*-marked *PRP28* plasmid. **B)** *prp8-tes* does not suppress U1/5'ss hyperstabilization. 5-fold serial dilutions of strains with *PRP8* or *prp8-P263L/W279G* and wild-type or U1/5'ss hyperstabilized Act-Cup splicing reporters (Staley and Guthrie 1999) were plated onto SD -Ura medium with 0.1 mM copper sulfate, and grown at 16°C for 6 days. In the presence of the U1/5'ss hyperstabilized Act1-Cup1 reporter, wild-type *PRP8* and *prp8-tes* strains grow equally poorly at 16°C on 0.1 mM copper sulfate. **C)** Prp39 and Prp40 bind similarly to wild-type Prp8-NTD, Prp8-NTD(P263L/W279G), Prp8-NTD(R226G), and Prp8-NTD(D273G). His_6 fusion Prp39 or Prp40 proteins were added to bead-bound GST-fusion Prp8-NTD proteins in a three-fold dilution series. GST-only beads were incubated with the highest amount of His-fusion protein, and "Input" lanes contain 25% of the lowest amount of His-fusion protein used in the binding reactions. **D)** Prp28 binds similarly to Prp8-NTD and Prp8-NTD-tes alleles. His_6 fusion Prp28 was added to bead-bound GST-fusion Prp8-NTD proteins in a four-fold dilution series. GST-only beads were incubated with the hightest amount of Prp28 protein, and "Input" lane contains 65% of the lowest amount of Prp28 used in the binding reactions.

Figure 2

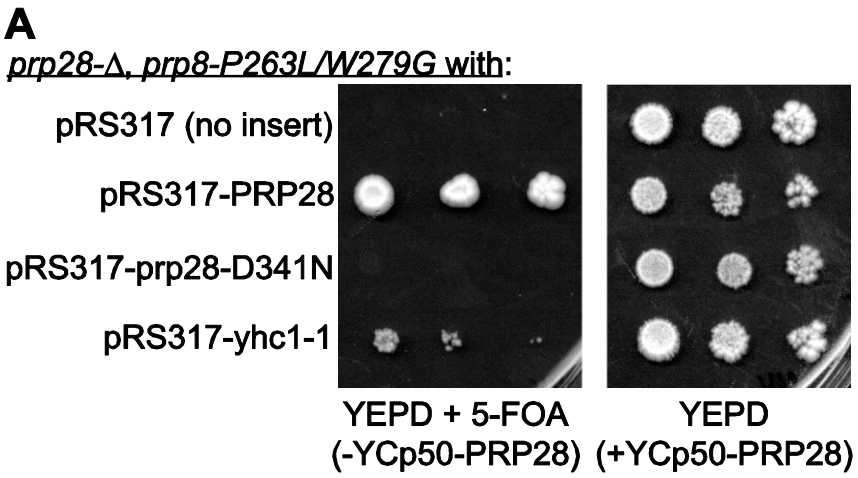
A
prp28-Δ, prp8-P263L/W279G with:
pRS317 (no insert)
pRS317-PRP28
pRS317-prp28-D341N
pRS317-yhc1-1
YEPD + 5-FOA
(-YCp50-PRP28)
YEPD
(+YCp50-PRP28)

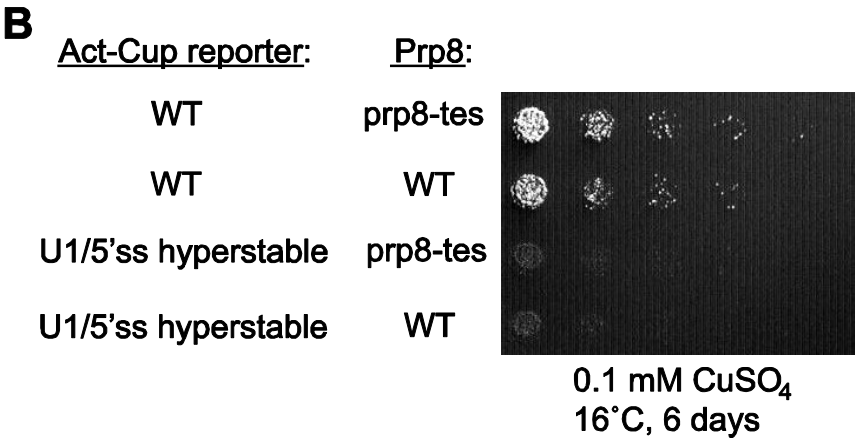
B
Act-Cup reporter:
Prp8:
WT
prp8-tes
WT
WT
U1/5'ss hyperstable
prp8-tes
U1/5'ss hyperstable
WT
0.1 mM CuSO4
16˚C, 6 days

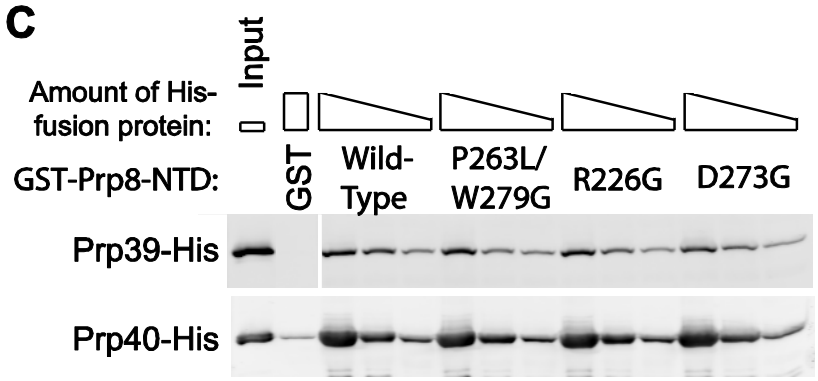
C
Amount of His-fusion protein:
Input
GST-Prp8-NTD:
GST
Wild-Type
P263L/W279G
R226G
D273G
Prp39-His
Prp40-His

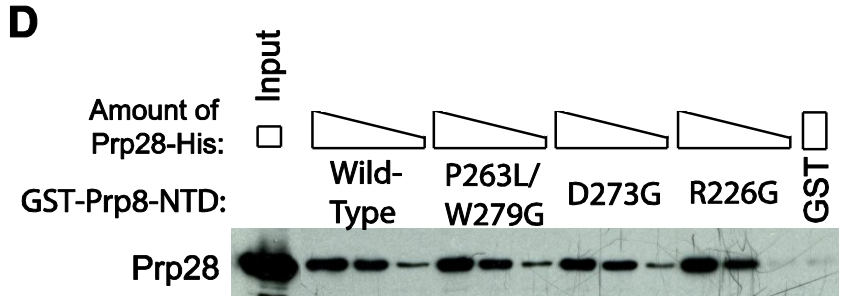
D
Amount of Prp28-His:
Input
GST-Prp8-NTD:
Wild-Type
P263L/W279G
D273G
R226G
GST
Prp28

Figure 3: The global splicing defect of the *prp28-1* mutant is partially suppressed by *prp8-P263L/W279G.* Each of 253 introns is represented by three probes on a DNA microarray (Pleiss et al. 2007): one in an exon to detect total RNA (lanes 1-4), one in the intron to detect unspliced pre-mRNA (lanes 5-8), and one across the exon-exon junction to detect spliced mRNA (lanes 9-12). Differentially labeled cDNA samples from pairs of strains were competitively hybridized to each array and log2-transformed normalized fluorescence ratios are presented. Yellow indicates an increase (ratio >0 (log2)) and blue a decrease (ratio <0 (log2)) in signal. Lanes 1, 5, and 9: *prp8-P263L/W279G* hybridized against wild-type. Lanes 2, 6, and 10: *prp28-1* against wild-type. Lanes 3, 7, and 11: *prp28-1* + *prp8-P263L/W279G* ("double") against wild-type. Lanes 4, 8, 12: *prp28-1* + *prp8-P263L/W279G* against *prp28-1* to directly measure suppression. Results presented are the average of two biological replicates, each with a dye-flip technical replicate.

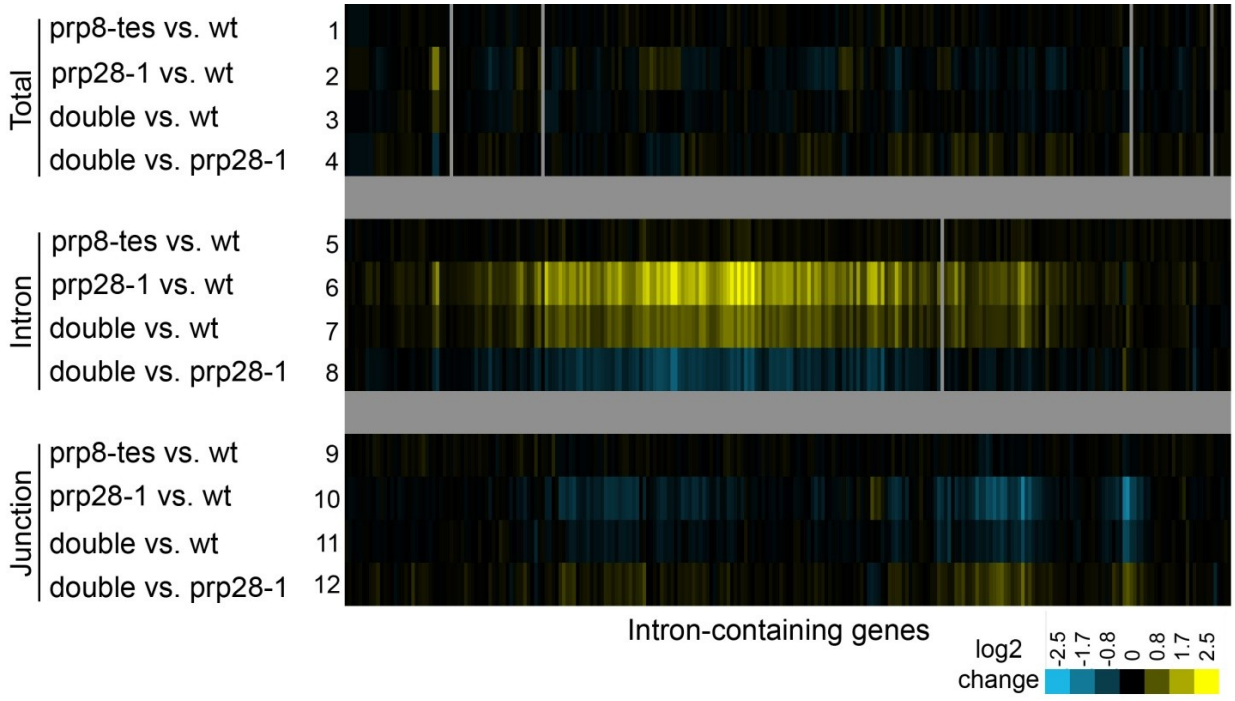

Figure 4: The *prp28-1* mutation delays cotranscriptional spliceosome assembly at the *ECM33* gene. A) Diagram of the expected order of snRNP and NTC occupancy of nascent transcripts along the *ECM33* gene. The short and long open rectangles represent the 5' and 3' exons, respectively. "RNAP" is RNA polymerase II. In order from the transcription start site (bent arrow), the splicing complexes are: CC1, CC2, pre-spliceosome, complete spliceosome, and active spliceosome. **B-E)** Data for four HA-tagged splicing factors, which are components of three snRNPs and the NineTeen Complex (NTC), as indicated on each panel. Diagrams at top show the positions of qPCR amplicons used for ChIP analysis of the gene *ECM33*. In the panels aligned below, data points are placed according to the positions of the PCR products along the gene. Crosslinking of each factor was assessed in strains with wild-type *PRP28* and *PRP8* (black line), *prp28-1* and wild-type *PRP8* (orange lines), and *prp28-1* and *prp8-P263L/W279G* (green lines). Strains were grown at 30°C (dashed lines) or 16°C (solid lines). The data represent the average of at least three independent experiments. Error bars represent the SEM.

Figure 4

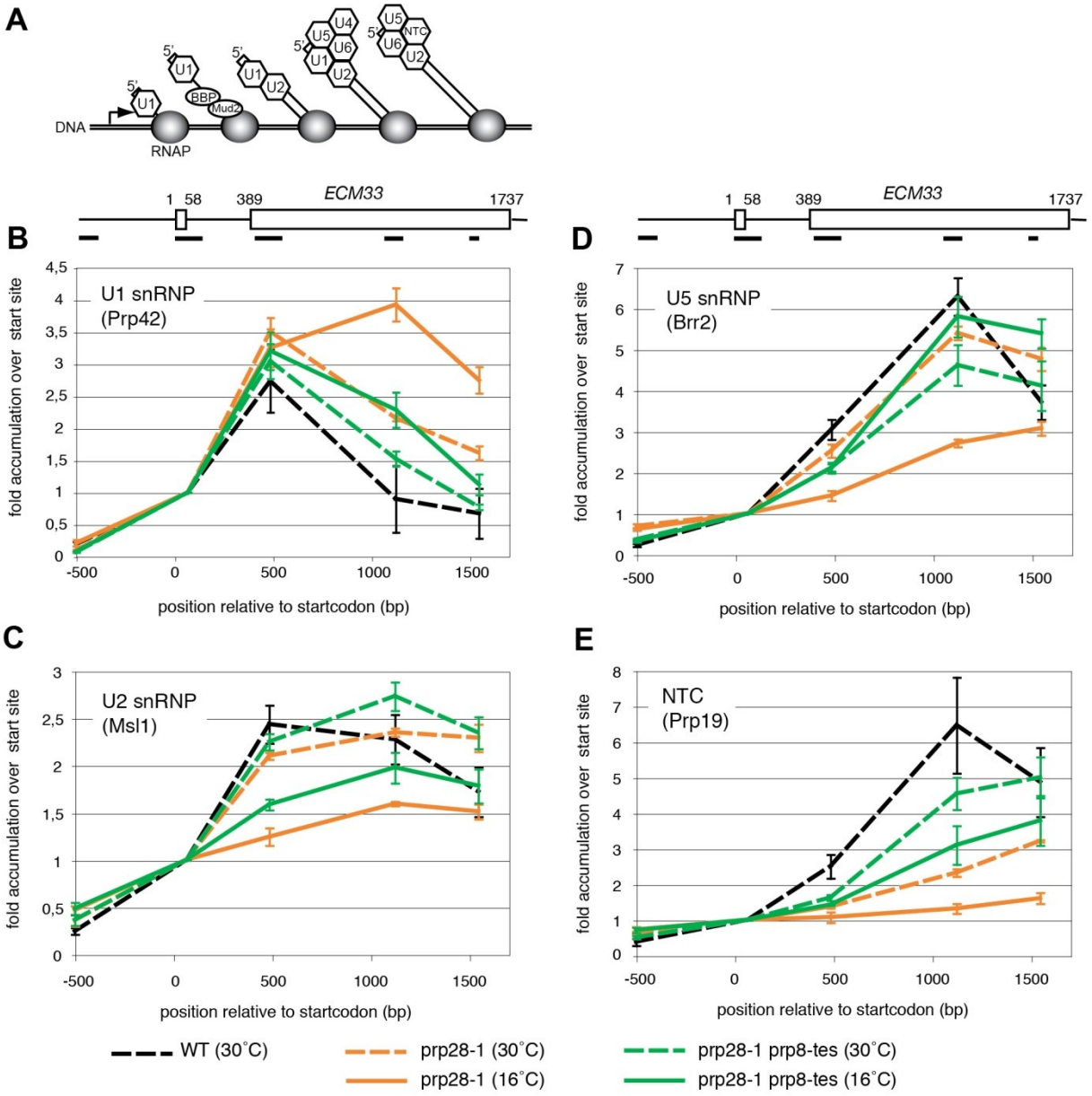
A
DNA
RNAP
5'
U1
BBP
Mud2
U2
U4
U5
U6
NTC
B
C
D
E
1 58 389 ECM33 1737
U1 snRNP (Prp42)
U2 snRNP (Msl1)
U5 snRNP (Brr2)
NTC (Prp19)
fold accumulation over start site
position relative to startcodon (bp)
WT (30˚C)
prp28-1 (30˚C)
prp28-1 (16˚C)
prp28-1 prp8-tes (30˚C)
prp28-1 prp8-tes (16˚C)

Figure 5: *In vitro*, *prp28-1* blocks U1 and U4 release and reduces stable U2, U5, and U6 association.

Splicing extracts made from four strains (wild-type: black, *prp28-1*: orange, *prp8-P263L/W279G*: blue, *prp28-1* + *prp8-P263L/W279G*: green lines) were incubated with biotinylated actin pre-mRNA at 16°C. Aliquots were taken at the indicated times and snRNAs bound to the pre-mRNA were detected by RT-qPCR. **A-E)** Pull-down results for U1, U4, U2, U5, and U6 snRNAs, respectively. Reactions with the 4 extracts were performed in parallel. The "-5 minute" time point represents background (mock pull-down without pre-mRNA). The data were normalized as described in Materials and Methods. Error = SEM after normalization.

Figure 5

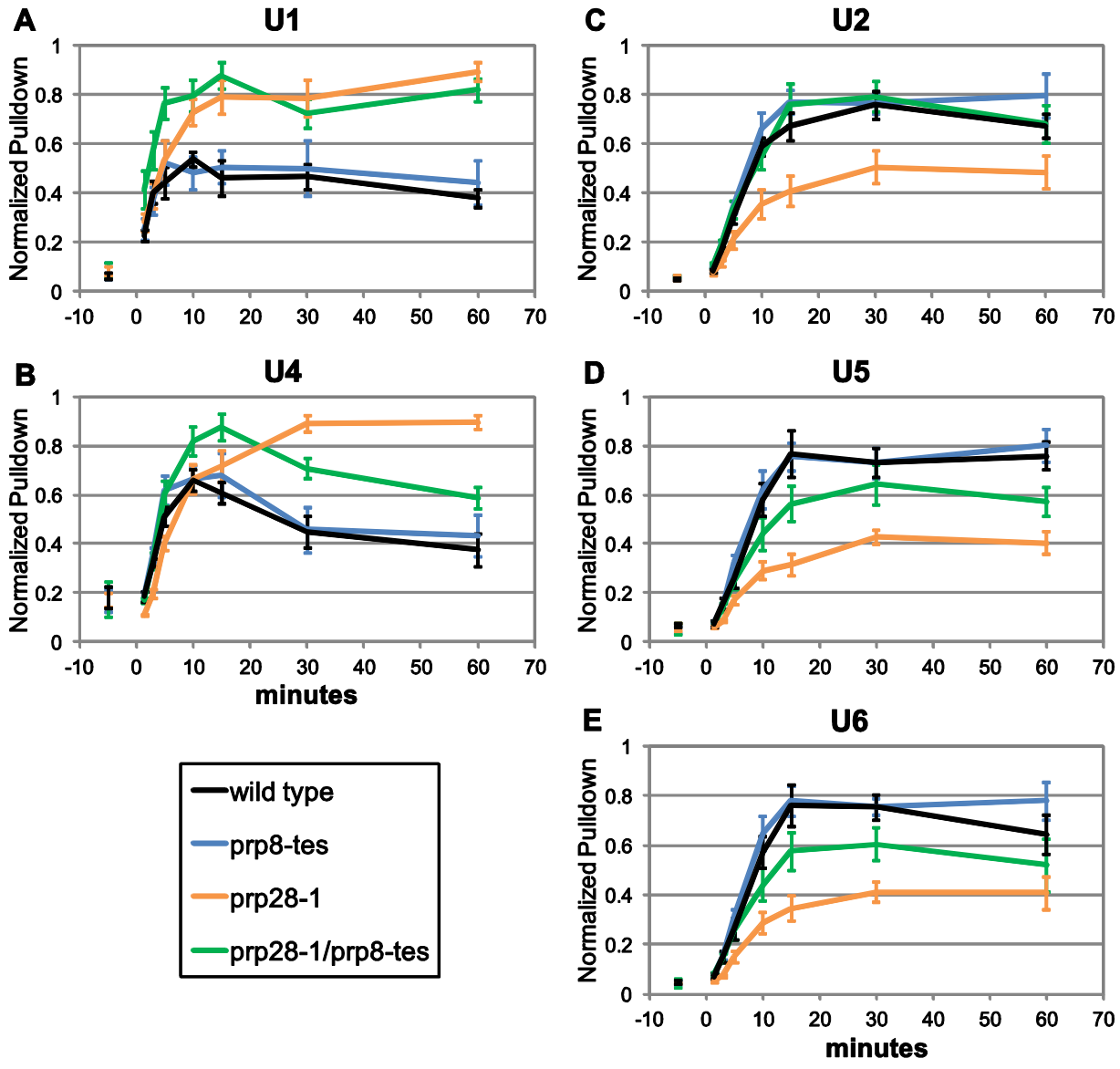
A
U1
C
U2
B
U4
D
U5
E
U6
Normalized Pulldown
minutes
wild type
prp8-tes
prp28-1
prp28-1/prp8-tes

Figure 6: *prp28-1* inhibits formation of CC2 and the transition from commitment complex to pre-spliceosome. Complexes assembled on ^{32}P-labeled RP51A pre-mRNA substrate in the presence or absence of ATP were resolved on a non-denaturing acrylamide/agarose composite gel. Lanes 1-4, 9: no ATP added, lanes 5-8, 10: 2 mM ATP added. Lanes 1, 5: wild-type extract; 2, 6: *prp8-P263L/W279G* extract; 3, 7: *prp28-1* extract; 4, 8: *prp28-1* + *prp8-P263L/W279G* extract; 9-10: extract from cells genetically depleted of Prp28. CC1: commitment complex 1, CC2: commitment complex 2, P/SP, pre-spliceosome/spliceosome, which co-migrate on these gels. Percentage of substrate in P/SP band, relative to the sum of P/SP, CC1, and CC2 bands, and ratio of CC2:CC1 are presented below. Error: SEM. * paired t-test conducted, pairing samples run on the same gel: significantly different, p=0.00023.

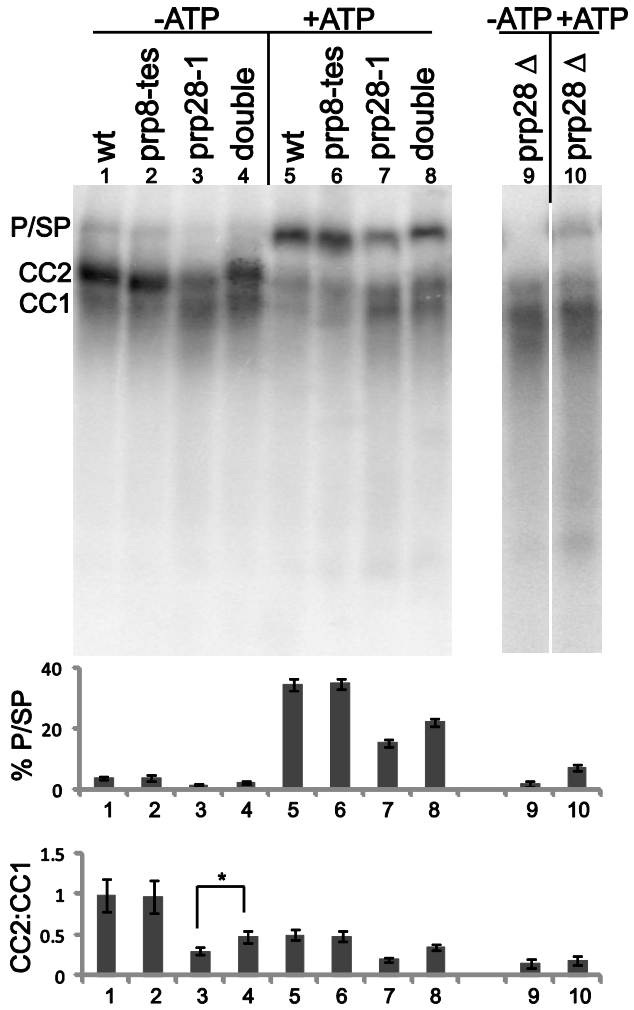

Figure 7: Model for the dual functions of Prp28 in spliceosome assembly and activation. Prp28 has an early, ATP-independent function in assembly of commitment complex 2 (CC2) and the pre-spliceosome (A), as well as a later, ATP-dependent function in conversion of the complete spliceosome (B) into the active spliceosome (B^{act}). Only selected splicing factors are shown.

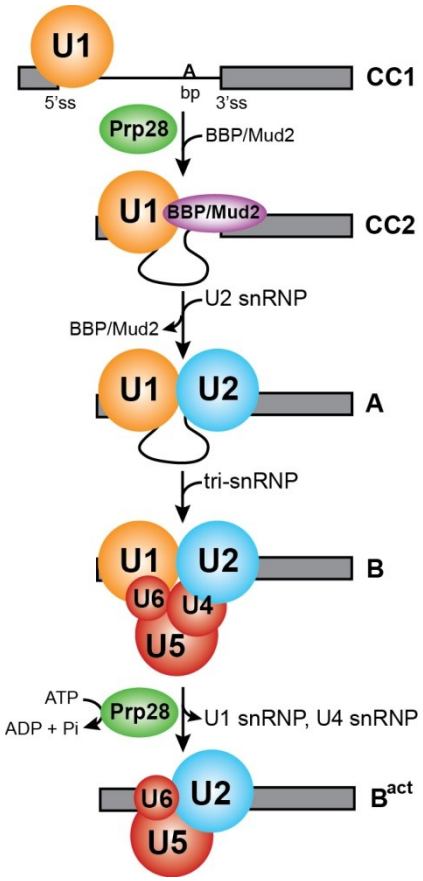

Supplementary Table 1: Strains used in this study

Strain name (parent)	Genotype	Source
ZRL102	*MAT***a** *snr14::TRP1 prp8Δ::ADE2 trp1 ura3 lys2 his3 ade2* (pRS317-U4-cs1) (YCp50-*PRP8)*	Kuhn and Brow 2000
ANK800	*MAT***a** *snr14::TRP1 prp8Δ::ADE2 trp1 ura3 lys2 his3 ade2* (pRS317-U4-wt)(YCp50-*PRP8*)	Kuhn and Brow 2000
ANK821	*MAT***a** *brr2-1 prp8Δ::ADE2 ura3 lys2 his3 ade2 leu2* (YCp50-*PRP8*)	Kuhn et al. 2002
ANK828	*MAT***a** *prp28-1 prp8Δ::ADE2 trp1 ura3 his3 ade2 lys2 (YCp50-PRP8)*	Kuhn et al. 2002
JG1	*MAT***a** *ade2 arg4 leu2-3,112 trp1-289 ura3-52 PRP40::6HA klTRP1*	Görnemann et al. 2011
KK37	*MAT***a** *ade2 arg4 leu2-3,112 trp1-289 ura3-52 PRP42::3HA kanMX6*	Görnemann et al. 2011
JG8	*MAT***a** *ade2 arg4 leu2-3,112 trp1-289 ura3-52 MSL1::6HA klTRP1*	Görnemann et al. 2011
JG10	*MAT***a** *ade2 arg4 leu2-3,112 trp1-289 ura3-52 BRR2::6HA klTRP1*	Görnemann et al. 2011
JG12	*MAT***a** *ade2 arg4 leu2-3,112 trp1-289 ura3-52 PRP19::6HA klTRP1*	Görnemann et al. 2011
JG110/AMP27 (ANK828)	*MAT***a** *prp28-1 prp8Δ::ADE2 trp1 ura3 his3 ade2 lys2 (pRS313-PRP8)*	this study
JG111 (JG110)	*MAT***a** *prp28-1 prp8Δ::ADE2 trp1 ura3 his3 ade2 lys2 MSL1::6HA-klTRP1 (pRS313-PRP8)*	this study
JG112 (JG110)	*MAT***a** *prp28-1 prp8Δ::ADE2 trp1 ura3 his3 ade2 lys2 PRP40::6HA-klTRP1 (pRS313-PRP8)*	this study
JG113 (JG110)	*MAT***a** *prp28-1 prp8Δ::ADE2 trp1 ura3 his3 ade2 lys2 PRP42::6HA-klTRP1 (pRS313-PRP8)*	this study
JG114 (JG110)	*MAT***a** *prp28-1 prp8Δ::ADE2 trp1 ura3 his3 ade2 lys2 NAM8::6HA-klTRP1 (pRS313-PRP8)*	this study
JG115 (JG110)	*MAT***a** *prp28-1 prp8Δ::ADE2 trp1 ura3 his3 ade2 lys2 BRR2::6HA-klTRP1 (pRS313-PRP8)*	this study
JG116 (JG110)	*MAT***a** *prp28-1 prp8Δ::ADE2 trp1 ura3 his3 ade2 lys2 PRP19::6HA-klTRP1 (pRS313-PRP8)*	this study
JG120/AMP28 (ANK828)	*MAT***a** *prp28-1 prp8Δ::ADE2 trp1 ura3 his3 ade2 lys2 (pRS313-prp8-P263L/W279G)*	this study
JG121 (JG120)	*MAT***a** *prp28-1 prp8Δ::ADE2 trp1 ura3 his3 ade2 lys2 MSL1::6HA-klTRP1 (pRS313-prp8-P263L/W279G)*	this study
JG122 (JG120)	*MAT***a** *prp28-1 prp8Δ::ADE2 trp1 ura3 his3 ade2 lys2 PRP40::6HA-klTRP (pRS313-prp8-P263L/W279G)*	this study
JG123 (JG120)	*MAT***a** *prp28-1 prp8Δ::ADE2 trp1 ura3 his3 ade2 lys2 PRP42::6HA-klTRP1 (pRS313-prp8-P263L/W279G)*	this study
JG124 (JG120)	*MAT***a** *prp28-1 prp8Δ::ADE2 trp1 ura3 his3 ade2 lys2 NAM8::6HA-klTRP1 (pRS313-prp8-P263L/W279G)*	this study
JG125 (JG120)	*MAT***a** *prp28-1 prp8Δ::ADE2 trp1 ura3 his3 ade2 lys2 BRR2::6HA-klTRP1 (pRS313-prp8-P263L/W279G)*	this study

JG126 (JG120)	*MAT**a** prp28-1 prp8Δ::ADE2 trp1 ura3 his3 ade2 lys2 PRP19::6HA-klTRP1 (pRS313-prp8-P263L/W279G)*	this study
JG140 (JG120)	*MAT**a** prp28Δ::kanMX6 prp8Δ::ADE2 trp1 ura3 his3 ade2 lys2 (pRS313-prp8-P263L/W279G)(YCp50-PRP28)*	this study
JG141 (JG140)	*MAT**a** prp28Δ::kanMX6 prp8Δ::ADE2 trp1 ura3 his3 ade2 lys2 (pRS313-prp8-P263L/W279G)(YCp50-PRP28)(pRS317-PRP28)*	this study
JG142 (JG140)	*MAT**a** prp28Δ::kanMX6 prp8Δ::ADE2 trp1 ura3 his3 ade2 lys2 (pRS313-prp8-P263L/W279G)(YCp50-PRP28)(pRS317-prp28-D341N)*	this study
JG144 (JG140)	*MAT**a** prp28Δ::kanMX6 prp8Δ::ADE2 trp1 ura3 his3 ade2 lys2 (pRS313-prp8-P263L/W279G)(YCp50-PRP28)(pRS317-yhc1-1)*	this study
EJS54	*MATα PRP28 trp1 ura3 his3 ade2 lys2.*	E. Strauss and C. Guthrie
AMP23 (ANK828 x EJS54)	*MATα PRP28 prp8Δ::ADE2 trp1 ura3 his3 ade2 lys2 (YCp50-PRP8)*	this study
AMP25 (AMP23)	*MATα PRP28 prp8Δ::ADE2 trp1 ura3 his3 ade2 lys2 (pRS313-PRP8)*	this study
AMP26 (AMP23)	*MATα PRP28 prp8Δ::ADE2 trp1 ura3 his3 ade2 lys2 (pRS313-prp8-P263L/W279G)*	this study
PR88	*MATα prp28Δ::TRP1 ura3 his3 trp1 leu2 ade2 (pSE362-Gal10-3HA-Prp28)*	P. Raghunathan and C. Guthrie
TB72	*Mat**a** prp8Δ::LYS2 his3 leu2 ura3 lys2 (YCp50-PRP8)*	T. Brenner and C. Guthrie
YS72	*MATα cup1Δ::ura3-52 ade2 trp1 lys2 leu2 ura3*	Burgess and Guthrie 1993
AMP24 (TB72 x YS72)	*Matα cup1Δ::ura3-52, prp8Δ::LYS2 ade2 his3 leu2 ura3 lys2 (YCp50-Prp8)*	this study
AMP39 (AMP24)	*MATα cup1Δ::ura3 prp8Δ::LYS2 ura3 lys2 trp1 his3 (pRS313-PRP8) (pCG90)*	this study
AMP40 (AMP24)	*MATα cup1Δ::ura3 prp8Δ::LYS2 ura3 lys2 trp1 his3 (pRS313-PRP8) (pCG91)*	this study
AMP41 (AMP24)	*MATα cup1Δ::ura3 prp8Δ::LYS2 ura3 lys2 trp1 his3 (pRS313-prp8-P263L/W279G) (pCG90*)	this study
AMP42 (AMP24)	*MATα cup1Δ::ura3 prp8Δ::LYS2 ura3 lys2 trp1 his3 (pRS313-prp8-P263L/W279G) (pCG91)*	this study

Supplementary Figure 1: In wild-type cells, the ChIP profile on ECM33 is very similar at 30°C and 16°C. ChIP was performed as in Figure 1 in wild-type cells grown at 30°C or shifted to 16°C for 45 min. PCR product positions are indicated on a map of ECM33 above, and plotted in corresponding positions on the horizontal axis. Solid line: 16°C, dotted line: 30°C.

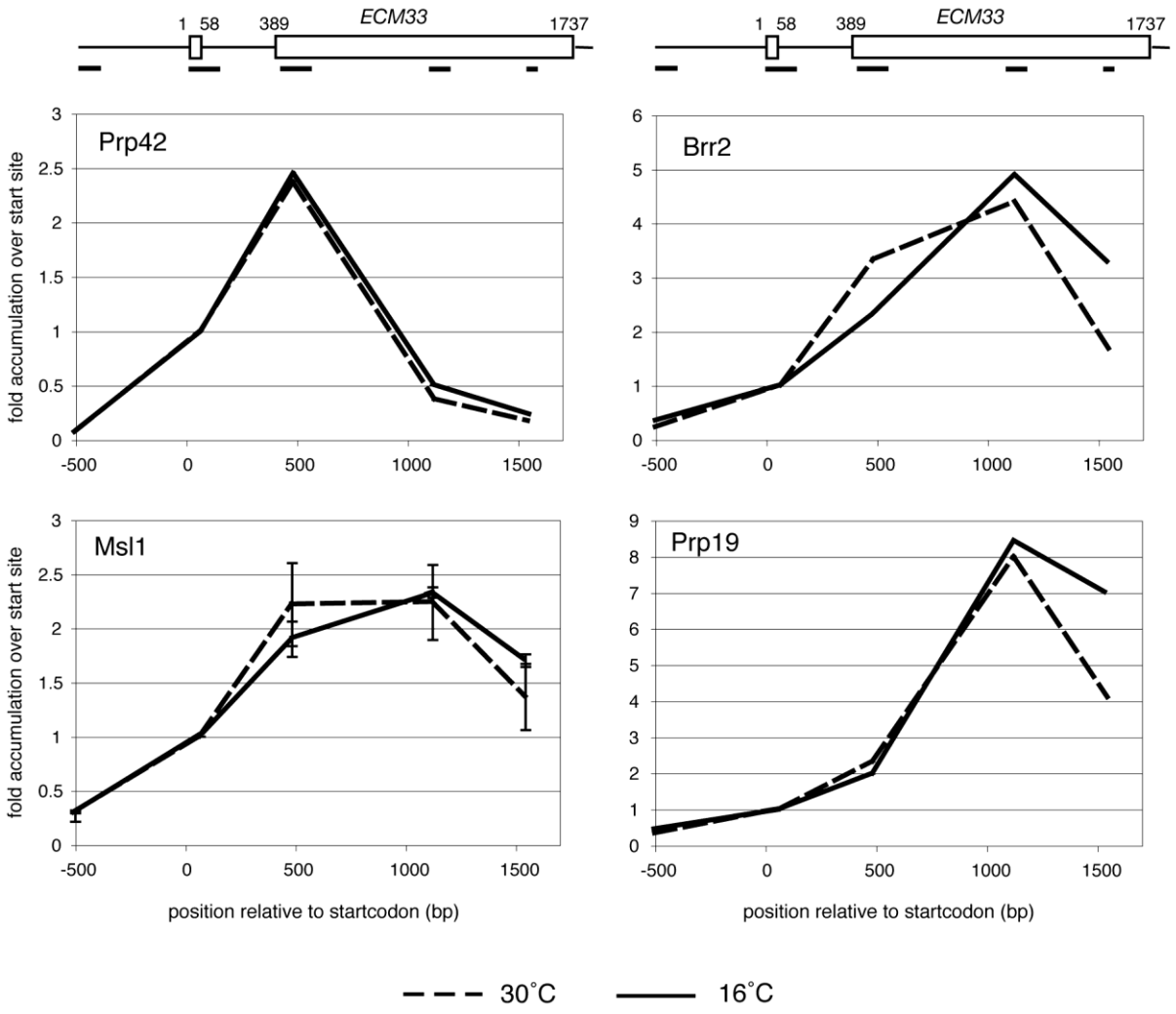

Supplementary Figure 2: Binding of U5 snRNP along *SEC27* is severely delayed and decreased in *prp28-1* strains. ChIP was conducted with HA tagged Brr2 as in Figure 1 but analyzed along *SEC27*, which has an exceptionally long second exon, allowing better resolution of U5 association and release. In *prp28-1* cells at 16°C (red solid line), U5 snRNP accumulation is dramatically delayed and reduced relative to *prp28-1* cells or wild-type cells grown at 30°C. PCR product positions are indicated in the SEC27 diagram above, with corresponding positions in the graph. The data represent the average of three independent experiments; error bars are the SEM.

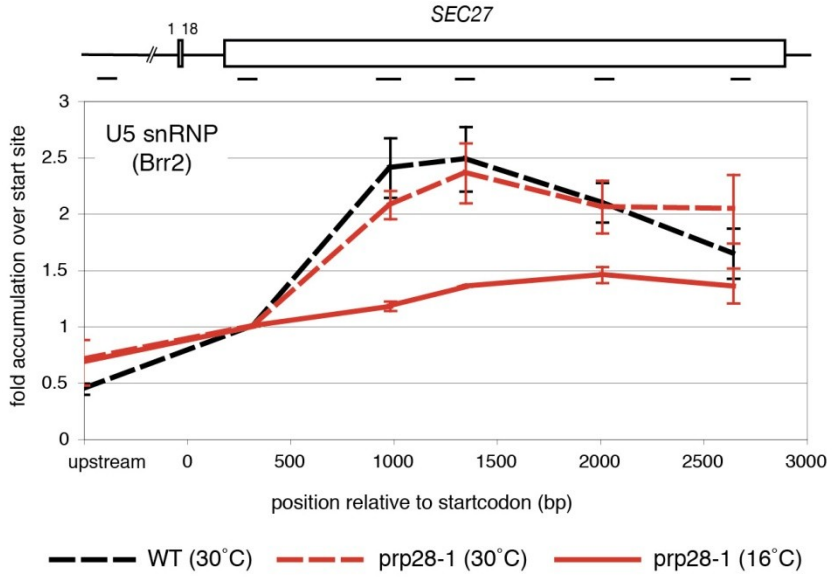

Chapter 2

Single molecule FRET analysis of commitment complexes formed with or without Prp28

Single molecule FRET analysis of commitment complexes formed with or without Prp28

Argenta Price*, Matthew Kahlscheuer*, Ramya Krishnan, Nils Walter, Christine Guthrie

Abstract

The earliest steps of spliceosome assembly are binding of the U1 snRNP to the 5' splice site, forming commitment complex 1, and binding of Branchpoint Binding Protein (BBP) and Mud2 to the branch sequence, forming commitment complex 2. Interactions between U1 and BBP/Mud2 are thought to bring the 5'ss and branch site into close proximity for the first time in commitment complex 2. We recently showed that formation or stability of commitment complex 2 required the presence of DEAD-box protein Prp28. Here we used single molecule FRET to measure the dynamics of Prp28-dependent formation of commitment complex 2. FRET probes were placed near the 5'ss and branch site of Ubc4 pre-mRNA so that we could measure the proximity of these sites. Surprisingly, we found that the pre-mRNA experienced high FRET states in equal frequency regardless of whether Prp28 was present or whether commitment complex 2 formation was blocked by mutating the branch site. We conclude that commitment complex 1 also allows the splice sites to come into close proximity. Possibly, BBP/Mud2 interacts with commitment complex 1 in a way that causes formation of high FRET states but is not stabilized on native gels the same way as commitment complex 2.

Introduction

The spliceosome assembles in a stepwise series of binding and rearrangement events. The first two steps are recognition of the 5' splice site by the U1 snRNP (forming commitment complex 1 - CC1) followed by binding of Branchpoint Binding Protein (Msl5) and Mud2 to the branch sequence (forming commitment complex 2 - CC2) (Seraphin and Rosbash 1989;

Legrain et al. 1988; Abovich and Rosbash 1997; Liao et al. 1992). We showed that Prp28, a DEAD-box ATPase that promotes U1 release later in the splicing cycle, has an earlier function in the ATP-independent formation of commitment complex 2 (Price et al. 2014). Native gels that separate CC1 from CC2 from higher order spliceosome complexes showed that in wild-type splicing reactions without ATP about half of the pre-mRNA is bound in CC2. However, in extracts made from yeast after shutting off Prp28 expression, very little CC2 formed and the mobility or crispness of CC1 was somewhat disrupted. These gels, which may stabilize the commitment complexes with gel-caging interactions, did not allow us to investigate the dynamics of stability of CC2 vs. CC1. We turned to single molecule fluorescence resonance energy transfer (FRET) using Ubc4 pre-mRNA with probes at the 5'ss and branch site to investigate these dynamics (Krishnan et al. 2013).

The commitment complexes were originally identified the earliest-forming stable complexes that commit the pre-mRNA to splicing and are resistant to competition with unlabeled pre-mRNA (Seraphin and Rosbash 1989; Legrain et al. 1988). These complexes contain the U1 snRNP (Seraphin and Rosbash 1989), the Mud2/Branchpoint Binding Protein dimer (Abovich et al. 1994; Abovich and Rosbash 1997; Rutz and Séraphin 1999), and some additional proteins including the cap binding complex (Colot et al. 1996; Zhang and Rosbash 1999). U1 binds to the 5'ss in commitment complex 1 and does not require the branch sequence to bind (Seraphin and Rosbash 1991). BBP and Mud2 join to form CC2, which requires the branch site. Both complexes form in the absence of ATP (Liao et al. 1992), and are thought to be in equilibrium with one another. Interestingly, Rutz and Séraphin (1999) showed that while depletion of BBP or Mud2 blocked CC2 formation and caused an increase in CC1, pre-spliceosome was still able to form and splicing was able to proceed in the presence of ATP. Therefore, CC2 formation may not be strictly required under optimal conditions for formation of later splicing complexes, even though Mud2 has been shown to help recruit U2 to the spliceosome (Abovich et al. 1994) and BBP binding improves splicing of suboptimal substrates (Rutz and Séraphin 1999, 2000).

Single molecule FRET can be used to monitor the dynamics of CC1 vs. CC2 formation in splicing reactions lacking ATP. Krishnan et al. (2013) describes the use of pre-mRNA with FRET probes near the 5'ss and branch site to monitor the distance between those sites. Abovich and Rosbash (1997) showed that the U1 snRNP protein Prp40 physically interacts with both BBP and Mud2, which would bring the 5'ss into closer proximity with the branch. Therefore, we expect that CC2 will bring the pre-mRNA into a high FRET state, while CC1 will have the branch and 3' end of the RNA unbound by spliceosomal proteins and in a lower FRET state, possibly more dynamic if the RNA is able to move around more freely. Because Prp28 changes the proportion of CC1 vs. CC2 that can be visualized by native gels, Prp28-depleted extracts allow us to visualize the differences in CC1 and CC2 FRET dynamics and learn how this equilibrium depends on Prp28.

Results

Commitment complex gels using Ubc4 pre-mRNA recapitulate previous results

Our single molecule FRET experiments used Ubc4 pre-mRNA with 20 nt exons and a Cy3 FRET donor attached 6 nucleotides downstream from the branch point and a Cy5 FRET acceptor attached 7 nucleotides upstream from the 5'ss, as described (Abelson et al. 2010; Krishnan et al. 2013). We wanted to test whether this substrate behaved the same as the RP51 pre-mRNA used previously to show that Prp28 has an effect on CC2 formation (Price et al. 2014). However, we were unable to see non-background bands on commitment complex gels using the fluorescent substrate, so we in vitro transcribed the same length Ubc4 pre-mRNA with 32-P labels and used that for CC gels. Figure 1 shows that CC1 and CC2 form as expected on Ubc4 pre-mRNA with wild-type substrate. In the absence of Prp28, CC1 forms but runs with slightly faster mobility, and formation of CC2 is severely inhibited. As expected, U2 depletion blocks formation of pre-spliceosome, but allows formation of CC2 only in WT extract. Interestingly, unlike with RP51 pre-mRNA (Seraphin and Rosbash 1989; Price et al. 2014), U2

depletion leads to a mix of CC1 and CC2 instead of predominantly CC2. We also planned on using branch site mutated pre-mRNA in the FRET experiments as a control for formation of just CC1. Previous papers had deleted the entire UACUAAC branch region to prevent CC2 formation (Seraphin and Rosbash 1991), but the branch site A to C mutation (BrC) had been shown to block binding of BBP to a branch site oligo in vitro (Garrey et al. 2008), so we tested whether BrC pre-mRNA would assemble CC2 using gels. Our results (Figure 1) show that BrC pre-mRNA stalls at CC1, and prp28 depleted extracts still have the somewhat altered mobility CC1.

Prp28 does not clearly affect the proximity of 5'ss and BP by single molecule FRET

We used single molecule FRET to investigate how Prp28 affects the dynamics and stability of commitment complex 2. Our prediction, based on the cross-intron bridging interactions between BBP and the U1 factor Prp40 (Abovich and Rosbash 1997), was that the 5'ss and branch site should be brought into closer proximity in CC2. Therefore, using our pre-mRNA with FRET probes at the 5'ss and branch site, we would expect to see high FRET states in CC2. When only CC1 has formed, we expect lower FRET states, or possibly more dynamic states because the pre-mRNA would be less constrained by bound spliceosomal components (Figure 2). Since Prp28 depletion blocks formation of CC2 on gels, we can monitor the FRET signature of CC1 vs. CC2 and can monitor the stability of CC2 and dynamics of transitions between FRET states in the presence or absence of Prp28.

Our preliminary experiments using extract from Prp28-depleted yeast (see materials and methods and Price et al. 2014) showed that in the absence of Prp28, the pre-mRNA experienced a mixture of high FRET and low FRET states and was fairly dynamic (supplementary figure 1A and data not shown). When purified Prp28 protein was added to the Prp28-depleted extract, we saw a shift to mostly high FRET states, which were still fairly dynamic (data not shown). This was consistent with our model that Prp28 would promote formation of the higher-FRET commitment complex 2, so we decided to investigate further.

We wanted to see if adding increasing concentrations of Prp28 would result in a dose-dependent shift toward higher FRET states. The amount of Prp28 added back to the splicing reactions lacking Prp28 was titrated from 0 nM to 160 nM. Then we took movies after allowing the splicing extract to incubate with pre-mRNA on the slide for about 10 minutes. Traces from single molecules that exhibited anti-correlation in the Cy3 and Cy5 channels, blinked or photobleached before the end of data collection, and appeared to only have one molecule of each dye, were selected for background correction and analysis. Surprisingly, even our reactions in which buffer instead of Prp28 were added to the splicing reaction, the predominant FRET states were high FRET states. Addition of any amount of Prp28 protein had very little effect on the distribution of FRET states (Figure 3). We also used biological replicates of the Prp28 depleted extract, tried adding different buffers for the no-Prp28 experiments, and added another DEAD-box ATPase, Ded1, as a negative control. The histograms for all of these experiments look very similar (Figure 3 and Supplementary figure 2).

In addition to using histograms to look at the data, we created Transition Occupancy Density Plots (TODPs; Krishnan et al. 2013; Blanco and Walter 2010) to look at the dynamics of FRET transitions. The proportion of molecules that undergo each transition from initial FRET (X-axis) to new "final" FRET (Y-axis) is plotted, with brighter spots indicating more molecules undergoing that transition. Static molecules without transitions are plotted along the diagonal. In Figure 3 B-H it is clear that molecules in these experiments transitioned between very many different FRET states, with few particularly preferred transitions except for the stable low FRET state that is present in all conditions. This indicates that these splicing reactions in the absence of ATP are incredibly dynamic, regardless of whether Prp28 is present. We also looked at Transition Density Plots (TDPs), which plot every transition that occurs, regardless of how many times that transition occurs in the same molecule, which also indicated that these molecules are highly dynamic (data not shown). While the addition of Prp28 didn't lead to an increase in the number of frames molecules spent in high FRET on the histograms, the TODPs do look like

there was an increase in molecules that had high FRET to high FRET transitions in the presence of the highest concentrations of Prp28. However, the molecules were still incredibly dynamic and the changes were subtle and not trending in a clear direction based on concentration of Prp28. In addition, we found from biological replicates (supplementary figure 1 and data not shown) that the TODP patterns were pretty variable from experiment to experiment in the absence of Prp28, so it is hard to draw conclusions based on subtle differences in TODP patterns.

During this set of experiments, the microscope was slightly out of alignment such that the edges of our field of view were unreliable and some molecules that we picked for analysis had different maximum possible intensities for Cy3 and Cy5, so some of our analysis may have been skewed because of that. However, repeats of the experiment including adding up to 400nM Prp28 still resulted in high FRET states throughout and very many FRET transitions. There may also have been differences in the timing of how long the splicing reactions were allowed to interact with pre-mRNA on the slide before being imaged. But, when we re-analyzed the preliminary set of data with a different person picking molecules and updated software doing the background correction, we also saw primarily high FRET states even in the absence of Prp28 (supplementary figure 1).

CC1 itself, blocked by BrC mutation instead of Prp28 depletion, is also high FRET

The branch site A to C mutation stalls spliceosome assembly at CC1 (Figure 1), so we used it as a control to see what the FRET dynamics are for CC1 formed by a different means. Both wild-type and Prp28 depleted extracts cause the BrC pre-mRNA to form high FRET states (supplementary figure 2). So the high FRET states seen in Prp28-depleted extracts with wild type substrate are also consistent with CC1.

Prp28 may affect the stability of the high FRET CC1/CC2 complexes

Although Prp28 didn't dramatically affect the FRET dynamics of our single molecule splicing reactions, we thought maybe it would affect the stability of the commitment complexes

once they formed, and this stability could be monitored by washing out the splicing extract and re-imaging the pre-mRNA and any stably bound spliceosomes after the wash-out. The commitment complexes were shown to be the first splicing complex "committed" to splicing because spliceosomes that had formed commitment complexes were still able to splice their bound substrates after being swamped out with unlabeled pre-mRNAs. Therefore, in a wild-type context, the commitment complexes should remain bound to the pre-mRNAs on the slide even after free spliceosomes in the extract are washed away. We tested whether Prp28 depleted extracts might have less stable commitment complexes that would be more sensitive to having extract washed out. We took movies of splicing reactions with or without Prp28 as previously described, then washed out the splicing reaction with a mix of splicing buffer and Buffer D (in the similar ratios to the initial splicing reaction - Buffer D replacing extract, slightly diluted with oxygen scavengers) and took another set of movies. Figure 4A shows that washing out the extract caused a decrease in the proportion of high FRET states and an increase in the low FRET state peak. This could be because loosely bound spliceosomes or other proteins in the extract were washed away, so the high FRET states could be partially caused by unstable/transient interactions with later splicing factors or with other proteins in the extract. The amount of background fluorescence is also reduced after the wash-out because the extract itself provides a lot of background fluorescence, which causes high background fluorescence.

The TODPs from the wash-out experiment are intriguing (figure4 E-G). There appears to be an increase in the stable high FRET (~0.8) states in the flow-out condition +Prp28 or wild-type compared to the Prp28 depleted condition. There may also be an increase in some mid-high and high-mid FRET transitions. The Prp28-depleted plus Prp28 protein condition does look more like wild-type. Unfortunately, we did not repeat these flow-out experiments after the microscope was behaving better or with different batches of extract to know how reproducible this is.

U2 depletion also causes high FRET, with subtle changes depending on the presence of Prp28

We depleted U2 from extracts that were wild-type or Prp28-depleted +/- Prp28 protein (Figure 5) to determine whether the absence of U2 would reveal any differences between extracts with and without Prp28. Since U2 joining requires ATP, we did not expect U2 to affect differences in the ATP-independent formation of commitment complexes. Based on the histograms, there was no clear difference between extracts with or without ATP in the absence of U2 - as usual, there were mostly high FRET states. The TODP for Prp28-depleted + Prp28p looks somewhat more similar to wild-type than Prp28-depleted does to wild-type, so the absence of U2 may reveal a difference between the presence or absence of Prp28. Interestingly, the U2-depleted/Prp28-depleted extract appears to have more high FRET to high FRET transitions than just Prp28 depleted extract (compare figures 5B and 3B or 4B). Possibly, U2 interacts with the pre-mRNA even in the absence of ATP, which reduces some of those high FRET transitions. This would be consistent with the small amount of pre-SP that we see in wild-type extracts in the absence of ATP (Figure 1). However, the TODPs for Prp28-depleted + buffer control experiments did tend to be quite variable and some biological replicates did have similar high FRET-high FRET transitions, so this difference may not be relevant.

Discussion

Although the Prp28 depleted extract behaves very differently on a gel compared to extracts containing Prp28, both extracts caused primarily high FRET states for pre-mRNA labeled at the 5'ss and branch site. This indicates that the splice sites are in close proximity in the absence of ATP either with or without Prp28 - in both CC1 and CC2. Our control with BrC pre-mRNA showed that CC1 is indeed primarily composed of high FRET states. One possible reason that CC1 would be high FRET is that the RNA in CC1 is highly dynamic like naked RNA, so the splice sites come into proximity because of RNA folding. Indeed, the TODPs show a very

large number of FRET states and transitions between different FRET states, indicative of highly dynamic RNA.

An alternative possibility is that the CC1 and CC2 complexes observed on gels are stabilized (or destabilized in the case of CC2 in Prp28 depleted extracts) by the gel, while in solution they are constantly interchanging, regardless of the presence or absence of Prp28. This would also be possible in the BrC situation because the single nucleotide change in the branch site might only partially destabilize BBP/Mud2 binding in a way that prevents that complex from being stable in the gel but not from forming transiently in the single molecule FRET experiments. Our experiments washing out unbound extract and taking movies after the flow-out did show that there was a Prp28-dependent slight increase in stable mid-high FRET states. This could mean that CC2 does bring the pre-mRNA into a higher FRET state that is stabilized by the presence of Prp28. Since CC1 and CC2 are expected to interchange easily, it isn't surprising that we would only detect a slight difference in CC2 stability in the more stringent condition with extract washed out.

Our results from titrating the amount of Prp28 protein added back to Prp28 depleted extracts showed very little difference in FRET state and transitions with or without Prp28, though at the highest concentrations of Prp28 there may have been greater representation of high FRET to high FRET transitions. We are unable to make strong conclusions based on these subtle differences, especially because in all of the movies there were an incredibly high number of FRET states identified by the Hidden Markov Modeling. One idea we have not yet tried is to restrict the software to only find a smaller number of FRET states to see if reducing the number of possible states would make differences in occupancy groups of states become easier to detect. The high number of FRET states and transitions could be partially due to complications with the alignment of the microscope during most of our experiments. We had trouble picking molecules that looked really excellent, had similar backgrounds and maximums for Cy3 and Cy5, and had a blink or photobleach long enough to do proper background collection. This may

have skewed our results toward having more FRET states than really existed. However, several of the experiments were repeated at a later time when the microscope was better aligned and still showed primarily high FRET states and many transitions, so our results are reproducible.

Because we found that the pre-mRNA samples high FRET states in equal frequency regardless of whether CC2 formation is blocked by Prp28 depletion or branch site mutation, we conclude that CC1 also allows the splice sites to come into close proximity. Possibly, BBP/Mud2 interacts with CC1 in a way that causes formation of high FRET states but is not stabilized on native gels in the same way as CC2. Supporting this, our wash-out experiments showed that there does appear to be a slight difference in the stable formation of high FRET states depending on the presence of Prp28. Thus there is some difference in the stability of the high FRET states seen in extracts that form CC1 vs. CC2; this difference may be distinguished on gels.

Materials and Methods

In vitro splicing assays and native gels

Splicing extract was prepared as described in Price et al. (2014). Wild-type extract was from Gal-driven Prp28 yeast (strain yPR88) grown in YEP + galactose (and shifted to fresh galactose for the final 3-5 hours). Prp28 depleted extract was the same strain shifted to YEP + glucose for 3-5 hours. Commitment complex gels were run as described in Price et al. (2014), except the pre-mRNA used was P32 labeled Ubc4 pre-mRNA with 20 nt exons - the same sequence of pre-mRNA used for the single molecule FRET experiments (Abelson et al. 2010). The branch site C mutated pre-mRNA used in the CC gel is Ubc4 pre-mRNA with the branch site A mutated to C. Both substrates were transcribed with 32-P UTP using the Ambion Megascript T7 kit. ATP was depleted from extracts by treatment with .05 U/µl Hexokinase (Roche) and 3 mM glucose for 30 minutes at room temperature followed by a second round of dialysis (1 x 2 L, 2 hr) before extracts were frozen in aliquots. U2 was depleted from splicing

reactions by treating with 400 nM U2 RNaseH oligo and 2 mM ATP for 30 minutes at 30 °C, then ATP was re-depleted with glucose prior to single molecule FRET analysis (but not gel).

Purification of Prp28 and Ded1 proteins

His-tagged Prp28 (plasmid from Matt K.) was purified from E. coli as described in Price et al. (2014). His-tagged Ded1 was expressed in E. coli on plasmid pET22b (a gift from I. Iost) and purified as described in (Iost et al. 1999).

Single molecule FRET experiments

100 µl splicing reactions (Lin et al. 1985) were mixed without pre-mRNA and incubated with 15 µl oxygen scavenger system (Trolox, PCA, and PCD) for about 10 min. The splicing reaction was flowed over a single molecule FRET slide pre-bound with pre-mRNA. pre-mRNA substrate was as described (Krishnan et al. 2013) - Ubc4 with a Cy3 FRET donor 7 nucleotides downstream from the branch and a Cy5 FRET acceptor 6 nucleotides upstream from the 5'ss. Slides were prepared and RNA bound as described in Mario methods paper reference. The splicing reaction on the slide was incubated at room temperature for about 10 minutes, then movies of five fields of view for each condition were recorded for ~2000 frames, with the red laser turned on to directly excite Cy5 for about 50 frames after the first 500 frames and again for the last ~400 frames. For the flow-out experiments, splicing reaction was flowed over the FRET slide, allowed to incubate for about 10 minutes, and data from several fields of view was collected. Then 200 µl buffer (52 mM KPO4, 35% Buffer D, and oxygen scavengers) was flowed over the slide to wash out un-bound spliceosomal components, and movies from 5 more fields of view were collected.

Data was analyzed using custom MatLab scripts developed in the Walter lab (Blanco and Walter 2010). After file conversion and TopHat background correction, molecules were selected by hand for analysis - molecules were only used if they contained signal from both fluorophores, had a Cy5 photo bleach or blink for individual fluorophore background correction, and had anti-correlation of the FRET probes. However, we did select molecules that had

differences in maximum Cy5 and Cy3 intensity - the microscope was not completely aligned so there were differences especially in the outer regions of the field of view, which may have made the FRET intensity results more variable. We used the vbFRET package to assign FRET values and transitions from the individual traces using Hidden Markov Modeling (Blanco and Walter 2010). Histograms were created from the FRET state of the first 100 frames of every molecule, except a trace from a single molecule was broken into several pieces (each of which was then counted as a separate single molecule) if there was a blink or if the fluorophores were still unbleached after the first flash with the green laser. TODPs which show the proportion of molecules that underwent each transition, and TDPs which show the number of times a transition occurred regardless of whether those transitions were in the same molecule, were created as described (Blanco and Walter 2010; Krishnan et al. 2013).

References

Abelson J, Blanco M, Ditzler MA, Fuller F, Aravamudhan P, Wood M, Villa T, Ryan DE, Pleiss JA, Maeder C, et al. 2010. Conformational dynamics of single pre-mRNA molecules during in vitro splicing. *Nat Struct Mol Biol* **17**: 504–512.

Abovich N, Liao XC, Rosbash M. 1994. The Yeast MUD2 Protein: An Interaction with PRP11 Defines a Bridge Between Commitment Complexes and U2 snRNP Addition. *Genes Dev* **8**: 843–854.

Abovich N, Rosbash M. 1997. Cross-intron bridging interactions in the yeast commitment complex are conserved in mammals. *Cell* **89**: 403–412.

Blanco M, Walter N. 2010. Analysis of Complex Single Molecule FRET Time Trajectories. *Methods Enzymol* **472**: 153–178.

Colot HV, Stutz F, Rosbash M. 1996. The yeast splicing factor Mud13p is a commitment complex component and corresponds to CBP20, the small subunit of the nuclear cap-binding complex. *Genes Dev* **10**: 1699–1708.

Garrey SM, Cass DM, Wandler AM, Scanlan MS, Berglund JA. 2008. Transposition of two amino acids changes a promiscuous RNA binding protein into a sequence-specific RNA binding protein. *RNA* **14**: 78–88.

Iost I, Dreyfus M, Linder P. 1999. Ded1p, a DEAD-box protein required for translation initiation in Saccharomyces cerevisiae, is an RNA helicase. *J Biol Chem* **274**: 17677–17683.

Krishnan R, Blanco MR, Kahlscheuer ML, Abelson J, Guthrie C, Walter NG. 2013. Biased Brownian ratcheting leads to pre-mRNA remodeling and capture prior to first-step splicing. *Nat Struct Mol Biol* **20**: 1450–1457.

Legrain P, Seraphin B, Rosbash M. 1988. Early commitment of yeast pre-mRNA to the spliceosome pathway. *Mol Cell Biol* **8**: 3755–3760.

Liao XC, Colot HV, Wang Y, Rosbash M. 1992. Requirements for U2 snRNP Addition to Yeast Pre-mRNA. *Nucleic Acids Res* **20**: 4237–4245.

Lin RJ, Newman AJ, Cheng SC, Abelson J. 1985. Yeast mRNA splicing in vitro. *J Biol Chem* **260**: 14780–14792.

Price AM, Görnemann J, Guthrie C, Brow DA. 2014. An unanticipated early function of DEAD-box ATPase Prp28 during commitment to splicing is modulated by U5 snRNP protein Prp8. *RNA New York N* **20**: 46–60.

Rutz B, Séraphin B. 2000. A dual role for BBP/ScSF1 in nuclear pre-mRNA retention and splicing. *EMBO J* **19**: 1873–1886.

Rutz B, Séraphin B. 1999. Transient interaction of BBP/ScSF1 and Mud2 with the splicing machinery affects the kinetics of spliceosome assembly. *RNA* **5**: 819–831.

Seraphin B, Rosbash M. 1989. Identification of functional U1 snRNA-pre-mRNA complexes committed to spliceosome assembly and splicing. *Cell* **59**: 349–358.

Seraphin B, Rosbash M. 1991. The yeast branchpoint sequence is not required for the formation of a stable U1 snRNA-pre-mRNA complex and is recognized in the absence of U2 snRNA. *EMBO J* **10**: 1209–1216.

Zhang D, Rosbash M. 1999. Identification of eight proteins that cross-link to pre-mRNA in the yeast commitment complex. *Genes Dev* **13**: 581–592.

Figures

Figure 1: Commitment complex gel with 32-P labeled Ubc4 pre-mRNA. Abbreviations: CC1: commitment complex 1, CC2: commitment complex 2, P/SP: pre-spliceosome/spliceosome co-migrating, 28D: extract from Prp28 depleted yeast, U2D: extract depleted of U2 with RNaseH oligo in vitro, BrC: Ubc4 pre-mRNA with the branch site A mutated to C.

Figure 1

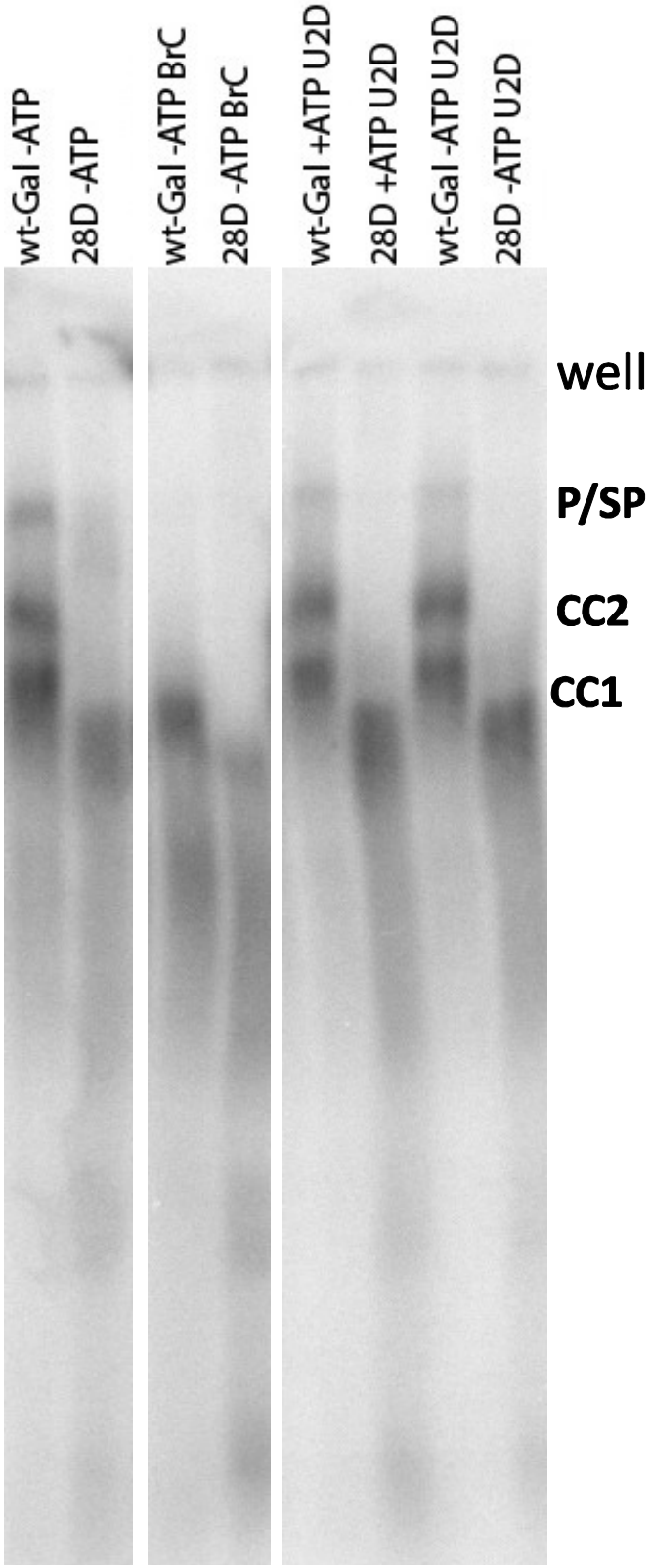
wt-Gal -ATP
28D -ATP
wt-Gal -ATP BrC
28D -ATP BrC
wt-Gal +ATP U2D
28D +ATP U2D
wt-Gal -ATP U2D
28D -ATP U2D
well
P/SP
CC2
CC1

Figure 2: Schematic of single molecule FRET set-up with Ubc4 pre-mRNA. CC1 would be predicted to be generally low FRET because the 5'ss and branch site are not yet brought into consistent proximity by the spliceosome. CC2 would be predicted to be higher FRET because cross-intron bridging interactions between BBP and U1 snRNP protein Prp40 (Abovich and Rosbash 1997) are expected to bring the splice sites into closer proximity.

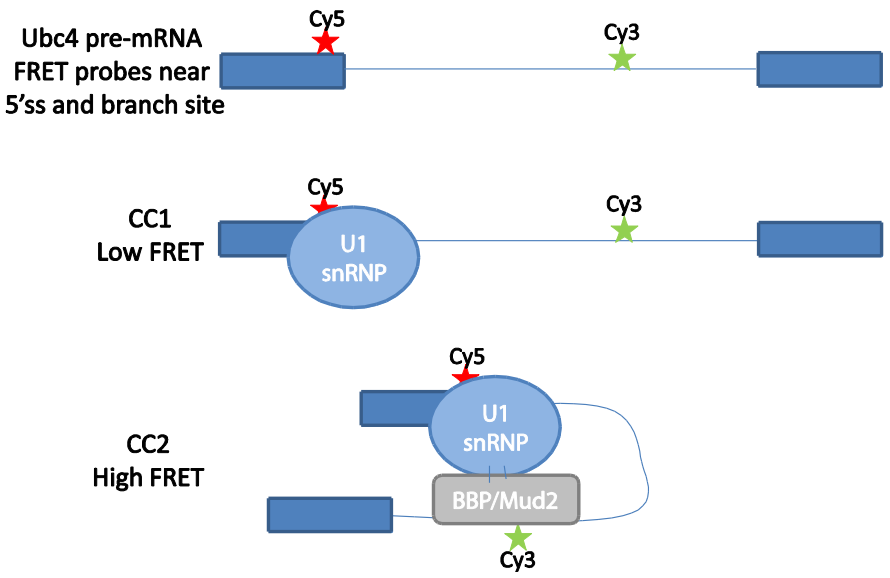

Figure 3: Prp28 depleted extracts cause Ubc4 pre-mRNA to experience primarily high FRET states, and the addition of Prp28 has only small effects on the dynamics of transitions between states. A) Histogram of FRET states of single Ubc4 pre-mRNA molecules interacting with Prp28-depleted splicing reactions + increasing concentrations of Prp28 protein. Several hundred molecules were collected for each condition. B-H) Transition Occupancy Density Plots (TODPs) showing initial FRET on the X axis and final FRET on the Y axis for reactions with increasing concentrations of Prp28 protein.

Figure 3

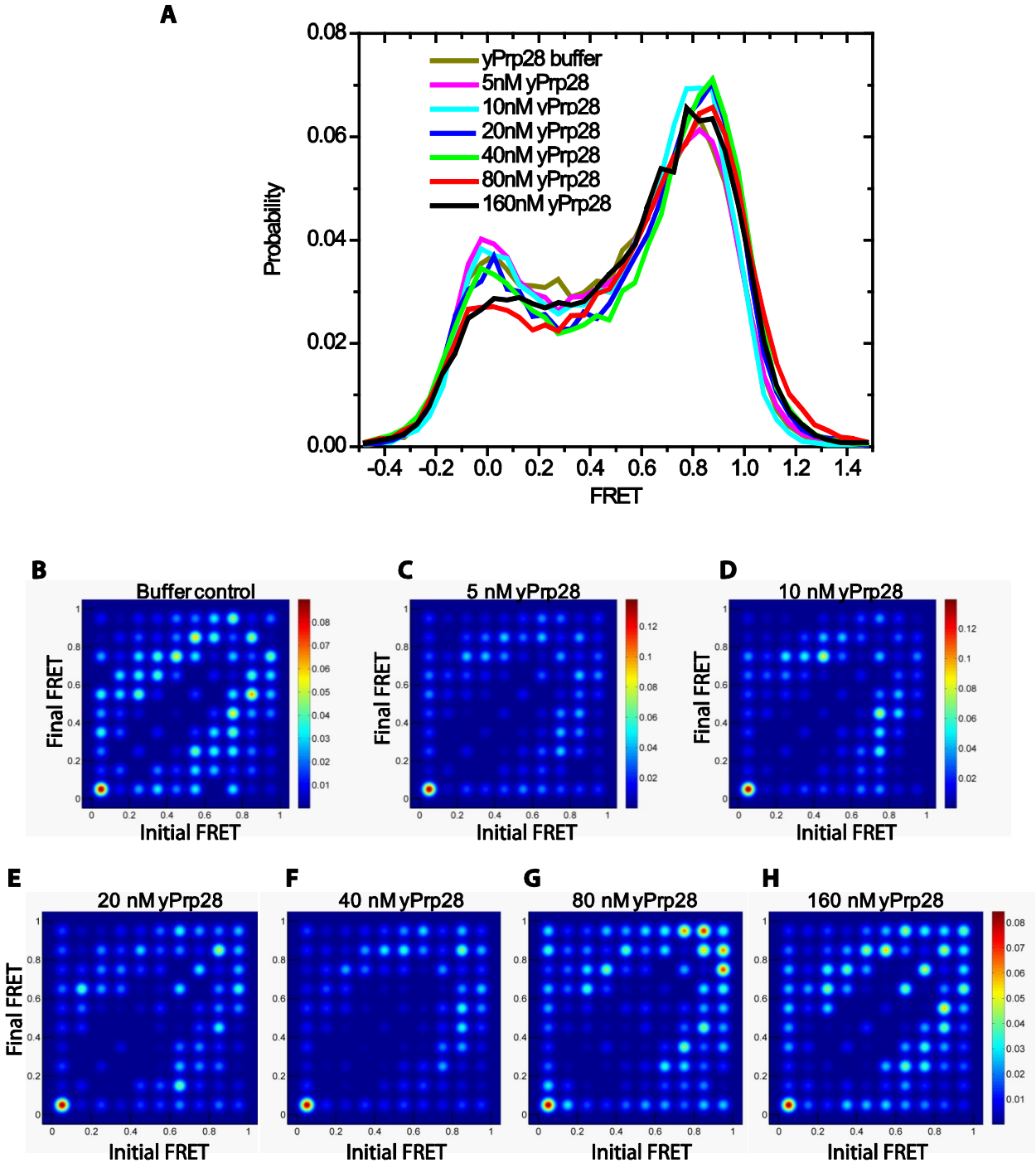
A
yPrp28 buffer
5nM yPrp28
10nM yPrp28
20nM yPrp28
40nM yPrp28
80nM yPrp28
160nM yPrp28
Probability
FRET
B
Buffer control
C
5 nM yPrp28
D
10 nM yPrp28
E
20 nM yPrp28
F
40 nM yPrp28
G
80 nM yPrp28
H
160 nM yPrp28
Final FRET
Initial FRET

Figure 4: Washing splicing extract off of the slide after pre-binding to form commitment complexes reduces the frequency of high FRET state, but Prp28 extracts behave similarly to wild-type. A) Histogram of FRET states of single Ubc4 pre-mRNA molecules interacting with wild-type or Prp28-depleted splicing reactions with or without added Prp28 protein. After an initial round of imaging, the slides were washed with 200 µl BufferD/splicing buffer and re-imaged ("after flowout" histograms) so that we could ask about the stability of the high FRET complexes after free spliceosome was washed away. B-D) TODPs before flow-out; B is a biological replicate of data in Figure 3B. E-G) TODPs after flow-out.

Figure 4

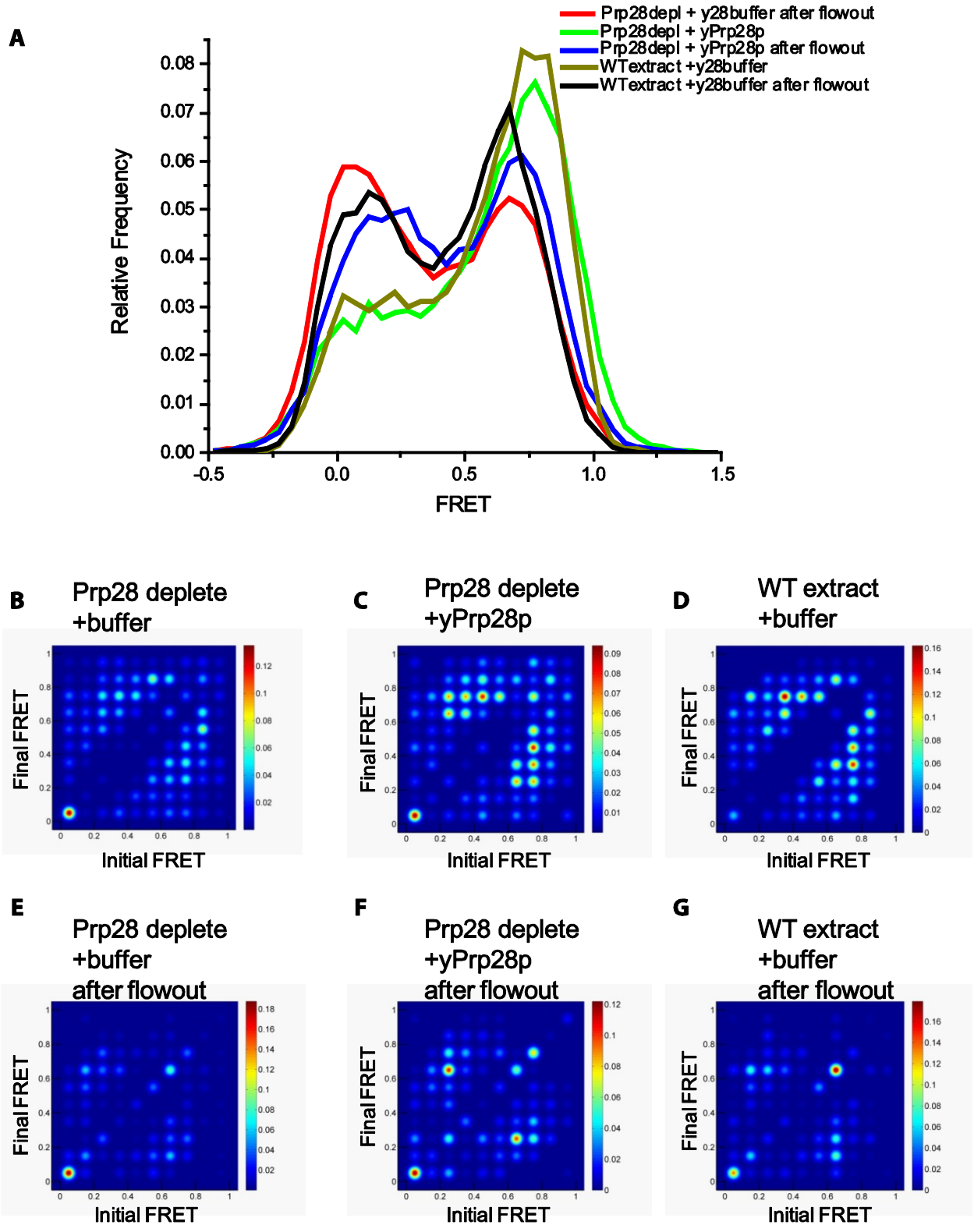
A
Prp28depl + y28buffer after flowout
Prp28depl + yPrp28p
Prp28depl + yPrp28p after flowout
WTextract +y28buffer
WTextract +y28buffer after flowout
Relative Frequency
FRET
B
Prp28 deplete
+buffer
C
Prp28 deplete
+yPrp28p
D
WT extract
+buffer
E
Prp28 deplete
+buffer
after flowout
F
Prp28 deplete
+yPrp28p
after flowout
G
WT extract
+buffer
after flowout
Final FRET
Initial FRET

Figure 5: U2 depleted extracts, which robustly form CC2 and also some CC1, form high FRET states, independent of the presence of Prp28. A) Histograms of the indicated extracts. B-D) TODPs (initial FRET on X axis, final FRET on Y axis) of the indicated extracts.

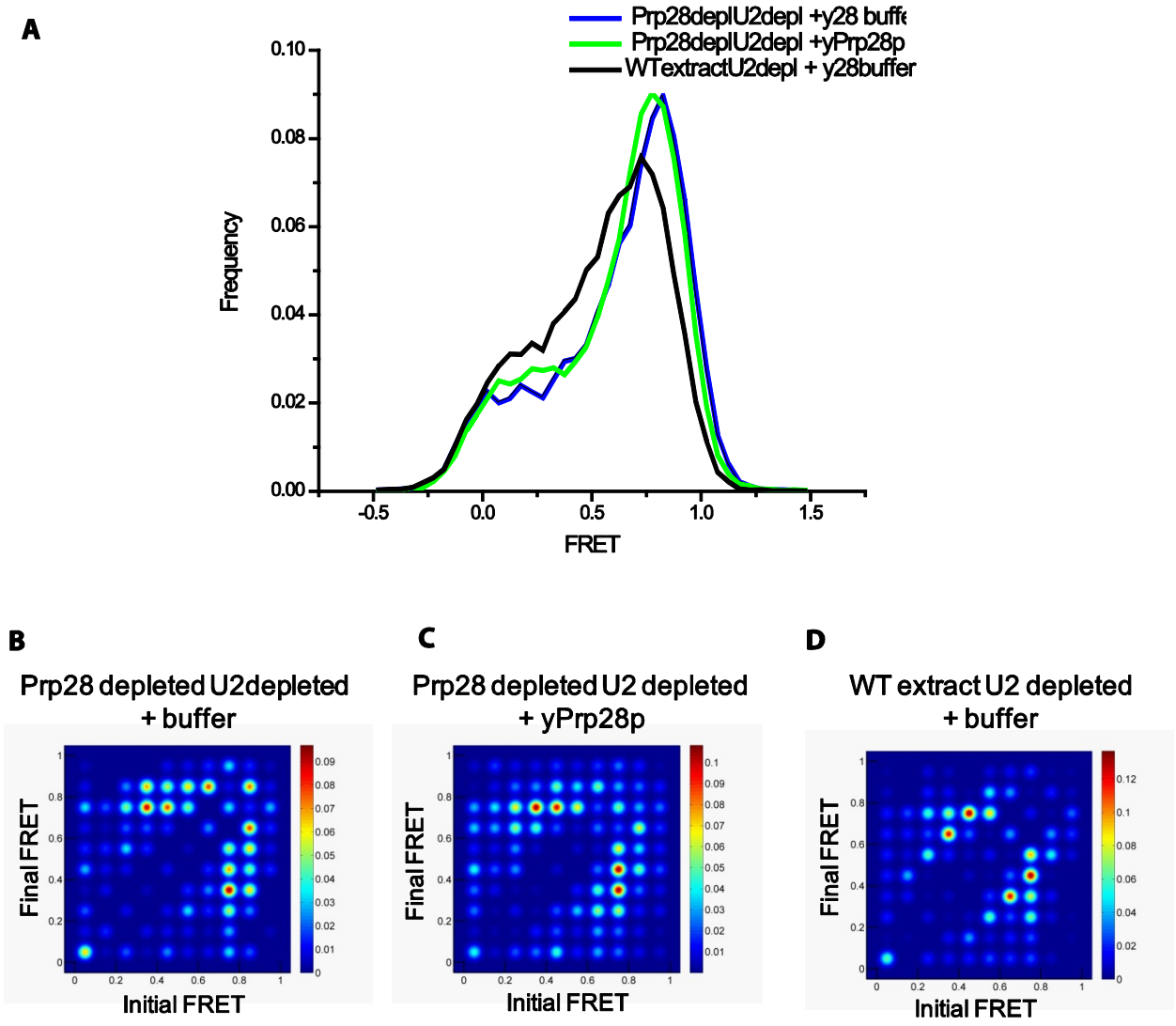

Supplementary Figure 1: Initial round of data and re-analysis of that data from Prp28 depleted extract. A) Histogram of the preliminary data from Prp28 depleted extract. B) Histogram of re-analyzed preliminary data, picking molecules based on the same standards as our other data and analyzing with the newer version of the background software dissection. C-D) Examples of traces of individual molecules that were picked in the re-analysis but not in the initial analysis.

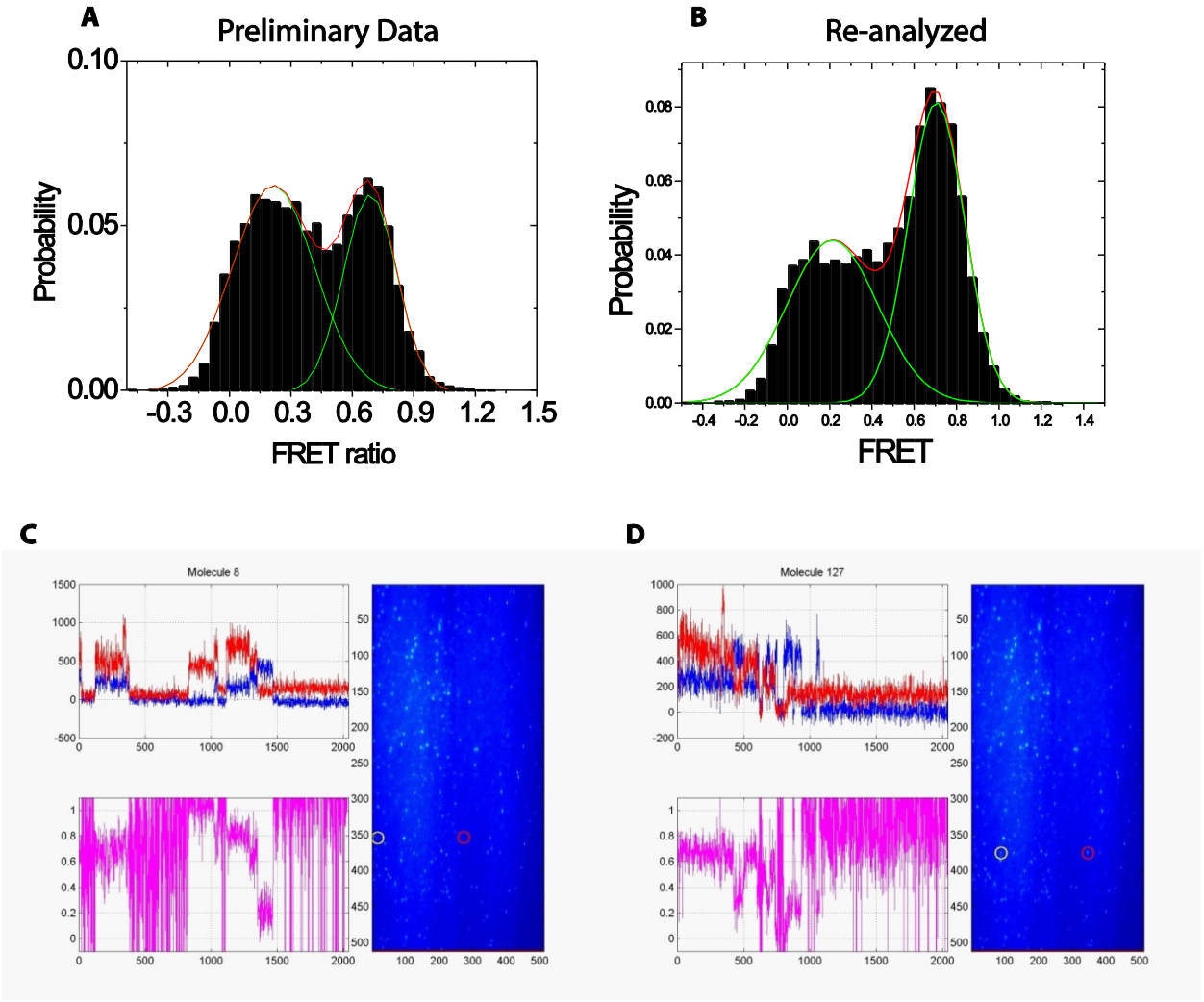

Supplementary Figure 2: Biological replicate controls (A-E) and control with Ded1 protein added (A and F). A) Histogram, and B-E) TODPs.

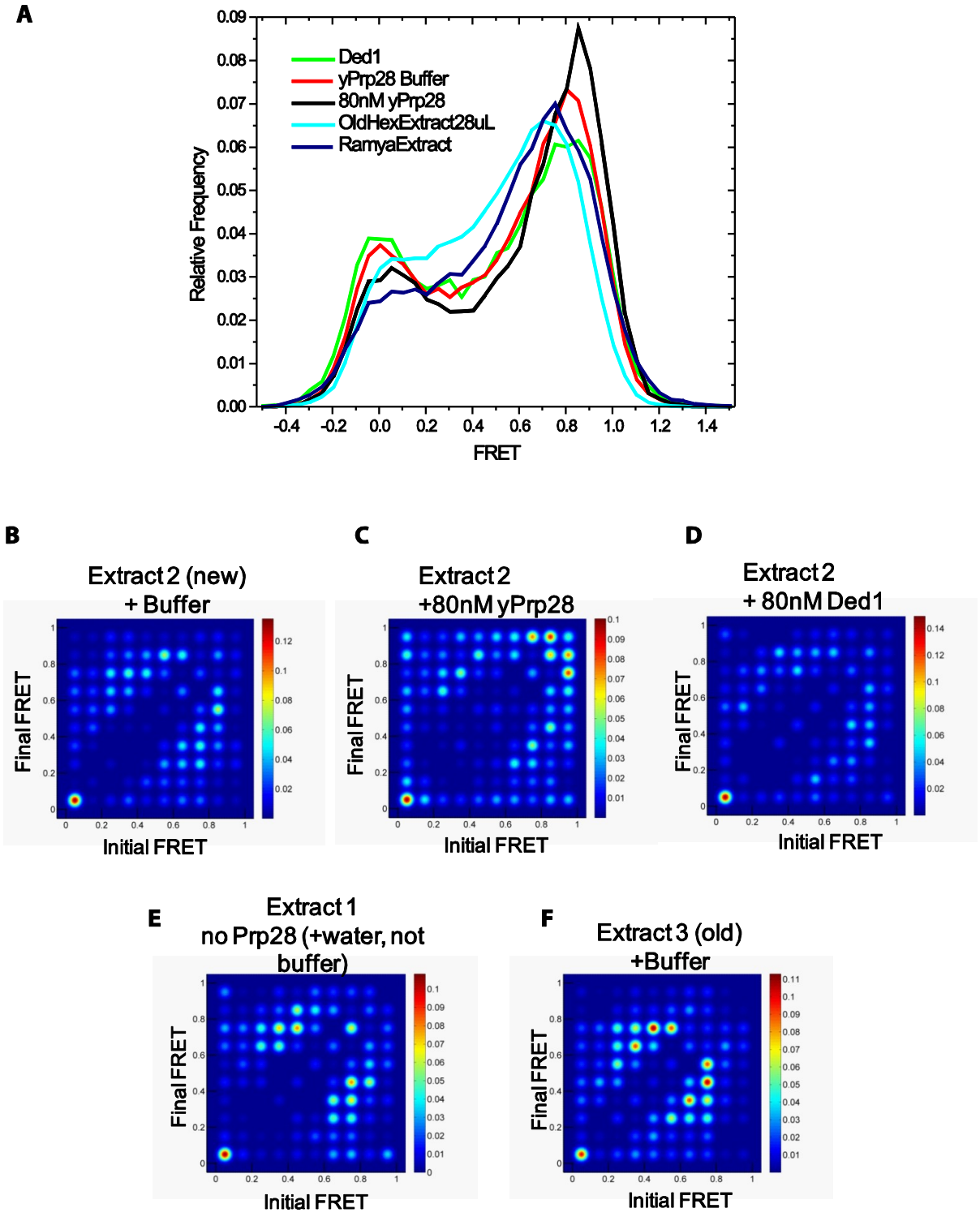

Supplementary figure 3: Histograms of A) wildtype and B) Prp28-depleted extracts interacting with BrC mutant Ubc4 pre-mRNA.

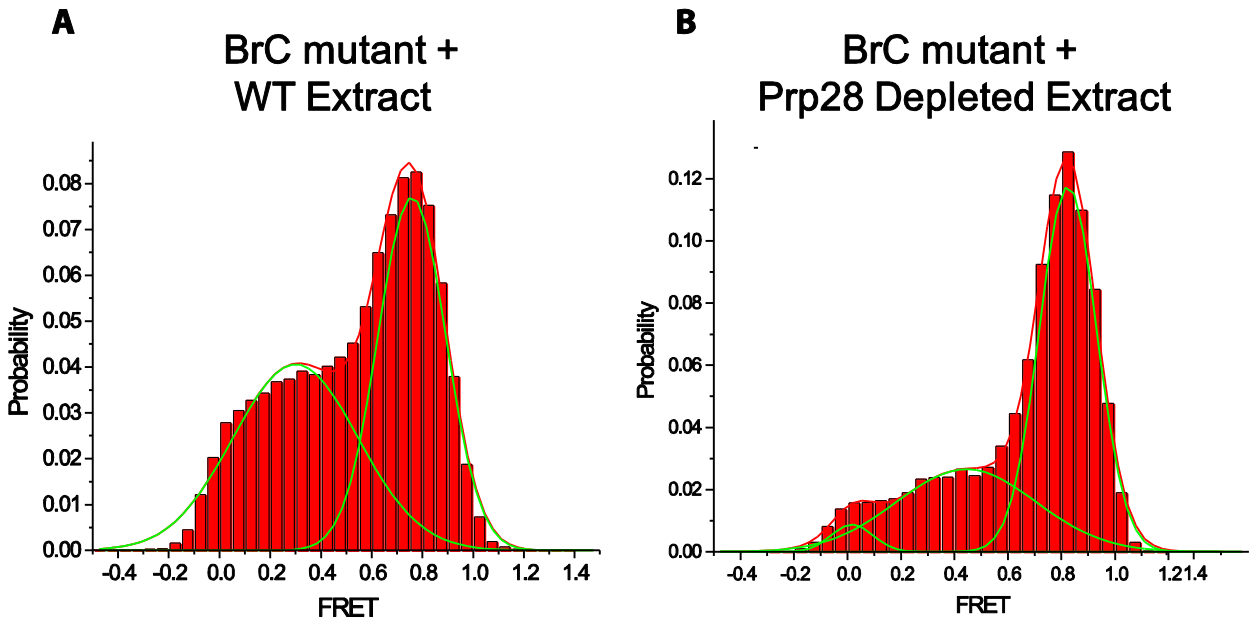

Chapter 3

A conformational change in the RNaseH domain of Prp8 biases the spliceosome toward catalytic or transitional conformations

A conformational change in the RNaseH domain of Prp8 biases the spliceosome toward catalytic or transitional conformations

Argenta Price*, Megan Mayerle*, Sarah Ledoux*, Erica Moehle, Haralambos Hadjivassiliou, Yangzi He, Senen Mendoza, Diana Velazquez, John Abelson, Christine Guthrie

Abstract

The structural rearrangements that take place in the catalytic center of the spliceosome are poorly understood. However, the group II ribozyme, which shares identical chemistry with the spliceosome, is much better understood from a structural perspective. The Pyle lab recently showed that the group II ribozyme toggles between two structurally similar catalytic conformations and rearranges through an obligate "silent" (we will call "transitional") conformation between catalytic steps. Here, we propose that the spliceosome, like the group II ribozyme, must also go through a transitional conformation between two, structurally similar, catalytic conformations. Genetic studies of the U5 snRNP protein Prp8 and other proteins that affect the catalytic steps of splicing led Query and Konarska to propose a two-state model in which the spliceosome transitions between two different catalytic conformations: one for the 1st step of splicing and one for the 2nd step. Mutations in Prp8 bias the spliceosome toward these two functionally distinct conformations. A recent structure, from the MacMillan lab, of the RNaseH domain of Prp8 identified a conformational change in a 17 amino acid hairpin/loop insertion that provides structural context to the different phenotypes of a cluster of 14 of these mutations. We test a model that the previously categorized 1st step alleles in this 17 amino acid insertion instead bias the spliceosome toward its catalytically inactive transitional conformation, and the previously categorized 2nd step alleles instead bias the spliceosome toward its catalytic conformations, which are similar for both steps of splicing. The existing genetic and biochemical

data could support both models, so we test two predictions to differentiate them: 1) catalytic alleles should be generally error prone for mutations that affect both steps of splicing and 2) catalytic alleles should efficiently catalyze the 1st chemical step while transitional alleles should be slow to catalyze the 1st step (if they are instead 1st step alleles, they would efficiently catalyze the 1st step). In support of our model, we found that catalytic alleles suppressed a wide range of mutations in a splicing fidelity reporter and were able to catalyze the 1st step of splicing in vitro similarly to wild-type. Transitional alleles were generally more sensitive to mutations in the splicing reporter, and some of the transitional alleles were unable to catalyze the 1st step of splicing as effectively in vitro.

Introduction

The spliceosome is a dynamic machine composed of five small nuclear RNAs (snRNAs) and over 100 proteins (reviewed in Wahl et al. 2009). It identifies and removes introns from pre-mRNA molecules by catalyzing two sequential trans-esterification reactions. In the first step of splicing, the spliceosome positions the pre-mRNA such that its branch-site Adenosine bulges out, positioning its 2' hydroxyl to attack the 5' splice site (5'ss). This first chemical step forms a branched lariat intermediate structure and a free 5' exon, which the spliceosome holds onto. Next, the spliceosome positions the 5' exon so that its newly formed 3' hydroxyl is properly oriented to attack the 3' splice site (3'ss). The second chemical step of splicing occurs, yielding the ligated pre-mRNA and releasing the branched lariat intron. How the spliceosome enters the first catalytic conformation then rearranges as it transitions between the two steps of catalysis is still poorly understood.

High resolution structures of the whole spliceosome or its catalytic core have not yet been solved, so the conformational changes at its catalytic core remain enigmatic. However structures do exist for the group II ribozyme, which is thought to be the evolutionary precursor of the spliceosome (Gordon et al. 2000). The chemical steps of splicing are identical for pre-mRNA

splicing and for splicing of the group II ribozyme. In the spliceosome, the RNA structure of the ribozyme is replaced by the proteins and RNAs of the spliceosome (Guthrie 1991; Sashital et al. 2004). In particular, the internal stem loop of the U6 snRNA forms a structure similar to stem V of the group II ribozyme, both of which have been shown to coordinate, with similar chemistry, magnesium ions necessary for catalysis (Yean et al. 2000; Fica et al. 2013; Marcia and Pyle 2012; Butcher 2011; Gordon et al. 2000). Because of the analogous chemistry and similarity of known structures, we can extrapolate how the catalytic core of the spliceosome behaves based on the structures of the group II ribozyme,

Interestingly, when Marcia and Pyle (Marcia and Pyle 2012; Marcia et al. 2013) crystallized the group II ribozyme in different monovalent salt conditions, they found that it formed two different conformations: a catalytic conformation that bound two Mg++ ions, and a silent (we will call "transitional") conformation that did not bind Mg++ because of a subtle rotation of two bases. The structures of the catalytic center during the two catalytic steps are remarkably similar. These crystal structures, combined with previous mutagenesis data, showed that the transitional conformation is an obligate conformation through which the ribozyme must transition between the two catalytic steps (Marcia and Pyle 2012; Boudvillain and Marie Pyle 1998; de Lencastre et al. 2005; Mikheeva et al. 2000). Other macromolecular complexes that catalyze sequential reactions, such as the ribosome (Frank and Agrawal 2001; Rodnina and Wintermeyer 2011) also undergo this sort of rearrangement: the enzyme catalyzes its reaction in a catalytic conformation, rearranges through a transitional conformation, and then returns to the catalytic conformation for the next reaction.

We propose that the spliceosome, like other multi-step macromolecular machines, and particularly like the group II ribozyme, must also go through a transitional conformation between two structurally similar 1st and 2nd step catalytic conformations.

The biological significance of this conformational toggling has been well studied in the ribosome (Zaher and Green 2009). Different classes of mutations promote the catalytic or

transitional conformations of the ribosome (called open and closed in conformations in the ribosome literature). In the ribosome, proofreading takes place in the transitional (open) conformation, so ribosomes that are stabilized in the transitional conformation are generally hyper-accurate (Vallabhaneni 2009). In contrast, mutations that stabilize the ribosome's catalytic conformation are generally error prone. In order for the ribosome to function properly, the time it spends in each conformation needs to be optimally balanced. Likewise, we predict that mutations in the spliceosome that disrupt the balance between catalytic and transitional conformations will affect the fidelity of splicing. Mutations that bias the spliceosome toward its catalytic conformation(s) will be error prone while mutations that bias it towards its transitional conformation will be hyper-accurate.

There are several particularly important components of the spliceosome that likely affect the structure of the catalytic core: the U5 snRNP protein Prp8, and the U6 and U2 snRNAs. Prp8 is a massive protein which is an integral component of the U5 and triple-snRNPs. It cross-links to multiple sites on the pre-mRNA (Reyes et al. 1996; Wyatt et al. 1992; Teigelkamp et al. 1997) and interacts genetically with both the pre-mRNA and many other spliceosomal components (for review see Grainger and Beggs 2005). U6, as discussed above, forms a structure that coordinates the essential magnesium ions for catalysis (Fica et al. 2014, 2013). U2 also plays a critical role, base-pairing with both U6 and the pre-mRNA branch sequence and bulging out the branch point A for the first chemical step.

Studies by Query and Konarska (Query and Konarska 2004; Liu et al. 2007; Query and Konarska 2012) identified Prp8 as a key protein that influences two different states of the spliceosome. One class of mutations in Prp8 makes the spliceosome more able to tolerate pre-mRNA mutations such as U2A, BSG, and A302U that inhibit the 2nd chemical step of splicing. Alleles in this class also promote the 2nd step in vivo, shown by primer extension of a BSG template (Query and Konarska 2004; Yang et al. 2008). A second class of mutations in Prp8 makes the spliceosome less tolerant of these same pre-mRNA mutations. By primer extension

of a BSC reporter, which is limiting for the 1st step of splicing, Liu et al. (2007) showed that this class of alleles also improves the 1st step of splicing at the expense of the 2nd step. Query and Konarska proposed an elegant two-state model of splicing catalysis in which the conformations of the spliceosome for the 1st and 2nd catalytic steps are distinct, and are stabilized by the two classes of alleles in Prp8. They also showed that mutations in the U6 snRNA affect the equilibrium between 1st step and 2nd step conformations, but combinations of U6 alleles with Prp8 alleles do not cancel in the same way that combinations of Prp8 alleles cancel each other, which indicates that U6 affects a different aspect of the 1st step to 2nd step conformation than does Prp8 (Liu et al. 2007; Query and Konarska 2012). These different yet similar effects could be because Prp8 and/or U6 actually influence the transitional conformation between catalytic steps rather than strictly promoting different 1st step or 2nd step catalytic conformations. Because the 2nd step Prp8 alleles tolerate a wide variety of pre-mRNA mutations (Siatecka et al. 1999; Query and Konarska 2004; Liu et al. 2007; Yang et al. 2008; Schellenberg et al. 2013) while U6-U57C only tolerates a more specific subset of mutations (our data not shown and Liu et al. 2007), we think that Prp8 is most likely to promote transitional and general catalytic conformations of the spliceosome rather than specific 1st step and 2nd step conformations.

Recent high resolution structures of parts of Prp8 begin to shed light on the structural context of a subset of Prp8 alleles (Figure 1). The structure of the domain of Prp8 that cross-links to the 5'ss has been solved by several labs - it forms an RNaseH-like fold but lacks the catalytic residues necessary for RNaseH activity (Yang et al. 2008; Ritchie et al. 2008; Pena et al. 2008; Galej et al. 2013; Schellenberg et al. 2013). The domain contains a 17 amino acid insertion that forms a β-hairpin, a loop, both, or a β-hairpin in different conformations, depending on the crystallography conditions. Schellenberg et al. (2013) found that when the insertion is in the loop conformation, the RNaseH domain is capable of binding magnesium and its ability to bind this Mg++ is required for second step catalysis. Strikingly, 14 individual mutations have been identified in this 17 aa insertion that have genetic interactions with other components of

the spliceosome and/or affect the fidelity of splicing. Most of these have been classified as either 1st step or 2nd step alleles, based on varying amounts of genetic interaction and primer extension data (Table 1, Collins and Guthrie 1999; Siatecka et al. 1999; Kuhn and Brow 2000; Query and Konarska 2004; Liu et al. 2007; Yang et al. 2008; Schellenberg et al. 2013). Schellenberg et al. (2013) solved crystal structures with four of these previously identified alleles and showed that two 2nd step alleles stabilize the loop conformation (or destabilize the hairpin thereby stabilizing the loop) while two 1st step alleles stabilize the hairpin conformation. By mixing wild-type and mutant proteins during crystallization, they showed that the Prp8 alleles do indeed preferentially form the conformation they stabilize. This provides an attractive structural basis for the different classes of Prp8 alleles. Importantly, all of the crystals in their study were composed of asymmetrical units containing both the loop and hairpin conformations of this insertion (Schellenberg et al. 2013). This indicates that the loop and hairpin conformations are similarly energetically favorable and the spliceosome needs Prp8 to be able to toggle between both structures.

A structure of a larger piece of Prp8 (Galej et al. 2013) shows that the RNaseH domain sits on one side of a cleft; on the other are the reverse-transcriptase and endonuclease-like domains of Prp8. The RNaseH domain cross-links to the 5'ss, and a region immediately across the cleft cross-links to the branch site (Galej et al. 2013; Reyes et al. 1996), suggesting that the catalytic center of the spliceosome lies in that cleft. The loop/hairpin insertion in the RNaseH domain interacts intimately, as a B-hairpin, with the U5 snRNP assembly factor Aar2 (which in the spliceosome is replaced with Brr2), and contacts the C-terminal Jab1/MPN domain of Prp8 (Galej et al. 2013). Therefore, conformational changes in this 17 aa loop/hairpin insertion could dramatically alter the structure of the catalytic core of the spliceosome (Figure 1).

Combining the new structural data for Prp8 and the group II ribosome with previous genetic and biochemical data, we propose that alleles in Prp8 that stabilize the hairpin structure in the RNaseH insertion and were previously classified as 1st step alleles actually bias the

spliceosome toward its transitional conformation. Alleles in this insertion that stabilize the loop structure and were identified as 2nd step alleles actually bias the spliceosome toward similar catalytic conformations for both steps of splicing. The relationships between the structures, previous Prp8 1st step/2nd step classifications, and our new transitional/catalytic classifications are presented in table 2. In this study, we test three main predictions about how spliceosomes biased toward the transitional state will behave in comparison to spliceosomes biased toward the catalytic state. Several of these predictions also allow us to differentiate between spliceosomes that promote the 1st or 2nd catalytic steps instead of stabilizing transitional and generally catalytic conformations.

First, by analogy to the ribosome and other machines that use kinetic proofreading, the transitional conformation would be the conformation that allows for proofreading before the 1st step and between the 1st and 2nd steps of splicing. Therefore, spliceosomes that are biased toward the transitional conformation by hairpin-stabilizing Prp8 mutations will spend more time proofreading and be generally hyper-accurate. In contrast, spliceosomes that are biased toward the catalytic conformation by loop-stabilizing Prp8 mutations will be primed for catalysis on any substrate and generally error prone. Using an array of Act1-Cup1 splicing fidelity reporters, we found that the predicted catalytic alleles are generally error prone while transitional alleles are generally unable to tolerate pre-mRNA mutations, consistent with our hypothesis. We will also use lariat sequencing to assess global in vivo 1st step splicing fidelity.

Second, transitional spliceosomes would be slow to catalyze splicing and therefore inefficient at both steps. Catalytic spliceosomes would be able to efficiently catalyze both steps of splicing, but might have difficulty transitioning between steps. We used in vitro splicing reactions with substrate that is only capable of the 1st step of splicing and found that the predicted transitional alleles, instead of improving the 1st step as they would if they are 1st step alleles, are bad at the first step while the catalytic alleles are able to splice the 1st step efficiently.

Third, catalytic spliceosomes may be able to reduce the requirement for accessory 1st step factors such as Cwc25, which Chiu et al. (2009) and Krishnan et al. (2013) showed is the last factor necessary to kick the spliceosome into its 1st step catalytic conformation. If the Prp8 alleles that were previously classified as 2nd step alleles actually promote a generally catalytic conformation of the spliceosome, they may reduce the requirement for Cwc25. We test this with a combination of genetics and in vitro splicing with Cwc25 depletion and reconstitution.

Results

Reclassification of the two classes of Prp8 RNaseH insertion alleles

Fourteen individual mutations that interact genetically with a variety of spliceosomal components and affect the fidelity of splicing have been identified in the 17 aa hairpin/loop insertion in the RNaseH domain of Prp8. Several were identified in screens for suppressors of pre-mRNA mutations (Siatecka et al. 1999; Collins and Guthrie 1999; Query and Konarska 2004), others were found based on genetic interactions with U4 or U6 snRNAs (Kuhn et al. 1999; Kuhn and Brow 2000; Liu et al. 2007; Query and Konarska 2004), and others were designed based on their position in the Prp8 crystal structure and tested for genetic interactions with splice site mutations (Yang et al. 2008). Many were also shown to genetically interact with other spliceosomal proteins (for example, Kuhn et al. 2002). Table 1 summarizes information about each mutation, how they were initially identified, and whether they have been characterized as alleles that stabilize either the 1st or 2nd step. Schellenberg et al. (2013) showed that two 1st step alleles stabilize the hairpin structure of the RNaseH extension, while two 2nd step alleles stabilize the loop (or destabilize the hairpin). They also predicted based on their structures that a third 2nd step allele (V1870D) would also stabilize the loop. Using the structures from Schellenberg et al. (2013), we modeled in each of the additional mutations and predicted whether they would form or prevent any hydrogen bonds that could stabilize either the hairpin or loop. Based on these predictions combined with whether the alleles were previously

classified as 1st step or 2nd step alleles, we grouped the mutations into what we expected to bias the spliceosome toward transitional or catalytic conformations: 1st step and/or hairpin = transitional; 2nd step and/or loop = catalytic (Table 2). We did not have enough information to classify the V1862A mutation. Our predicted structural effects and predicted categories are also listed in Table 1.

Previous studies on these alleles were conducted in a variety of different strain backgrounds with different sets of genetic interactions tested. We created a set of strains in a consistent background for direct comparison. Each mutation was cloned into Prp8 on a pRS313 (His marked) plasmid transformed into a Prp8 delete strain (covered with Prp8-YCp50 that is later selected against with 5FOA) also that has Cup1 deleted (yAMP24, Price et al. 2014. This strain is similar to strain yJU75 (Umen and Guthrie 1996), which has been used in previous studies). Strains with all of the previously identified Prp8 alleles as their only copy of Prp8 grew similarly to wild-type on rich media, similar to previous studies (Figure 2), though on minimal media, N1869D was slightly temperature sensitive (Figure 2).

The ability of Prp8 to toggle between loop and hairpin structures as the spliceosome toggles between catalytic and transitional conformations should be important for splicing and yeast viability. The result that most of the previously identified alleles grow similarly to wild-type in rich media suggests that these mutations do not stabilize one conformation over the other in a way that is so strong it negatively affects spliceosome function under optimal conditions. To further exacerbate phenotypes caused by stabilizing one conformation over the other, we generated plasmids with multiple mutations that we predicted would extra-stabilize either the loop or hairpin. All four strains with mutations that should extra-stabilize the hairpin were viable, though V1860D+T1865K , V1860D+A1871E, and V1860D+T1865K+T1872E were sick even at 30 degrees (Figure 2). All three strains with two mutations that should extra-stabilize the loop were very sick and picked up suppressors too quickly for us to assess the growth of the strains further. We also deleted the entire 17 aa insertion, on the hypothesis that the absence of hairpin

might function like the loop, but this deletion was lethal. In addition, we generated T1855K, which lies outside of the insertion but would form contacts with several of the mutations that stabilize the hairpin. Yeast with this mutation were also inviable.

Prp8-transitional alleles are accurate and catalytic alleles are error prone

Our first prediction about how spliceosomes biased toward the transitional state would behave in comparison to those biased toward the catalytic conformation is that transitional spliceosomes will be hyper-accurate while catalytic spliceosomes will be error prone. We tested this using the Act1-Cup1 splicing fidelity reporter system developed by (Lesser and Guthrie 1993). In this reporter, the 5' exon and intron from Act1 are fused to the Cup1 gene such that splicing is required for expression of Cup1 protein. The amount of Cup1 protein produced is directly proportional to the amount of copper that yeast can tolerate, so this reporter can be used to measure the efficiency of splicing based on yeast growth on copper (Figure 2A). By using reporter constructs with mutations in the intron, we can ask about the fidelity of splicing - error prone spliceosomes are more efficient at splicing mutant pre-mRNA reporters and will allow yeast to grow on higher concentrations of copper.

All 18 viable (and without suppressors) Prp8 strains were transformed with wt, G1A, U2A, G5A, C256A, BSC, BSG, U301G, A302G, or G303/304C Act1-Cup1 reporter plasmids (Figure 3A). These strains were grown, serially diluted, and plated onto -Leu + CuSO4 plates containing a series of Cu++ concentrations, described in materials and methods. After growth at 30°C for 3-4 days, each strain was scored for the maximum concentration of copper with a small amount of growth. Representative plates at Cu++ concentrations when differences in growth become apparent for BSC and BSG Act1-Cup1 reporters are shown in Figure 3B. Each Cu++ plate contained 6-8 Prp8 strains with the same Act1-Cup1 reporter plasmid, and every plate contained Prp8-wt, prp8-V1860D (transitional), and prp8-V1870D (catalytic) Prp8 alleles with that reporter, so each strain could always be compared to a matched wild-type and control transitional and catalytic allele to control for variability in plate preparation and/or growth

conditions. The ratio of copper tolerance values of each Prp8 mutant vs. its matched wild-type was calculated and Log2 transformed. At least three biological replicates were averaged and the results are plotted in Figure 3C. Blue represents growth on copper worse than wild-type, while yellow represents growth better than wild-type.

The Prp8 alleles that we had classified as transitional are, as predicted, generally less able to tolerate mutations in the Act1-Cup1 intron - they are hyper-accurate across a broad array of reporter mutations. Similarly as predicted, the alleles that we had classified as catalytic are generally better at splicing mutant Act1-Cup1 reporters and are therefore error prone. The alleles that we could not classify based on previous data appears to be a strong transitional alleles, though V1862D has a mixed phenotype depending on the Act1-Cup1 reporter, which is unsurprising given that Yang et al.(2008) reported that that allele behaved similarly to wild-type with the reporters they tested. These results are more comprehensive than, but consistent with, previous Act1-Cup1 data reported for some of these alleles in the literature (Query and Konarska 2004; Liu et al. 2007; Yang et al. 2008; Schellenberg et al. 2013). Aside from a couple of alleles that have been studied extensively with this assay (notably V1870D), this is a more extensive array of cup reporter data within the same strain background, showing that the hyper accuracy or error prone nature of the Prp8 mutants broadly affects mutations in the 5'ss, branch, and 3'ss.

There are exceptions. For example, G1A is not spliced any less efficiently by the transitional alleles, possibly because wild-type is already very inefficient at splicing this mutant reporter. Query and Konarska (2004) previously reported a similar inability of Prp8 alleles to suppress G1A. In addition, there are a few Prp8 alleles that are generally hyper-accurate but splice one or two reporters more efficiently than wild-type. Similarly there are a couple generally error prone alleles that splice a reporter less efficiently than wild-type. There are also differences in the strength of individual alleles. This variability is expected. Different alleles will stabilize the loop or hairpin to different degrees, which may affect the ability to transition from

transitional to catalytic spliceosome differently thus causing variability in the degree of tolerance of particular splice site mutations. The splice site mutations themselves also inhibit different aspects of splicing (Liu et al. 2007), so it is not surprising that different Prp8 mutations would affect different reporters to different degrees. The results in aggregate strongly support our model that catalytic spliceosomes (stabilized by mutations that stabilize the loop structure of Prp8's RNaseH insertion) are generally error prone, while transitional spliceosomes (stabilized by mutations that stabilize the hairpin structure of Prp8's RNaseH insertion) are generally hyper-accurate.

Global effects of Prp8 Transitional/Catalytic alleles on splicing fidelity

The Act1-Cup1 reporter assay allows us to measure the fidelity of splicing by requiring splicing for growth using a single reporter gene using strong mutations in the splice sites. Because it introduces mutations that the spliceosome does not ordinarily encounter, we decided to investigate the fidelity of splicing during normal growth. The spliceosome encounters natural variation in splice site sequences in the approximately 260 intron containing genes in yeast. The spliceosome also uses cryptic and alternative splice sites at some frequency, even in yeast (Kawashima et al. 2014). These natural errors that the spliceosome makes in vivo could tell us more about the general error prone or hyper-accurate nature of the different Prp8 mutations. We plan to use lariat sequencing in collaboration with Jeff Pleiss to measure the global fidelity of the first step of splicing (Awan et al. 2013). Lariat sequencing will tell us the sequence of the 5'ss and branch that was used in each spliced lariat, from which we can identify aberrant, cryptic, or previously unknown splice sites as well as compare the frequency of splicing at consensus vs. non-consensus splice sites.

We compared several methods for isolating lariats for sequencing. Using Dbr1Δ strains, we isolated RNA, then used 2D gels as described in Awan et al. (2013) to isolate lariats. We compared that method to using a RiboMinus kit followed by RNaseR, and Xrn1 to deplete rRNA and degrade other linear RNAs. We compared these methods using RT-qPCR and looked at

the enrichment of lariat vs. exon for three genes with different sized lariats. Our results are presented in Supplementary Figure 1, but we have not yet determined the best method for isolating lariats, because only in some cases did we enrich for lariat above the abundance in total RNA. This could be because our RNA preparations were nicked or degraded before analysis. Once we have decided on the best (good enough enrichment + easy enough) method for isolating lariats, we will send them to Jeff Pleiss for sequencing. Reverse transcriptase reads through the 2'-5' linkage between the 5'ss and branch point a small proportion of the time (Awan et al. 2013), which will result in sequencing reads through 5'ss then skipping to the branch site (see supplementary figure 1). The sequence of the 5'ss and branch that was used in each sequenced lariat can then be mapped to the genome so that we can identify non-consensus, aberrant, cryptic, or previously unknown splice sites.

Our hypothesis is that Prp8-catalytic alleles will generally be more error prone and will splice genes with non-consensus splice sites more efficiently while also having an increase in use of aberrant and cryptic splice sites that are not normally used by wild-type spliceosomes. The Prp8-transitional alleles might be even more accurate than wild-type, but we are not yet sure how much dynamic range we will have (wild type is expected to be fairly accurate already). Interestingly, because the lariat sequencing will be looking at the fidelity of the product of the first step of splicing (lariats), this assay should allow us to determine whether transitional alleles are instead biasing the spliceosome toward the first step of splicing - if they are, they might actually decrease the fidelity of lariat choice and we would see results opposite to our predictions. These experiments are currently underway.

Some transitional alleles are inefficient at the first step of splicing in vitro

The second prediction from our model is that spliceosomes biased toward the transitional conformation will be slow and inefficient at completing the first step of splicing, while catalytic-biased spliceosomes will be able to catalyze both steps quickly. We used in vitro splicing reactions with actin pre-mRNA truncated after the branch (Schellenberg et al. 2013) to

monitor the efficiency of the first step of splicing. This substrate is truncated before the 3'ss and does not undergo the second step of splicing, which simplifies quantification of just the first step of splicing. Since the sequence of the pre-mRNA is otherwise wild-type, this assay measures speed and efficiency of the 1st step, not fidelity.

Splicing reactions were incubated at various temperatures (25, 30, 33, and 37 °C) to exacerbate potential defects in the first step of splicing, because none of the yeast strains exhibited strong growth defects in rich media. Figure 4A shows time courses of the first step of splicing in extracts from three Prp8 alleles. The first step of splicing was inhibited in a temperature-dependent manner in extract made from one of the transitional Prp8 alleles - V1860D. The catalytic allele, V1870N, spliced the first step as efficiently and quickly as wild-type. This experiment was repeated with extracts from multiple different Prp8 alleles and also with different extract preparations from the same strain to determine the reproducibility and generality of the transitional allele causing a 1st step defect. We quantified the Lariat/pre-mRNA ratio, shown in Figure 3B-C for the gels shown plus additional Prp8 alleles tested at 33 and 37 °C. Repeats of these gels are still in progress so we have not yet confirmed that differences in extract batch quality cannot account for the observed differences in 1st step efficiency, but the temperature dependency of the defect is suggestive of a defect caused by the Prp8 mutation, not extract quality. Extracts from different strains do have different effects on 1st step efficiency. Notably, V1860D has a TS defect, but A1871E splices like wild-type. However, the combination of V1860D and A1871E exhibits an even stronger TS defect, suggesting that while A1871E does not inhibit the 1st step in vitro itself, it exacerbates the defect caused by V1860D, consistent with both alleles stabilizing a non-catalytic state of the spliceosome.

These data support our model that transitional Prp8 alleles stabilize a transitional state instead of a 1st step catalytic conformation because at least some transitional alleles are inefficient at the first catalytic step of splicing, while the catalytic alleles are competent at the first step. These transitional alleles have been previously characterized as alleles that improve the

first step of splicing based on genetics and primer extension of Act1-Cup1 reporters. However, our in vitro experiment shows that they are in fact less efficient at catalyzing the first step of splicing in vitro.

Prp8-catalytic alleles do not allow bypass of Cwc25

Several 1st step accessory factors are required for the spliceosome to form its 1st step catalytic conformation and actually catalyze the 1st step of splicing. DEAH-box ATPase Prp2 with its co-factor Spp2 catalyze rearrangements in the spliceosome, then Cwc25 binds and finally kicks the spliceosome into its 1st step conformation ((Krishnan et al. 2013; Chiu et al. 2009)). Chiu et al. (2009) showed that Cwc25 binds after the activity of Prp2 and is essential for efficient 1st step catalysis. In addition, Krishnan et al. (2013) used single molecule FRET to show that Cwc25 is the factor that finally causes the 5'ss and branch site stably be in close proximity (ie the 1st step has occurred). Therefore, binding of Cwc25 may change the conformation of the spliceosome from its pre-1st step transitional state into its catalytic conformation. Our third prediction to test whether Prp8 alleles stabilize catalytic and transitional conformations of the spliceosome was that Prp8 alleles that stabilize the catalytic conformation would reduce the requirement for Cwc25.

We tested whether Prp8 alleles that we predict bias the spliceosome toward its catalytic conformation would be able to bypass the normally essential Cwc25 gene. We mated our Prp8/Cup1 delete strain with a Cwc25 delete strain carrying Cwc25 on a Leu plasmid. After passing the diploid several times on media to maintain the Prp8 plasmid but allow passive loss of the Cwc25 plasmid, we obtained diploids heterozygous for Prp8 and Cwc25 with a plasmid for Prp8-wt or one of 5 catalytic alleles or 6 transitional alleles (including a double-hairpin allele). The diploids were sporulated and tetrads dissected. If any of the Prp8 alleles allowed bypass of Cwc25, we would see tetrads with more than two viable spores. The viability of any of these that have Prp8 deleted depends on that spore also containing the Prp8 plasmid, but the Prp8 plasmid was constantly selected for in the diploid up until sporulation, so it shouldn't have been

lost too frequently. Many tetrads had one or two viable spores, but in no case did we see more than two viable spores (Figure 5). None of the Prp8 alleles, whether transitional or catalytic, allowed bypass of Cwc25. However, to bypass the essential nature of Cwc25, the Prp8 alleles would have had to promote the catalytic or 1st step conformation of the spliceosome strongly enough to completely overcome the function that Cwc25 normally performs; that is a tall order.

Prp8 catalytic alleles may reduce the requirement for Cwc25 in vitro.

The Prp8 alleles are viable and most likely able to toggle between conformations relatively easily, because we believe the ability to transition between these conformations is important for splicing. It is therefore not surprising that the Prp8 alleles were unable to bypass Cwc25. We are now using an in vitro approach to determine whether Prp8 mutants can reduce the requirement for Cwc25 for the first step of splicing even though they cannot bypass it entirely.

Extracts were prepared from yeast strains containing different Prp8 alleles and HA-tagged Cwc25. HA antibody can be used to deplete Cwc25 from these extracts, which prevents splicing in vitro (Chiu et al. 2009 and data not shown). We are in the process of titrating in purified Cwc25 protein to determine how much Cwc25 is required for in vitro splicing in several different Prp8 backgrounds. These data will tell us whether any Prp8 alleles push the balance toward a spliceosomal conformation that is catalytic for the first step of splicing, thus reducing the amount of Cwc25 required for first step catalysis. We predict that catalytic alleles will allow splicing to occur with lower amounts of Cwc25 than wild-type or transitional alleles.

Discussion

We and others (Schellenberg et al. 2013; Yang et al. 2008; Liu et al. 2007; Query and Konarska 2004) have shown that the 17aa insertion in the RNaseH fold of Prp8 affects the catalytic function of the spliceosome by promoting two distinct states of the spliceosome. Our data show that the conformation promoted by one set of alleles is generally error prone,

efficiently catalyzes the first step of splicing in vitro, and we are investigating if it reduces the need for 1st step factor Cwc25. Most of the Prp8 alleles in this category have been previously characterized as 2nd step alleles, based on their ability to promote the second step of splicing. We re-classify them as "catalytic" alleles because our data suggests they promote a catalytic conformation of the spliceosome, which should be similar for both steps of splicing (by analogy to the group II ribozyme - Marcia et al. 2013). The other set of alleles promote a state that is generally hyper-accurate, is less efficient at promoting the 1st step of splicing in vitro, and we are investigating whether it doesn't change or even increases the need for Cwc25 for the 1st step of splicing. Most of the Prp8 alleles in this category have been previously characterized as 1st step alleles which improve the 1st step of splicing on a BrC mutant splicing reporter. We propose that these alleles in fact stabilize the transitional conformation of the spliceosome as it rearranges between the first and second catalytic steps. We call this set of alleles "transitional" alleles. Our model for the roles of the different classes of Ppr8 alleles is represented in Figure 6.

We used a variety of Act1-Cup1 reporters at the 5'ss, branch site, and 3'ss to show that the catalytic alleles are generally error prone and the transitional alleles are generally accurate. All of these pre-mRNA mutations inhibit the second step of splicing in vivo (Lesser and Guthrie 1993; Liu et al. 2007). Several also affect the first step, but only BSC is actually limiting for the first step (Liu et al. 2007). Because of this, we can't easily use this assay to differentiate between whether the catalytic alleles are error prone because they promote the 2nd step of splicing or because they stabilize the catalytic conformation of the spliceosome. However, none of our catalytic alleles strongly suppress the BSC mutation, which could support the model that these alleles promote the 2nd but not 1st step catalytic conformation. In addition, this assay cannot differentiate between transitional and 1st step alleles. We would expect 1st step alleles to improve the 1st step, but they would still make yeast growth worse and appear hyper-accurate by this growth assay because they would inhibit the 2nd step. Transitional alleles would make both steps of splicing less efficient, so would also result in less growth on copper. Therefore,

these results are consistent with both models about the role of Prp8 alleles in the transitions at the catalytic steps of splicing.

Previous studies have used primer extension to more specifically see whether the 1st or 2nd step is improved or inhibited by some of these Prp8 strains with specific Act1-Cup1 reporter constructs. They found that 1st step alleles such as V1860D in fact improve the 1st step of splicing of the BSC reporter (Yang et al. 2008; Schellenberg et al. 2013) while 2nd step alleles such as V1870N improve the 2nd step of splicing of the BSG reporter but do not improve the 1st step (Query and Konarska 2004; Liu et al. 2007; Schellenberg et al. 2013). The two-state model proposed by Query and Konarska (Query and Konarska 2004; Liu et al. 2007; Query and Konarska 2012; Konarska and Query 2005) is strongly supported by these data. However, we believe that this primer extension data could also be consistent with the model that 1st step alleles instead promote the spliceosome's transitional conformation. In our model, the spliceosome must transition through its transitional conformation between the 1st and 2nd catalytic steps. Transitional alleles would therefore stabilize the conformation that forms immediately after the 1st step of splicing, while also inhibiting the 2nd step of splicing and possibly making the backwards reaction less likely. This would lead to accumulation of products of the 1st step of splicing in vivo. We also predict that the spliceosome would also form its transitional conformation before the first step of splicing. Therefore, our model requires that the energy well for the transitional state between catalytic steps be deeper than the well for the transitional state prior to the 1st step. The catalytic conformations would be high energy intermediate states (Figure 5B).

In vitro experiments measuring the efficiency of the 1st step of splicing and the requirement for 1st step factor Cwc25 allow us to more directly probe whether the catalytic alleles (aka 2nd step alleles) and not the transitional alleles (aka 1st step alleles) actually catalyze the 1st step of splicing efficiently. In support of our model, our results show that the 1st step of splicing is inhibited in a temperature-dependent manner by some transitional alleles, but not

catalytic alleles. One caveat is that these alleles could also affect the assembly of the spliceosome, and thus reduce the efficiency of the 1st step because earlier assembly steps are inhibited, not specifically because they are bad at catalyzing the 1st step.

The model in which opposing classes of Prp8 alleles promote either the 1st or 2nd step of splicing is not necessarily mutually exclusive with our model that the spliceosome toggles between catalytic and transitional conformations. The 1st and 2nd step catalytic conformations must be slightly different because the lariat-intermediate 2nd step substrate is structurally different from the pre-mRNA 1st step substrate. This would allow sub-sets of Prp8 alleles to affect either the 1st step/2nd step equilibrium or the catalytic/transitional conformation, or both, depending on the Prp8 allele. Many mutations have been identified elsewhere in Prp8 that also affect the fidelity of splicing and the equilibrium between 1st step and 2nd step, perhaps in different ways. Other alleles in Prp8 do not affect this transition but interact with other components, indicating that the functions of Prp8 are diverse and central to spliceosome function.

Conformational changes in Prp8 stabilize catalytic and transitional conformations of the spliceosome's catalytic core within the larger context of the spliceosome as a whole. Conformational changes in other parts of the spliceosome have also been reported that affect the catalytic nature of the spliceosome, so it will be interesting to investigate how those components work together. The U6 snRNA forms a stem-loop that coordinates the two catalytic magnesium ions, and mutations in the U6 snRNA near this stem-loop were shown to affect the fidelity of splicing in similar but subtly different ways to the Prp8 alleles described here (McPheeters 1996; Liu et al. 2007). These subtly different effects indicate that the structures of the two catalytic conformations and their transitional conformation are more complicated and may entail multiple slightly different conformations that are affected differently by mutations in different components of the spliceosome. Indeed, Liu et al. (2007) proposed that Prp8 1st step alleles could affect substrate repositioning, which we would expect to happen in the transitional

conformation, while U6 alleles could affect the opening and closing of the catalytic center - a different function that would also influence the transitional vs. catalytic conformation.

Interestingly, the U2 snRNA also toggles between two conformations. It forms two mutually exclusive base-pairing interactions, stem IIa and stem IIc and has been shown to toggle between these conformations during spliceosome assembly and during catalysis (Perriman and Ares 2007; Hilliker et al. 2007). Data using Act1-Cup1 reporters has been used to conclude that U2 forms its stem IIc conformation in the active, catalytic form of the spliceosome, and forms stem IIa during spliceosome assembly and when the spliceosome is transitioning between the 1st and 2nd catalytic step (Perriman and Ares 2007; Hilliker et al. 2007). The parallel sets of data and conclusions involving the U2 and Prp8 conformational changes leads to interesting questions about whether and how U2 and Prp8 collaborate to form the catalytic center of the spliceosome. Even if Prp8 alleles promote specifically different 1st step and 2nd step catalytic conformations of the splcieosome instead of catalytic and transitional conformations, the U2 and U6 snRNAs or other components of the spliceosome may change conformations to form the transitional conformation. We will only fully understand how these components work together once we have structures of the catalytic core of the spliceosome.

Materials and Methods

Yeast strains and plasmids

Strains and plasmids used in this chapter are described in supplementary table 1.

In vitro splicing assays

Splicing extracts from each strain of yeast were prepared as described in Price et al. (2014) from 3 L yeast grown to OD 1.6-1.8. For 1st step splicing assays, Actin pre-mRNA truncated after the branch (described in Schellenberg et al. 2013) was transcribed (Megascript T7 kit - Ambion) with 5% of the UTP replaced by Cy5-labeled UTP, then gel purified and tested empirically for concentration of RNA that gave good visibility of lariat product on splicing gels

(turned out to be ~1 nM final concentration; 10 fmol loaded per lane). 70 µl splicing reactions (Lin et al. 1985) containing 28 µl extract (approximately 50 mg/ml) in Buffer D, 60 mM KPO4 pH 7, 3% PEG 8000, 2.5 mM MgCl2 were pre-incubated at the reaction temperature for 2-3 minutes. Then 8.4 µl of 1st step pre-mRNA + ATP was added to start the reaction (final concentration 2 mM ATP and ~1 nM pre-mRNA). 10 µl aliquots were removed and stopped on ice at the indicated time points. After the final time point, 5 µl of Proteinase K mix (2.5 µl Proteinase K (Roche), 2.5 µl PK buffer: 2% SDS, 100 mM Tris pH 8, 100 mM EDTA) was added and samples were spun briefly then incubated at ~55°C for 10 minutes. Finally 15 µl Formamide loading dye (96% Formamide, 20 mM EDTA, Bromophenol Blue) was added and samples were run on denaturing 6% acrylamide (19:1)-urea-TBE gels. Gels were scanned for Cy5 on a Typhoon scanner and bands quantified using Image J (Schneider et al. 2012). For 1st step gels, only the lariat product and pre-mRNA precursor were quantified because the free 5' exon tended to have very low signal - similar intensity to background smudges. Graphs reported indicate the ratio of lariat/pre-mRNA.

Yeast growth assays

Strains containing Act1-Cup1 splicing reporters were grow in SD -Leu media to maintain the reporter plasmid. Overnight cultures were back-diluted then allowed to grow at 30°C for 2-4 doublings (3-7 hours) to log phase (OD 0.3-0.7), then were diluted again to OD 0.1 and serially diluted 5 times in 4-fold dilutions and spotted onto SD -Leu plates with the following Cu++ concentrations (mM): 0, 0.013, 0.025, 0.05, 0.75, 0.1, 0.18, 0.25, 0.3, 0.4, 0.5, 0.75, 1.0, and 1.5 mM. Strains wt, V1860D (transitional allele), and V1870N (catalytic allele) were grown with every set of strains to allow direct comparisons and control for differences in number of doubling times, final OD, and media or plate batch. For any given set of strains, the amount of dilution and final OD was similar, except for the double-mutant strains which tended to grow more slowly and therefore had to be back-diluted and frogged at lower OD than the corresponding wild-type and other alleles. Strains were grown on Cu++ plates at 30°C for 3-4 days before

being scored for maximum concentration of copper on which they were viable - small colonies in the most concentrated spot of yeast were considered "viable." If two strains of the same set were both able to tolerate the same maximum concentration of copper, but one grew clearly better or worse than the other, we adjusted the "tolerated copper" value up by 10% (or down by 10% if one strain grew worse than several others on the same plate but still had the same maximum concentration tolerated). To generate figure 2B, these values were Log2-transformed (because the concentrations of copper on which yeast were grown were generally double the previous concentration with a few extras added in) then the wild-type yeast value was subtracted from the value for each Prp8 mutant. Log2-transformed growth relative to wild-type was averaged for 3-X biological replicates then color-scaled: bright blue = -1.5 or more (Log2 fold worse than wt), black = equal to wt, bright yellow = +1.5 or more (Log2 fold better than wt). Yeast strains without Act1-Cup1 reporters were grown in YPD or -His media, and back diluted then spotted as described above onto plates and temperatures as indicated.

Test for bypass suppression of Cwc25

A cwc25Δ::Kan strain covered with a Cwc25-Leu plasmid was crossed to Prp8 mutant strains. Diploids were selected on +Kan/-His plates, then passaged 2x on -His plates, grown overnight in -His media, then plated for single colonies on -His plates. These plates were replica plated onto -Leu and colonies that did not grow on -Leu (had lost the Cwc25 plasmid) were grown on -His then sporulated for 5-10 days. Tetrads were dissected and numbers of viable spores recorded. Two plates (22-24 tetrads) were dissected for each Prp8 allele.

Lariat isolation

Dbr1Δ yeast with various Prp8 mutant alleles were grown to OD 0.6. 15 ml culture was spun down and frozen, then RNA extracted with hot acid phenol as described (Pleiss et al. 2007). RNA was resuspended in water to concentration ~5 µg/µl. We tested several methods for isolation of lariats: 2D gels and RNase digestions. The gels were 7.5% acrylamide + urea/TBE

in the 1st dimension, then 15% in the second dimension run similar to the method described for Pombe lariat isolation in Awan et al. (2013).

We compared side-by side three different ways of extracting RNA from three separate 2D gels run with the same batch of RNA: a conservative cut-out of the off-diagonal RNA eluted overnight at 4 °C in RNA elution buffer, a similar conservative cut-out of the off-diagonal RNA followed by transfer to a Hybdond N+ membrane then stripping the membrane and concentrating with sec-butanol to allow for smaller volume ethanol precipitation, or taking essentially everything above the diagonal that wasn't clearly a clump of rRNA and eluting overnight in RNA elution buffer (0.3 M NaOaC, 1 mM EDTA) then treating with RNaseR and Terminator RNases. We also compared these gel based methods to treating 10 ng total RNA with the RiboMinus kit, then treating with units RNaseR and Terminator enzymes at 37°C for 2 hr and phenol-chloroform extracting the RNA.

We compared these methods by RT-qPCR of several genes with varying lariat lengths. Supplementary figure 2 shows the distribution of lariat sizes in *Saccharomyces cerevisiae* (based on information in Ares lab database, Grate and Ares 2002). RNA from each method was resuspended in 20 µl H2O and quantified by nanodrop. 8 µl of the enzyme-treated (not gel) sample was treated with 1 U DNase, phenol chloroform extracted, and re-precipitated. 1 µg of total RNA was similarly treated with DNase. 4-8 µl of each sample (277 ng Total no RT, 323 ng Total + RT, 109 ng Enzyme treated, 160 ng Lariat gel transferred, 77 ng Lariat gel eluted then enzyme treated) was reverse transcribed with 250 nM random 9-mer primer and superscript III RT following the manufacturer's instructions. Unfortunately all of the "standard" gel sample was used up while troubleshooting the RT reaction and qPCR reactions with different RT conditions. After RT, the samples were diluted 1:20 and 10 µl was used in a 25 µl qPCR reaction with NEB Taq. 300 ng of primers for the intron (primer pairs between 5'ss and branch) and exon 2 of Scs22, Asc1, and Rps24b were used in each qPCR reaction. Genomic DNA from S288C was

used for a standard curve. Supplementary figure 1 shows results of intron/exon sample vs. total (normalized to ng of RNA put into the RT reaction).

References

Awan AR, Manfredo A, Pleiss JA. 2013. Lariat sequencing in a unicellular yeast identifies regulated alternative splicing of exons that are evolutionarily conserved with humans. *Proc Natl Acad Sci* 201218353.

Boudvillain M, Marie Pyle A. 1998. Defining functional groups, core structural features and inter-domain tertiary contacts essential for group II intron self-splicing: a NAIM analysis. *EMBO J* **17**: 7091–7104.

Butcher SE. 2011. The spliceosome and its metal ions. *Met Ions Life Sci* **9**: 235–251.

Chiu Y-F, Liu Y-C, Chiang T-W, Yeh T-C, Tseng C-K, Wu N-Y, Cheng S-C. 2009. Cwc25 Is a Novel Splicing Factor Required after Prp2 and Yju2 To Facilitate the First Catalytic Reaction. *Mol Cell Biol* **29**: 5671–5678.

Collins CA, Guthrie C. 1999. Allele-specific genetic interactions between Prp8 and RNA active site residues suggest a function for Prp8 at the catalytic core of the spliceosome. *Genes Dev* **13**: 1970–1982.

Fica SM, Mefford MA, Piccirilli JA, Staley JP. 2014. Evidence for a group II intron-like catalytic triplex in the spliceosome. *Nat Struct Mol Biol* **21**: 464–471.

Fica SM, Tuttle N, Novak T, Li N-S, Lu J, Koodathingal P, Dai Q, Staley JP, Piccirilli JA. 2013. RNA catalyses nuclear pre-mRNA splicing. *Nature* **503**: 229–234.

Frank J, Agrawal RK. 2001. Ratchet-like movements between the two ribosomal subunits: their implications in elongation factor recognition and tRNA translocation. *Cold Spring Harb Symp Quant Biol* **66**: 67–75.

Galej WP, Oubridge C, Newman AJ, Nagai K. 2013. Crystal structure of Prp8 reveals active site cavity of the spliceosome. *Nature* **493**: 638–643.

Gordon PM, Sontheimer EJ, Piccirilli JA. 2000. Metal ion catalysis during the exon-ligation step of nuclear pre-mRNA splicing: extending the parallels between the spliceosome and group II introns. *RNA* **6**: 199–205.

Grainger RJ, Beggs JD. 2005. Prp8 protein: at the heart of the spliceosome. *RNA* **11**: 533–557.

Grate L, Ares M. 2002. Searching yeast intron data at Ares lab Web site. *Methods Enzymol* **350**: 380–392.

Guthrie C. 1991. Messenger RNA splicing in yeast: clues to why the spliceosome is a ribonucleoprotein. *Science* **253**: 157–163.

Hilliker AK, Mefford MA, Staley JP. 2007. U2 toggles iteratively between the stem IIa and stem IIc conformations to promote pre-mRNA splicing. *Genes Dev* **21**: 821–834.

Kawashima T, Douglass S, Gabunilas J, Pellegrini M, Chanfreau GF. 2014. Widespread use of non-productive alternative splice sites in Saccharomyces cerevisiae. *PLoS Genet* **10**: e1004249.

Konarska MM, Query CC. 2005. Insights into the mechanisms of splicing: more lessons from the ribosome. *Genes Dev* **19**: 2255–2260.

Krishnan R, Blanco MR, Kahlscheuer ML, Abelson J, Guthrie C, Walter NG. 2013. Biased Brownian ratcheting leads to pre-mRNA remodeling and capture prior to first-step splicing. *Nat Struct Mol Biol* **20**: 1450–1457.

Kuhn AN, Brow DA. 2000. Suppressors of a cold-sensitive mutation in yeast U4 RNA define five domains in the splicing factor Prp8 that influence spliceosome activation. *Genetics* **155**: 1667–1682.

Kuhn AN, Li Z, Brow DA. 1999. Splicing factor Prp8 governs U4/U6 RNA unwinding during activation of the spliceosome. *Mol Cell* **3**: 65–75.

Kuhn AN, Reichl EM, Brow DA. 2002. Distinct domains of splicing factor Prp8 mediate different aspects of spliceosome activation. *Proc Natl Acad Sci U S A* **99**: 9145–9149.

De Lencastre A, Hamill S, Pyle AM. 2005. A single active-site region for a group II intron. *Nat Struct Mol Biol* **12**: 626–627.

Lesser CF, Guthrie C. 1993. Mutational analysis of pre-mRNA splicing in Saccharomyces cerevisiae using a sensitive new reporter gene, CUP1. *Genetics* **133**: 851–863.

Lin RJ, Newman AJ, Cheng SC, Abelson J. 1985. Yeast mRNA splicing in vitro. *J Biol Chem* **260**: 14780–14792.

Liu L, Query CC, Konarska MM. 2007. Opposing classes of prp8 alleles modulate the transition between the catalytic steps of pre-mRNA splicing. *Nat Struct Mol Biol* **14**: 519–526.

Marcia M, Pyle AM. 2012. Visualizing group II intron catalysis through the stages of splicing. *Cell* **151**: 497–507.

Marcia M, Somarowthu S, Pyle AM. 2013. Now on display: a gallery of group II intron structures at different stages of catalysis. *Mob DNA* **4**: 14.

McPheeters DS. 1996. Interactions of the yeast U6 RNA with the pre-mRNA branch site. *RNA New York N* **2**: 1110–1123.

Mikheeva S, Murray HL, Zhou H, Turczyk BM, Jarrell KA. 2000. Deletion of a conserved dinucleotide inhibits the second step of group II intron splicing. *RNA* **6**: 1509–1515.

Pena V, Rozov A, Fabrizio P, Luhrmann R, Wahl MC. 2008. Structure and function of an RNase H domain at the heart of the spliceosome. *EMBO J* **27**: 2929–2940.

Perriman RJ, Ares M Jr. 2007. Rearrangement of competing U2 RNA helices within the spliceosome promotes multiple steps in splicing. *Genes Dev* **21**: 811–820.

Pleiss JA, Whitworth GB, Bergkessel M, Guthrie C. 2007. Transcript specificity in yeast pre-mRNA splicing revealed by mutations in core spliceosomal components. *PLoS Biol* **5**: e90.

Price AM, Görnemann J, Guthrie C, Brow DA. 2014. An unanticipated early function of DEAD-box ATPase Prp28 during commitment to splicing is modulated by U5 snRNP protein Prp8. *RNA New York N* **20**: 46–60.

Query CC, Konarska MM. 2012. CEF1/CDC5 alleles modulate transitions between catalytic conformations of the spliceosome. *RNA* **18**: 1001–1013.

Query CC, Konarska MM. 2004. Suppression of multiple substrate mutations by spliceosomal prp8 alleles suggests functional correlations with ribosomal ambiguity mutants. *Mol Cell* **14**: 343–354.

Reyes JL, Kois P, Konforti BB, Konarska MM. 1996. The Canonical GU Dinucleotide at the 5' Splice Site Is Recognized by P220 of the U5 snRNP Within the Spliceosome. *RNA* **2**: 213–225.

Ritchie DB, Schellenberg MJ, Gesner EM, Raithatha SA, Stuart DT, MacMillan AM. 2008. Structural elucidation of a PRP8 core domain from the heart of the spliceosome. *Nat Struct Mol Biol* **15**: 1199–1205.

Rodnina MV, Wintermeyer W. 2011. The ribosome as a molecular machine: the mechanism of tRNA-mRNA movement in translocation. *Biochem Soc Trans* **39**: 658–662.

Sashital DG, Cornilescu G, McManus CJ, Brow DA, Butcher SE. 2004. U2-U6 RNA folding reveals a group II intron-like domain and a four-helix junction. *Nat Struct Mol Biol* **11**: 1237–1242.

Schellenberg MJ, Wu T, Ritchie DB, Fica S, Staley JP, Atta KA, LaPointe P, MacMillan AM. 2013. A conformational switch in PRP8 mediates metal ion coordination that promotes pre-mRNA exon ligation. *Nat Struct Mol Biol* **20**: 728–734.

Schneider CA, Rasband WS, Eliceiri KW. 2012. NIH Image to ImageJ: 25 years of image analysis. *Nat Methods* **9**: 671–675.

Siatecka M, Reyes JL, Konarska MM. 1999. Functional interactions of Prp8 with both splice sites at the spliceosomal catalytic center. *Genes Dev* **13**: 1983–1993.

Teigelkamp S, Mundt C, Achsel T, Will CL, Lührmann R. 1997. The human U5 snRNP-specific 100-kD protein is an RS domain-containing, putative RNA helicase with significant homology to the yeast splicing factor Prp28p. *RNA* **3**: 1313–1326.

Umen JG, Guthrie C. 1996. Mutagenesis of the yeast gene PRP8 reveals domains governing the specificity and fidelity of 3' splice site selection. *Genetics* **143**: 723–739.

Vallabhaneni H. 2009. *Translational Accuracy: Ribosomal Protein-protein Interactions and Stop Codon Recognition by Variant-code Release Factors*. ProQuest.

Wahl MC, Will CL, Lührmann R. 2009. The spliceosome: design principles of a dynamic RNP machine. *Cell* **136**: 701–718.

Wyatt JR, Sontheimer EJ, Steitz JA. 1992. Site-specific cross-linking of mammalian U5 snRNP to the 5' splice site before the first step of pre-mRNA splicing. *Genes Dev* **6**: 2542–2553.

Yang K, Zhang L, Xu T, Heroux A, Zhao R. 2008. Crystal structure of the B-finger domain of Prp8 reveals analogy to ribosomal proteins. *Proc Natl Acad Sci* **105**: 13817–13822.

Yean SL, Wuenschell G, Termini J, Lin RJ. 2000. Metal-ion coordination by U6 small nuclear RNA contributes to catalysis in the spliceosome. *Nature* **408**: 881–884.

Zaher HS, Green R. 2009. Fidelity at the molecular level: lessons from protein synthesis. *Cell* **136**: 746–762.

Table 1: Prp8 alleles in the RNaseH insertion: origins, classification, and structural prediction.

Prp8 allele	References	Originally found how?	1st step/ 2nd step classification
V1860D	Kuhn and Brow 2000; Yang et al. 2008	U4-cs1 suppression	1st
V1860N	Kuhn and Brow 2000	U4-cs1 suppression	?
V1862D	Kuhn and Brow 2000; Yang et al. 2008	U4-cs1 suppression	?
T1865K	Yang et al. 2008	designed in hairpin/loop	1st
A1871E	Yang et al. 2008	designed in hairpin/loop	1st
T1872E	Yang et al. 2008	designed in hairpin/loop	1st
T1861P	Kuhn et al. 1999; Schellenberg et al. 2013	U4-cs1 suppression	2nd
V1862Y	Kuhn and Brow 2000; Schellenberg et al. 2013	U4-cs1 suppression	2nd
V1862A	Kuhn and Brow 2000	U4-cs1 suppression	?
H1863E	Yang et al. 2008	designed in hairpin/loop	2nd
K1864E	Collins and Guthrie 1999	5'ss suppression	2nd
N1869D	Siatecka et al. 1999; Collins and Guthrie 1999; Query and Konarska 2004	5'ss (and other splice site) suppression	2nd
V1870N	Query and Konarska 2004; Liu et al. 2007	BSG suppression	2nd
I1875T	Kuhn and Brow 2000	U4-cs1 suppression	?

Prp8 allele	Position (human Prp8)	Structural prediction (bold = Schellenberg et al. 2013)	Reason for structural prediction (based on structure of human protein from Schellenberg et al.)	Prediction: Catalytic or Transitional
V1860D	V1788	**hairpin**	Structure solved: H-bond with Y1786 stabilizes hairpin	Transitional
V1860N	V1788	hairpin	H-bond with Y1786	Transitional?
V1862D	I1790	hairpin	H-bond with T1800	Transitional?
T1865K	T1793	hairpin	H-bond with N1797?	Transitional
A1871E	T1799	hairpin	H-bond with H1791	Transitional
T1872E	T1800	**hairpin**	Structure solved: Water-mediated H-bond with Y1786 stabilizes hairpin	Transitional
T1861P	T1789	**loop**	Structure solved: proline disrupts hairpin	Catalytic
V1862Y	I1790	**loop**	Structure solved: H-bond with N1797 stabilizes loop	Catalytic
V1862A	I1790	?	?	?
H1863E	H1791	loop	?	Catalytic
K1864E	K1792	loop	?	Catalytic
N1869D	N1797	loop	?	Catalytic
V1870N	L1798	**loop**	Structure predicted.: H-bond with G1796	Catalytic
I1875T	I1803	loop	H-bond with R1787	Catalytic?

Table 2: Relationship between Prp8 RNaseH insertion structures and classifications of functions of Prp8 alleles

Structure stabilized in insertion in RNaseH domain	**1st step/2nd step Classification**	**Transitional/Catalytic Classification**	**Prp8 alleles in this class**
Hairpin	1st step	Transitional	V1860D, V1860N, V1862D, V1862A, T18675K, A1871E, T1872E
Loop	2nd Step	Catalytic	T1861P, V1862Y, H1863E, K1864E, N1869D, V1870N, I1875T

Figures

Figure 1: Mutations can stabilize either the loop or hairpin conformation of Prp8's RNaseH domain extension. A) Structure (PDB ID: 4I43 Galej et al. 2013) of the C-terminal 2/3 of Prp8. The RNaseH domain is highlighted in blue, and the 17 aa insertion (which is in the hairpin conformation in this structure) is teal. B) The RNaseH domain insertion can form either a loop or hairpin conformation. This structure (PDB ID: 4JK7 Schellenberg et al. 2013) shows the two different conformations - hairpin (yellow-green) or loop (blue) and their change in orientation. C) Structure of the RNaseH domain with the insertion in its hairpin conformation (PDB ID: 4JK7 Schellenberg et al. 2013). Mutations in the loop/hairpin insertion used in this study are highlighted. Mutations that favor the spliceosome's catalytic conformation and the insertion's loop conformation are highlighted in blue. Mutations that favor the spliceosome's transitional conformation and the insertion's hairpin conformation are highlighted in yellow. Different substitutions in one position (green) can bias the spliceosome to either conformation. Aside from the four mutations actually shown by Schellenberg et al. (2013) to stabilize the loop or hairpin, the mutations are assigned to each category based on our predictions (from genetic phenotype or analysis of the structure).

Figure 1

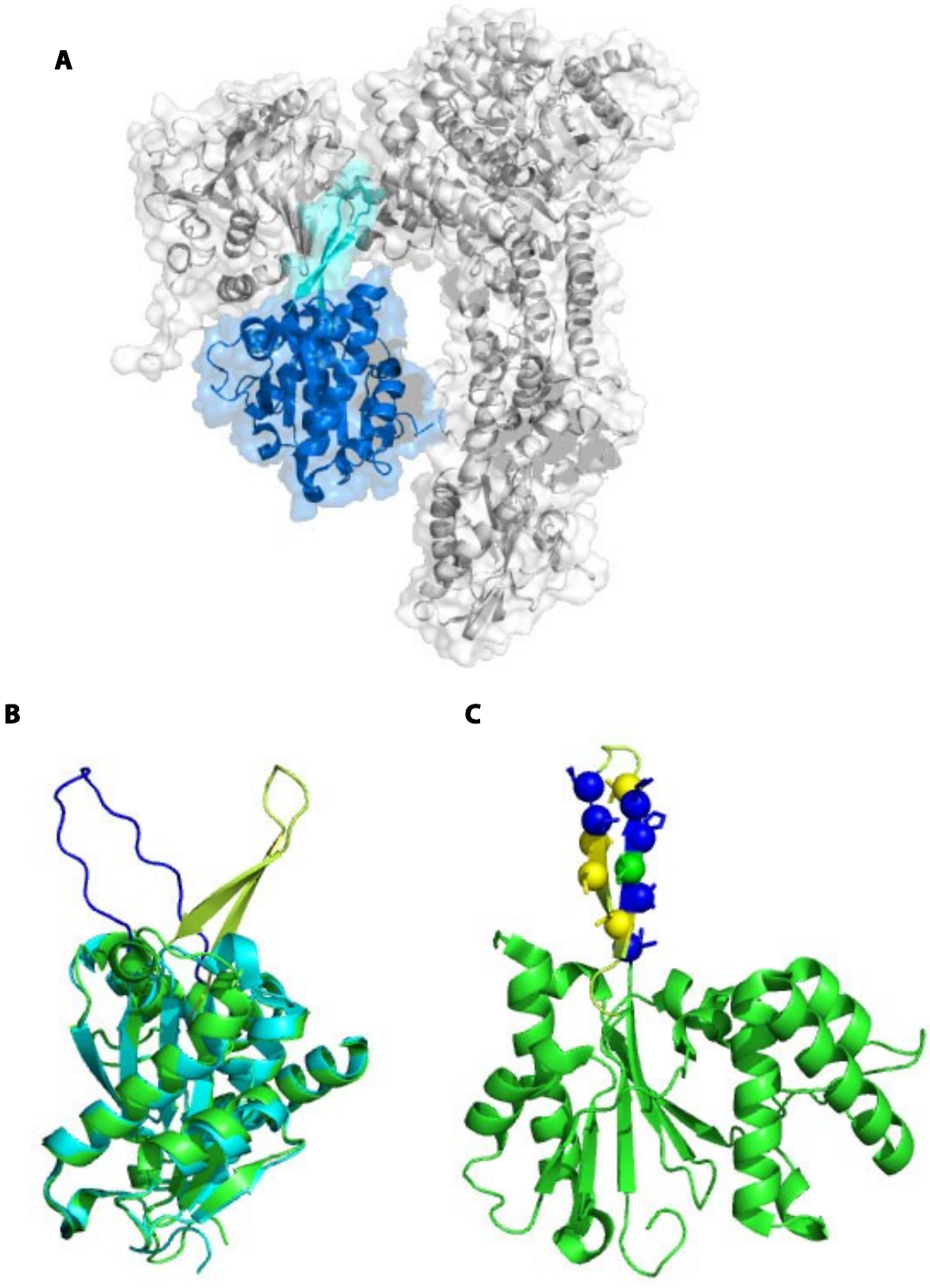

Figure 2: Prp8 alleles used in this study in general do not have growth defects, except for double and triple mutants. Strains were grown in YDP and plated in serial dilutions on -His plates at various temperatures.

-His, 37 degrees

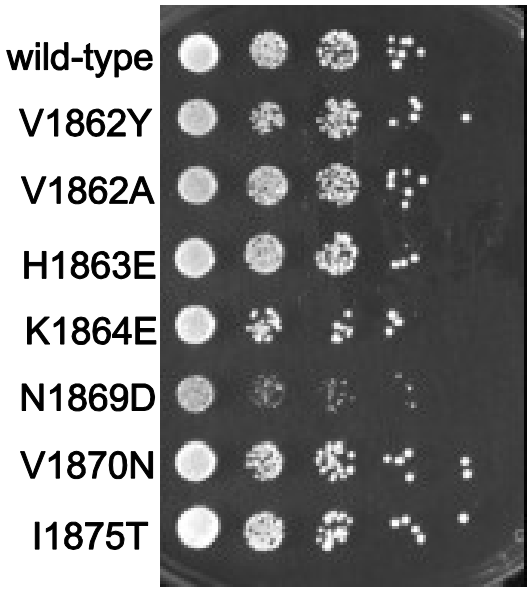

-His, 37 degrees

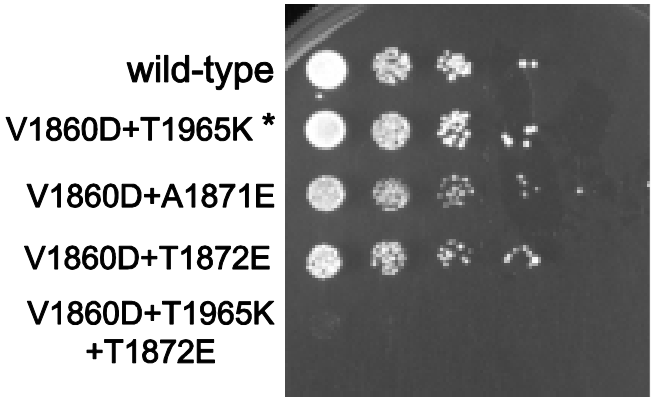

-His, 30 degrees

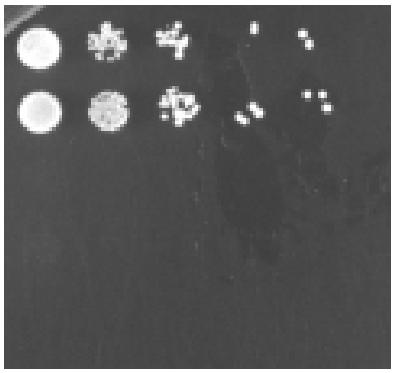

-His, 37 degrees

* normally very sick - picked up suppressor

Figure 3: Prp8 alleles in the RNaseH extension fall into two classes: generally hyper-accurate or generally tolerant of pre-mRNA mutations. A) Schematic (adapted from Query and Konarska 2004) of the Act1-Cup1 reporter system, in which the Cup1 gene is fused to the 5' exon and intron of Act1 such that splicing is required for expression of Cup1 and growth on copper. Red letters: mutations in the intron used in this study to test splicing fidelity. B) Serial dilutions of wt and Prp8-RNaseH mutant yeast plated onto the indicated concentrations of copper. Left panel: Act1-Cup1 reporter with the branch site A mutated to C (BSC), which with a wild-type spliceosome inhibits both the 1^{st} and 2^{nd} step of splicing and is limiting for the 1^{st} step (Liu et al. 2007). Right panel: Act1-Cup1 reporter with the branch site A mutated to G (BSG) which with a wild-type spliceosome inhibits the 2^{nd} step of splicing (Liu et al. 2007). C) Summary of all of the Prp8 alleles tested and all of the Act1-Cup1 reporter mutations tested. Strains were scored based on the maximum concentration of copper they were able to tolerate, then their copper tolerance was compared to that of Prp8-wt yeast containing the same Act1-Cup1 reporter. The numbers, which are the average of at least 3 biological replicates, indicate the Log2-transformed copper tolerance of each strain relative to wild-type. The colors indicate growth on copper better than wild-type (yellow) or growth worse than wild-type (blue); black indicates growth the same as wild-type.

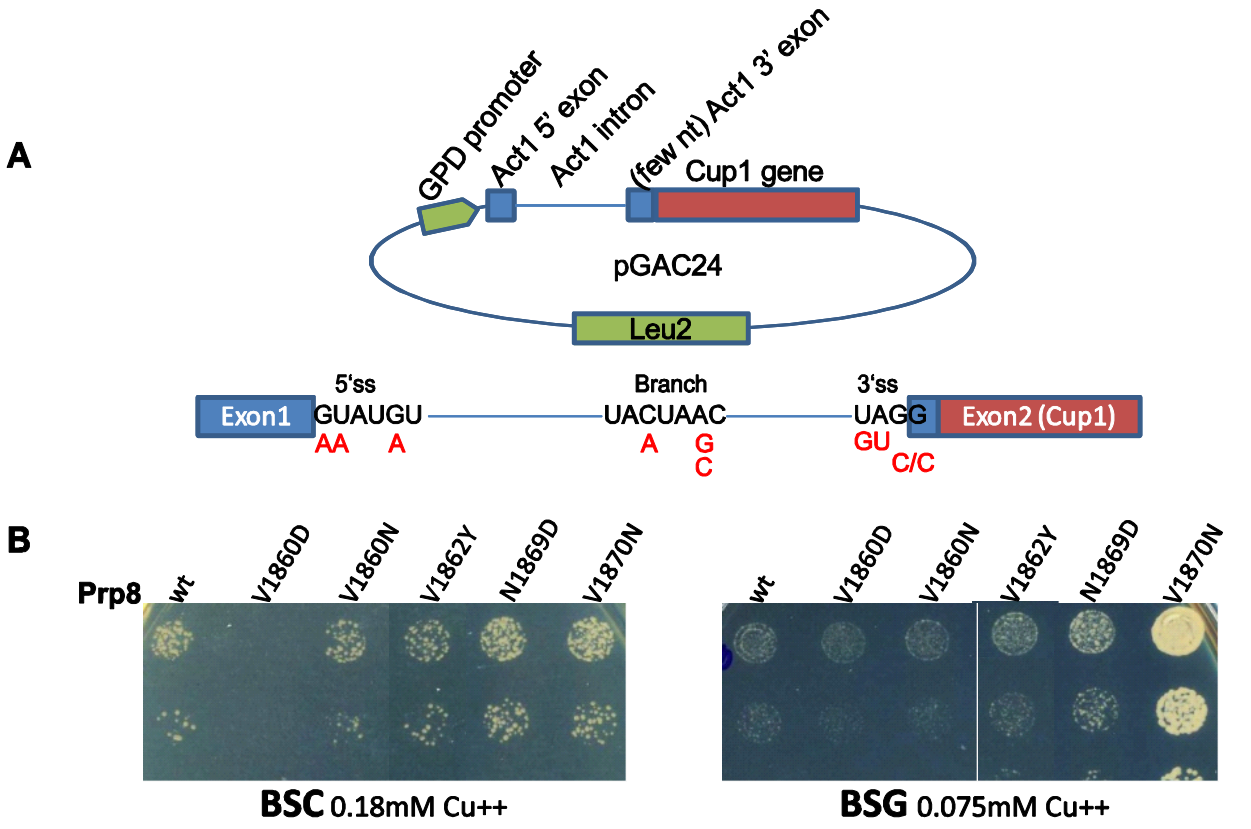

C

Act1-Cup1 reporter

Prp8 allele	wt	G1A	U2A	G5A	C256A	BSC	BSG	U301G	A302G	G303/4C	Classification (predicted):
	5'ss				Branch			3'ss			
wild-type											
V1860D	0.0474	-0.0507	-0.0507	-0.256	0.0615	-0.8074	-0.0965	-0.4875	-0.1576	-0.0862	Transitional
V1860N				-0.0459		-0.316	-0.0965	-0.1073	-0.0507	-0.3382	Transitional
T1865K				-0.7125	0.384	-0.3137		-0.969	-0.2767		Transitional
A1871E			-0.4717		0.0459	-0.2086	-0.0507	-1.2778	-0.7037	0.1842	Transitional
T1872E			-0.421		0.0877	-1.7888	-0.1383	-1.2778	-0.9863	-0.1383	Transitional
V1860D+T1965K	-1.1998	-0.8987	-1.1315	-1.3023	-0.926	-1.774	-0.8927	-3.8746	-1.3219	-1.848	Transitional
V1860D+A1871E	-0.6208	-0.3752	-0.7962	-0.4973	-0.2767	-0.6951	-0.5594	-3.7363	-1.1247	0.6315	Transitional
V1860D+T1872E	-0.195		0.2457		0.0877				-0.5653		Transitional
V1860D+T1965K +T1872E	-0.963	-1.1315	-1.424	-1.8813	-1.768	-1.2653	-1.1383	-3.8746		-1.848	Transitional
V1862D			-0.0507	-0.4609		-0.0459	0.4668	0.4543	0.4543	-0.2875	?
V1862A	-3.2402	-0.616	-0.9493	-1.1668	-0.811	-1.4406	-0.9493	-1.1269	-1.0877		?
T1861P			0.0468	0.0615					0.0918		Catalytic
V1862Y		-0.0507	-0.0507			-0.316	0.0418	0.353		-0.2875	Catalytic
H1863E		0.2555	0.8246		0.1335	0.1802	0.1375	1.1884	0.6297	0.3225	Catalytic
K1864E		0.232	0.195		0.1335	0.0925	0.0459	0.158	0.384	0.5594	Catalytic
N1869D	0.0507		0.848	-0.0459		0.0917	0.0877	0.768	0.6052	0.0917	Catalytic
V1870N		0.0685	1.2479		0.3889	0.0616	1.2958	1.5309	1.6837	0.795	Catalytic
Log2 difference from wt:				-1.5	-1	-0.5	0	0.5	1	1.5	

Figure 4: Some transitional Prp8 alleles are inefficient at the 1st step of splicing in vitro. A) Time course of in vitro splicing using a Cy5 labeled Actin pre-mRNA molecule that lacks the 3' exon but is able to proceed through the first step of splicing (Schellenberg et al. 2013). Splicing reactions with wild-type, V1860D (transitional) and V1870N (catalytic) extracts were incubated at 37°C and aliquots were removed to ice after the indicated times. The mobility of pre-mRNA, lariat product, and 5' exon product are indicated. B-C) Quantification of Lariat/(Lariat+pre-mRNA) from 1st step splicing reaction time courses at B) 33 °C, and C) 37 °C, showing the temperature dependent decrease in splicing activity in extracts from some of the transitional Prp8 alleles. Red/orange: transitional alleles. Greens: catalytic alleles. Black: wild-type.

Figure 4

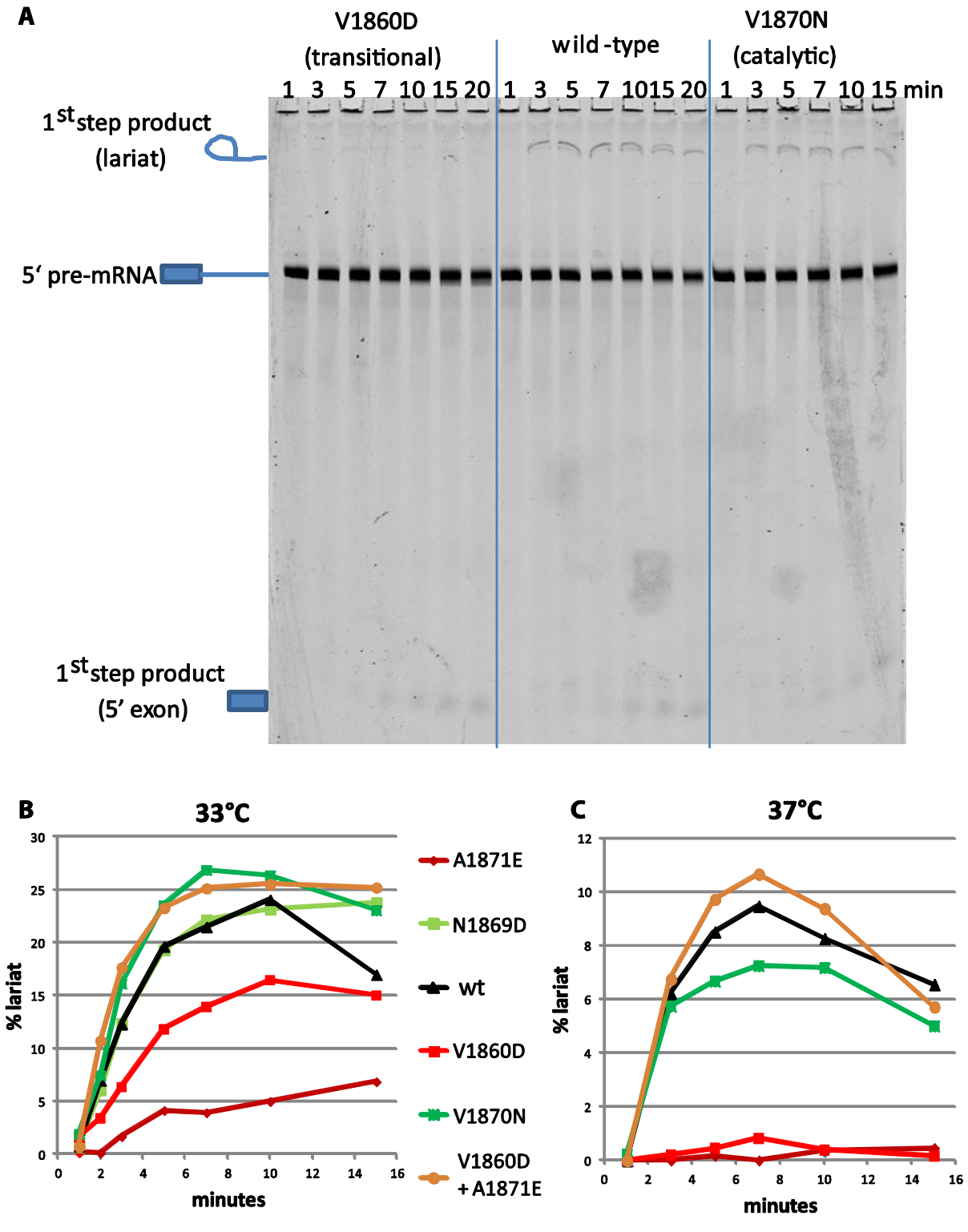
A
V1860D
(transitional)
wild -type
V1870N
(catalytic)
1 3 5 7 10 15 20 1 3 5 7 1015 20 1 3 5 7 10 15 min
1st step product
(lariat)
5' pre-mRNA
1st step product
(5' exon)
B
33°C
% lariat
minutes
A1871E
N1869D
wt
V1860D
V1870N
V1860D
+A1871E
C
37°C
% lariat
minutes

Figure 5: Neither Prp8 catalytic nor transitional alleles allow bypass of Cwc25. Plates are shown of tetrad dissections from diploids heterozygous for Prp8 and Cwc25 containing plasmids for wild-type Prp8, prp8-V1860D (transitional), and prp8-V1870N (catalytic). Note: some spots on these plates are contamination, indicated by blue marks on top of colony. None of the other Prp8 alleles tested (V1860N, V1862D, A1871E, T1872E, V1860D+A1871E, V1862Y, K1864E, N1869D, nor V1870N) gave rise to tetrads with more than 2 viable spores either.

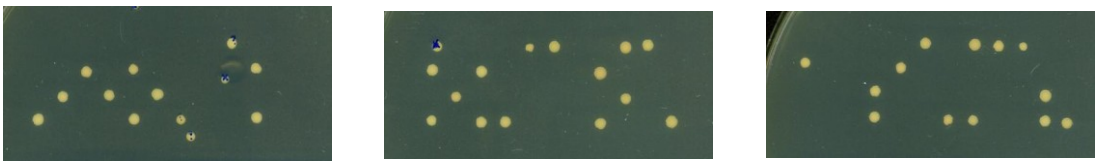

Figure 6: A) Model figure showing when the spliceosome is in its catalytic vs. transitional conformations and when Prp8's RNaseH insertion forms its loop vs. hairpin structure. B) Energy well diagram showing how transitional alleles could cause accumulation of the 1st step products seen by primer extension.

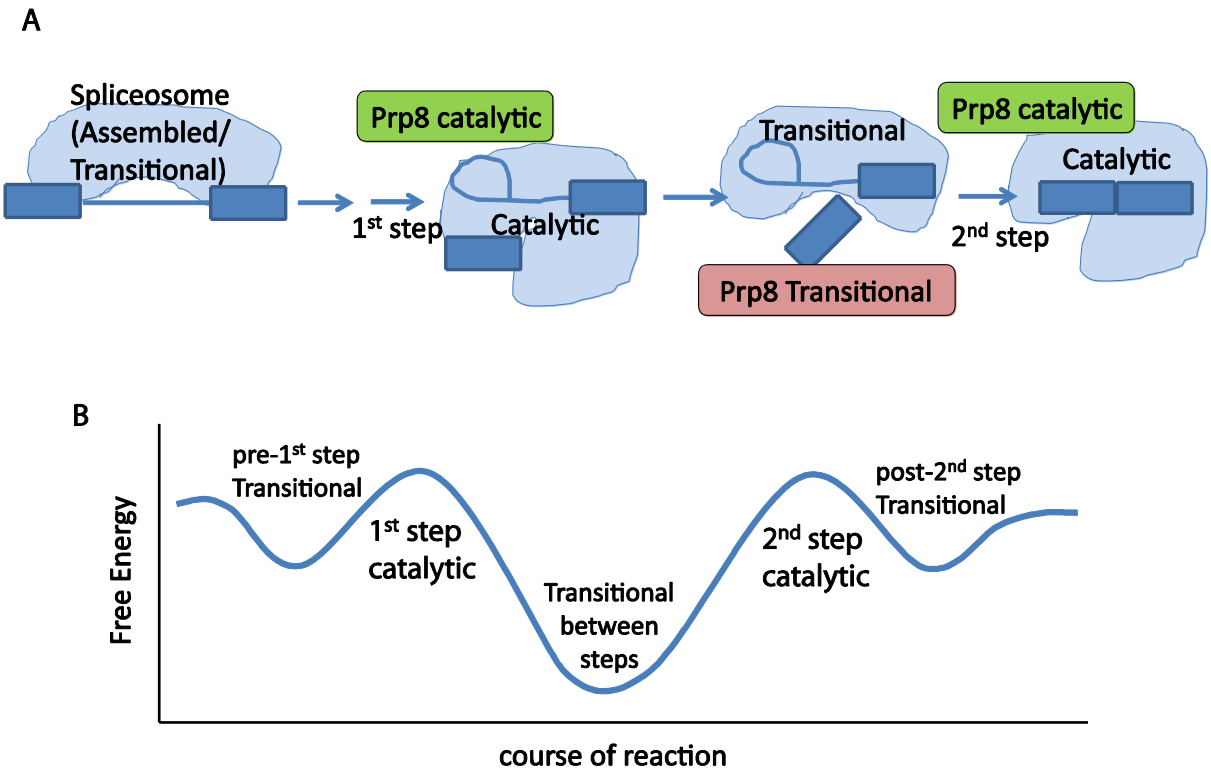

Supplementary Figure 1: Set-up for lariat sequencing. A) Two dimensional gel to isolate lariat introns from dbr1Δ yeast total RNA. The denaturing Urea-TBE gels were 7.5% acrylamide in the first dimension and 15% acrylamide in the second dimension. B) Schematic of RT reading through the 2'-5' linkage and the lariat cDNAs that will be analyzed after sequencing. C-E) qPCR results comparing enrichment of lariats isolated by 2D gel vs. enzymatic method to deplete rRNA and other linear RNAs. qPCR primer sets in the exon and lariat of Rps24b (C, long lariat), Asc1 (D, medium lariat), and Scs22 (E, short lariat) were used to amplify cDNA from total RNA, lariat RNA isolated from 2D gels (either by electro-elution or passive elution), or lariat RNA treated with the RiboMinus kit followed by RNaseR and Terminator (Xrn1) enzymes to degrade linear RNA from both ends.

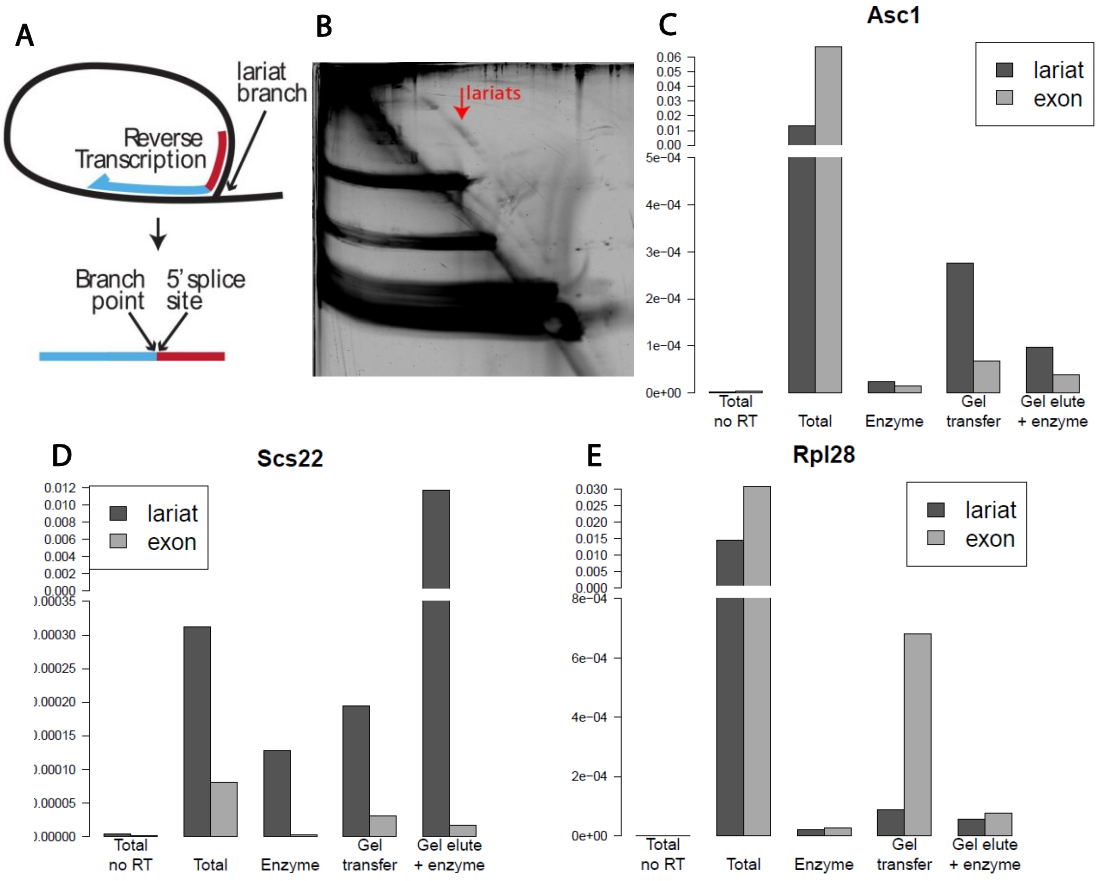

Supplementary Figure 2: Lariat lengths in *S. cerevisiae*, based on Ares lab database (Grate and Ares 2002). The genes checked with qPCR are indicated (lariat length in parentheses).

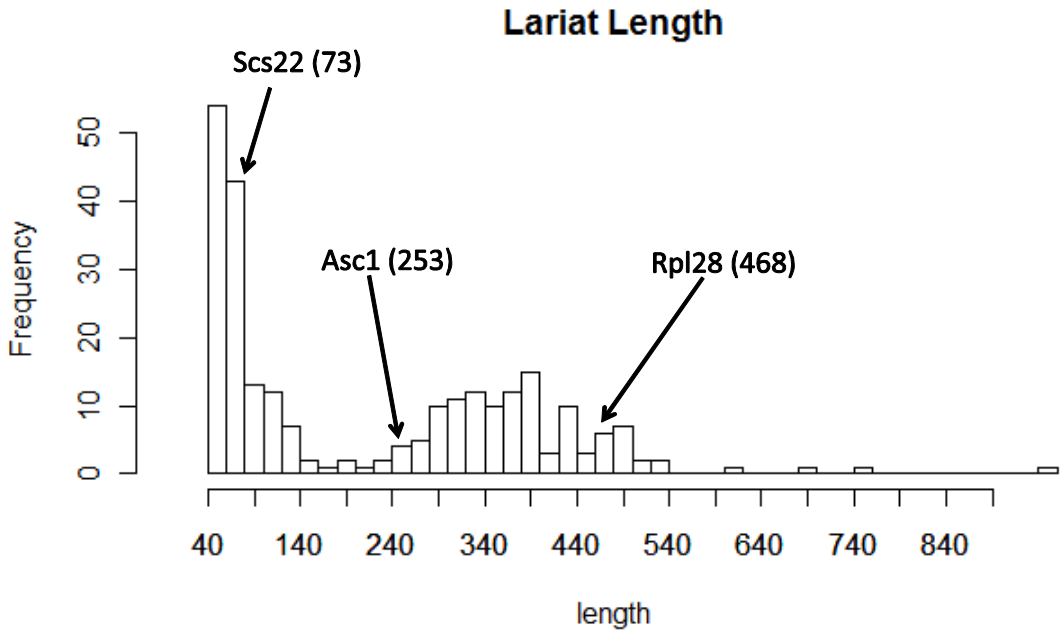

Supplementary Table 1: Strains used in the study

Strain Name	Parent Strain + plasmid information	Genotype
yAMP24	yTB72 x yTK102	prp8Δ::LYS, cup1Δ::ura3-52, ade-, Trp+, his-, leu-, Mat a, (plasmid yCP50-Prp8-URA-Cen)
yTT81	yAMP24 + Prp8-wt plasmid (His-Cen)	
yTT83	yAMP24 + Prp8(V1860D) plasmid (His-Cen)	
yTT85	yAMP24 + Prp8(V1860N) plasmid (His-Cen)	
yTT87	yAMP24 + Prp8(V1862D) plasmid (His-Cen)	
yTT89	yAMP24 + Prp8(V1862Y) plasmid (His-Cen)	
yTT93	yAMP24 + Prp8(N1869D) plasmid (His-Cen)	
yTT95	yAMP24 + Prp8(V1870N) plasmid (His-Cen)	
yTT157	yAMP24+Prp8-A1871E-His	
yTT159	yAMP24+Prp8-T1872E-His	
yTT161	yAMP24+Prp8-H1863E-His	
yTT163	yAMP24+Prp8-K1864E-His	
yTT165	yAMP24+Prp8-V1860D/T1865K-His	
yTT167	yAMP24+Prp8-V1860D/A1871E-His	
yTT169	yAMP24+Prp8-V1860D/T1872E-His	
yTT171	yAMP24+Prp8-V1860D/T1865K/T1872E-His	
yTT97	yTB72 +Dbr1D::KAN (equivilent to yEM466)	Mat a, his3D, leu2D, lys2D, ura3D, Prp8Δ::LYS, (yCP50 Prp8 WT URA Cen), Dbr1Δ::Kan
yTT344	consortium - sporulated from heterozygous diploid collection	cwc25Δ::Kan (cwc25-Leu plasmid) Mat alpha lys-, his-

Epilogue

Epilogue

My journey with Prp8 and Prp28 from the earliest steps of spliceosome assembly to the heart of the catalytic spliceosome has been motivated by a desire to learn how splicing can be simultaneously precise and accurate yet flexible enough to be regulated by cells in response to changing environmental signals. The specific rearrangements in the spliceosome that I've studied are points at which the fidelity or activity of the spliceosome could be modulated. My hope is that by learning about how spliceosomal components such as Prp8 and Prp28 control these individual steps, we will be able to later interrogate more effectively how the cell regulates these components to regulate splicing. It will be particularly interesting to study how Prp8 itself is regulated, since it influences everything from assembly to catalysis and may itself be the master regulator of spliceosome activity. One hint is that ubiquitin may regulate certain aspects of splicing - the activity of Brr2 is in part regulated by ubiquitin (Small et al. 2006), and an essential splicing factor Prp19 is a ubiquitin ligase (Song et al. 2010). Tantalizingly, Prp8 both binds ubiquitin (Bellare et al. 2006) and a mass spec study found that Prp8 can be ubiquitylated (Bellare et al. 2008).

This is a particularly exciting time in the splicing field because high resolution crystal structures of more and more pieces of the spliceosome are being solved. Eventually structures of the catalytic core of the spliceosome and of the complexes formed during spliceosome assembly will allow us to understand more completely how decades of genetic and biochemical data fit together. We will then be able to rationally probe what happens during each conformational rearrangement in the spliceosome, which will have important implications for understanding how the activity of the spliceosome is regulated in different contexts. The structure of the ribosome revolutionized the translation field, with the power to design better

experiments to test better hypotheses. Hopefully we will have similar opportunities with the spliceosome.

Chapter 3 is one example of how new structural insights provide context for years of genetic and biochemical data and help us refine models. However, the catalytic and transitional conformations model proposed in chapter 3 is probably more complicated than what we described. In addition to the contributions that the RNaseH domain of Prp8 makes to the structure of the spliceosome's catalytic core, many other components of the spliceosome are intricately coordinated. Mutations in other parts of Prp8 also influence the fidelity of splicing and the equilibrium between two opposing conformations (Query and Konarska 2004; Liu et al. 2007; Kuhn et al. 2002), as do mutations in the U2 and U6 snRNAs (Hilliker et al. 2007; Perriman and Ares 2007; Query and Konarska 2004; Liu et al. 2007; Chang and McPheeters 2000) as well as NTC component Cef1 (Query and Konarska 2012). The DExD/H-box ATPases, which catalyze conformational rearrangements to promote each step of splicing, are layered on top of this. Do the rearrangements promoted by these ATPases affect the structure of Prp8 or other aspects of the catalytic core? Does Prp8 play a more active role in actually activating the ATPases? Biochemical and genetic studies combined with the power of structures would help us answer these questions and open up more questions.

We can expand our model based on our current understanding. Mutations in Prp16 and Prp22 have been shown to antagonize the different classes of Prp8 alleles, with wild-type Prp16 thought to promote the 2nd step conformation and wild-type Prp22 to promote the 1st step conformation (or a similar conformation for mRNA release) (Liu et al. 2007; Query and Konarska 2004). How could all of this fit together with our model that the spliceosome toggles between catalytic and transitional conformations? The spliceosome, like the ribosome, can be compared to a Brownian ratchet (Frank and Agrawal 2001; Krishnan et al. 2013) in which the ATPase promotes a rearrangement that pushes the spliceosome forward, and an accessory factor binds to serve as a pawl to prevent backwards steps. In the case of Prp2, we know that the activity of

Prp2 destabilizes the SF3a/3b subunits of U2 (Wlodaver and Staley 2014; Lardelli et al. 2010). Then the pawl, Cwc25, binds and only then does 1st step catalysis occur (Krishnan et al. 2013). In our working model (Figure 1), Prp2 activity and the proofreading it allows would occur while the spliceosome's catalytic core is in a transitional conformation before the first catalytic step. Binding of Cwc25 pushes it into its high-energy catalytic conformation. Next, Prp16 hydrolyzes ATP which releases Cwc25 from the spliceosome and returns the spliceosome to its transitional conformation but also allows for substrate repositioning and moves the spliceosome forward toward the 2nd catalytic step by allowing 2nd step factors to bind (Tseng et al. 2011). In our working model, binding of second step factors Prp22, Prp18, and Slu7 (and/or conformational arrangements in Prp8 and other spliceosomal components that either affect or are affected by binding of these proteins) push the spliceosome into its 2nd step catalytic conformation. After 2nd step catalysis occurs, Prp22 hydrolyzes ATP, returning the spliceosome to its transitional conformation, from which mRNA is released. The connection between catalytic and transitional states and the individual protein components in this model can be tested by studying genetic interactions between all of these factors and the two classes of Prp8 alleles. In addition, single molecule FRET studies with the purified system described in Krishnan et al. (2013) could be used to probe how pre-mRNA dynamics are affected by all of these factors including the Prp8 alleles.

While the catalytic center of the spliceosome is controlled by a fascinating cascade of proteins and rearrangements, the assembly of the spliceosome is equally complex and enigmatic. Spliceosome assembly, even more than catalysis, is a target for regulation by cells needing to control the efficiency of splicing. For example, splicing often occurs co-transcriptionally (Görnemann et al. 2005; Lacadie et al. 2006), and perturbations that affect polymerase affect the efficiency of splicing at the level of spliceosome assembly and recruitment of early subunits (for example, Moehle et al. 2014; Alexander et al. 2010). The roles we

identified for Prp28 and Prp8 in the earliest steps of spliceosome assembly could therefore have implications how spliceosome assembly is regulated.

An open question from my work on Prp28 was how does Prp28 actually promote CC2 formation and how do Prp8 mutations affect this when Prp8 isn't even thought to join the spliceosome until much later. Discussions with Aaron Hoskins at our annual lab retreat, RNA camp, led to an intriguing hypothesis. The U5 snRNP and U1 snRNP may need to interact during spliceosome assembly, but only at the appropriate time, i.e. when the triple-snRNP is recruited to the spliceosome before U6 replaces U1. Too early of an interaction or one between inappropriate complexes could prevent CC2 formation. U1 physically interacts with both BBP/Mud2 (in CC1; Abovich and Rosbash 1997) and Prp8 (Li et al. 2013; Grainger and Beggs 2005; Wiesner et al. 2002) (presumably during tri-snRNP joining), so too early of an interaction between Prp8 and U1 could compete with BBP/Mud2 and therefore inhibit CC2 formation. Intriguingly, an assembly intermediate of the U5 snRNP actually co-immunoprecipitates with the U1 snRNP (Gottschalk et al. 2001). Prp28 is not a component of this assembly intermediate, nor is it a stable component (in yeast) of the triple-snRNP (Small et al. 2006; Stevens et al. 2001; Gottschalk et al. 1999; Fabrizio et al. 2009) which should interact with U1 during tri-snRNP joining. Prp28 is only a stable component of the free U5 snRNP (Stevens et al. 2001), the snRNP whose interactions with U1 might prevent CC2 formation. Perhaps the role of Prp28 is to prevent interactions between Prp8/U5 and U1 until the proper time? This model could also explain how mutations in the N-terminus of Prp8 could suppress defects in Prp28. These mutations are in the part of Prp8 that interacts with U1 proteins, so they could reduce the ability of Prp8 to interact with U1, reducing these possible improper interactions. Although we did not see changes in binding of Prp8 to U1 snRNP proteins in vitro (Price et al. 2014), we used only a small piece of the N-terminus of Prp8 in our experiment, so in the context of the whole protein or the entire spliceosome, the prp8-tes alleles may still affect interactions between Prp8 and U1. It will be interesting to test whether Prp28 affects the formation of improper U1-U5 interactions.

The highly dynamic nature of the spliceosome makes it particularly fascinating but also particularly difficult to study. The future of the splicing field is bright with new discoveries and new questions about the regulation of splicing, the conformational rearrangements of the spliceosome, and the structure and nature of its catalytic core.

Figures

Figure 1: Model of how Prp2, Prp16, Prp22 and accessory factors play into the conformational changes during the catalytic steps of splicing.

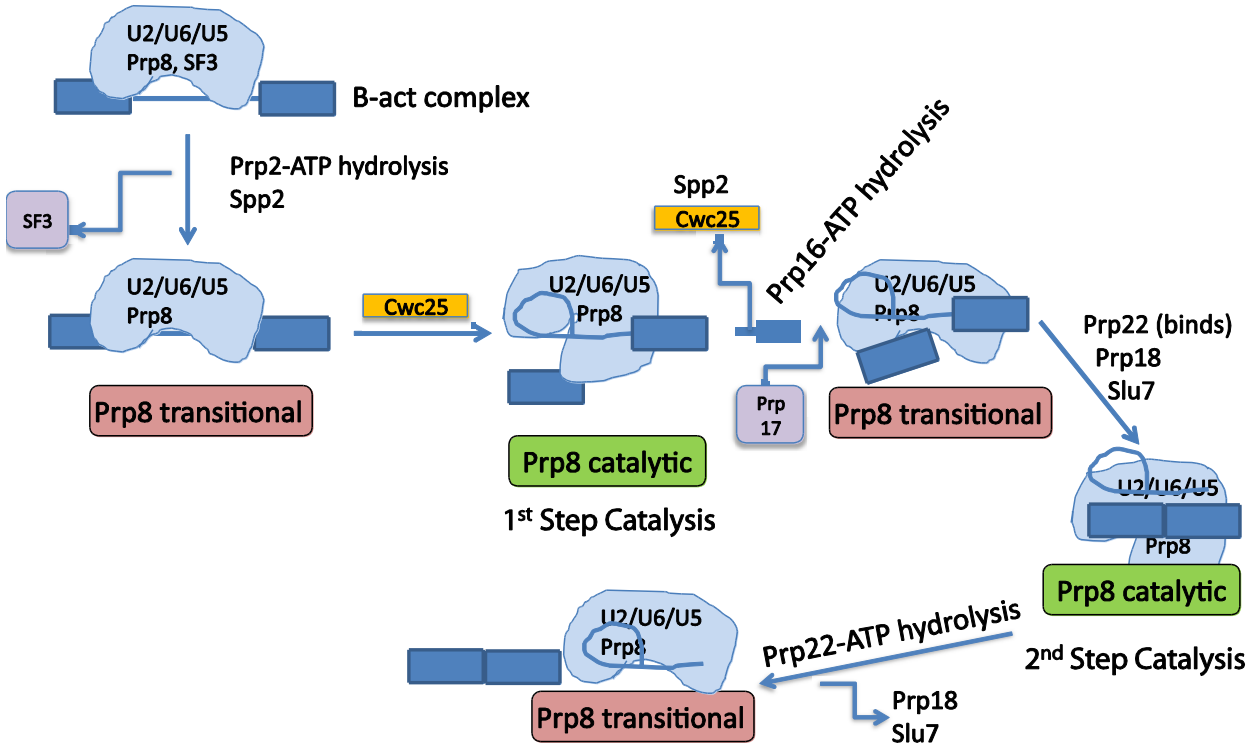

Appendix

Appendix

Prp28's role in Commitment Complex 2 formation is not a side effect of blocking other assembly steps also impacted by Prp28

I did two controls to confirm that Prp28's role in commitment complex 2 formation is not a side effect of, or caused by feedback from, blocking other assembly steps also impacted by Prp28. We did not include these in our publication (Price et al. 2014), but I include them here for reference.

First, Prp28 was previously known to be required for maximal triple-snRNP binding (Staley and Guthrie 1999; Mathew et al. 2008), so one question was whether inhibiting triple-snRNP association would feed back to cause a build-up of CC1 instead of CC2. CC2 formation occurs several steps before triple-snRNP joining, so we did not expect tri-snRNP to affect CC2. I tested this by depleting the U6 snRNA from extract with oligo U6-d to target U6 for cleavage by RNaseH (Fabrizio et al. 1989). Depleting U6 should break apart the triple-snRNP and prevent tri-snRNP from binding to the pre-mRNA. Commitment complex gels from splicing reactions depleted of U6 (Figure 1A) looked similar to those containing U6 (see Price et al. 2014). Furthermore, prp28-1 was still deficient at forming CC2 even in the absence of U6 (Figure 1A). Therefore, we conclude that triple-snRNP association does not feed back to promote CC2 formation and Prp28's role in CC2 formation is not dependent on U6.

Second, Prp28 was known to catalyze the release of U1 from the 5'ss to allow U6 to stably interact with the 5'ss (Staley and Guthrie 1999; Chen et al. 2001). Staley and Guthrie (1999) had blocked U1 snRNP release in vitro and in vivo by extending the base pairing between U1 and the 5'ss (Figure 1B adapted from Staley and Guthrie 1999). This was synthetic lethal with *prp28-1* in vivo, and blocked U1 release and inhibited triple-snRNP joining in vivo,

phenocopying *prp28-1* (Staley and Guthrie 1999). I used this method to test whether blocking U1 snRNP unwinding, separate from prp28-1, would also cause a decrease in CC2. I cloned mutations into the RP51 in vitro transcription template and used the extended U1 snRNA from Staley and Guthrie (1999) to increase the base-pairing between the 5'ss of RP51 and U1. The 9 base-pair template is the equivalent of the "like wild-type" template from Staley and Guthrie (1999), while the 11 base-pair template is hyperstabilized (Figure 1B). Commitment complex gels run from splicing reactions with these constructs showed that the "like wild-type" base pairing between U1 and the 5'ss resulted in mostly CC1 (Figure 1C) - less CC2 than normally present in a completely wild-type context. Surprisingly, increasing the base pairing to hyperstabilize the U1/5'ss helix dramatically increased the amount of CC2 (and pre-spliceosome +ATP) that formed (Figure 1C). This suggests that the ability of U1 to form a stable interaction with the 5'ss is actually important for CC2 formation. Perhaps having a less stable U1/5'ss interaction prevents cross-intron bridging interactions between U1 and BBP/Mud2 from stabilizing CC2. Based on this, one hypothesis about the role of Prp28 in CC2 formation is that Prp28 actually helps to stabilize U1 binding to the 5'ss early in the spliceosome assembly process, which in turn helps to stabilize CC2. This is supported by results in Price et al. (2014), which show that CC1 formed in the absence of Prp28 has a slightly altered mobility. In this model ATPase activity of Prp28 would only be activated at the appropriate time, after tri-snRNP joining, to change Prp28's role from stabilizing U1 to catalyzing its release. It will be interesting in the future to test this model and compare it to the model regarding competition between U1-U5 and U1-BBP/Mud2 interactions, proposed in the epilogue.

Figure 1: Commitment complex gels with U6 depleted or U1/5'ss hyperstabilization. A) Splicing reactions (+/- ATP) with U6 depleted from wt or prp28-1 extracts were run on a commitment complex gel. B) Schematic of U1/5'ss hyperstabilization on RP51 pre-mRNA, adapted from Staley and Guthrie (1999). C) Commitment complex gel (+/- ATP) with U1/5'ss either hyperstabilized or not hyperstabillized.

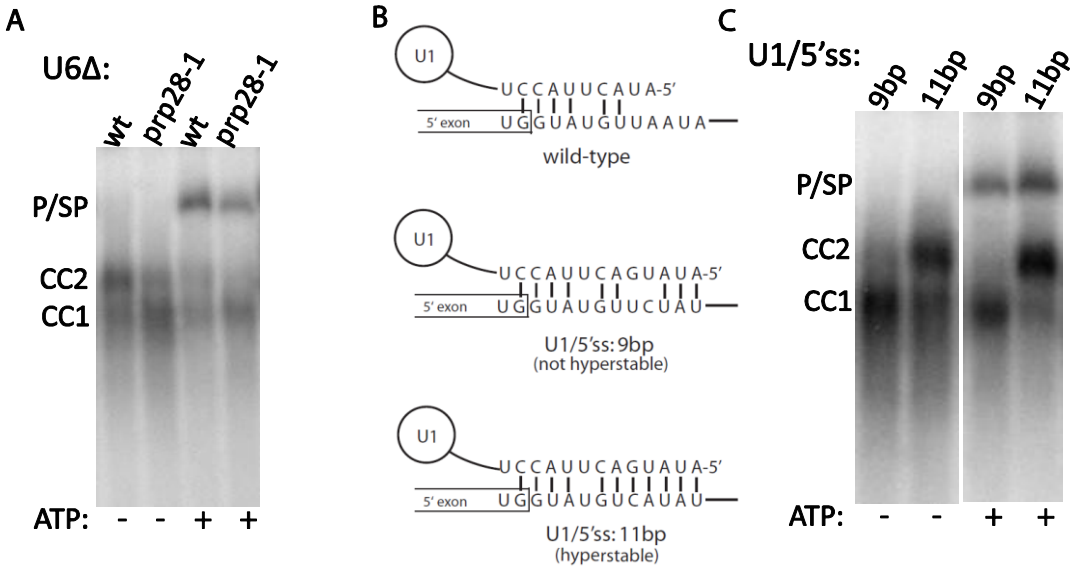

References (Epilogue and Appendix)

Abovich N, Rosbash M. 1997. Cross-intron bridging interactions in the yeast commitment complex are conserved in mammals. *Cell* **89**: 403–412.

Alexander RD, Innocente SA, Barrass JD, Beggs JD. 2010. Splicing-dependent RNA polymerase pausing in yeast. *Mol Cell* **40**: 582–593.

Bellare P, Kutach AK, Rines AK, Guthrie C, Sontheimer EJ. 2006. Ubiquitin binding by a variant Jab1/MPN domain in the essential pre-mRNA splicing factor Prp8p. *RNA New York N* **12**: 292–302.

Bellare P, Small EC, Huang X, Wohlschlegel JA, Staley JP, Sontheimer EJ. 2008. A role for ubiquitin in the spliceosome assembly pathway. *Nat Struct Mol Biol* **15**: 444–451.

Chang JS, McPheeters DS. 2000. Identification of a U2/U6 helix Ia mutant that influences 3' splice site selection during nuclear pre-mRNA splicing. *RNA New York N* **6**: 1120–1130.

Chen JY-F, Stands L, Staley JP, Jackups Jr. RR, Latus LJ, Chang T-H. 2001. Specific alterations of U1-C protein or U1 small nuclear RNA can eliminate the requirement of Prp28p, an essential DEAD box splicing factor. *Mol Cell* **7**: 227–232.

Fabrizio P, Dannenberg J, Dube P, Kastner B, Stark H, Urlaub H, Lührmann R. 2009. The evolutionarily conserved core design of the catalytic activation step of the yeast spliceosome. *Mol Cell* **36**: 593–608.

Fabrizio P, McPheeters DS, Abelson J. 1989. In vitro assembly of yeast U6 snRNP: a functional assay. *Genes Dev* **3**: 2137–2150.

Frank J, Agrawal RK. 2001. Ratchet-like movements between the two ribosomal subunits: their implications in elongation factor recognition and tRNA translocation. *Cold Spring Harb Symp Quant Biol* **66**: 67–75.

Görnemann J, Kotovic KM, Hujer K, Neugebauer KM. 2005. Cotranscriptional spliceosome assembly occurs in a stepwise fashion and requires the cap binding complex. *Mol Cell* **19**: 53–63.

Gottschalk A, Kastner B, Lührmann R, Fabrizio P. 2001. The yeast U5 snRNP coisolated with the U1 snRNP has an unexpected protein composition and includes the splicing factor Aar2p. *RNA* **7**: 1554–1565.

Gottschalk A, Neubauer G, Banroques J, Mann M, Lührmann R, Fabrizio P. 1999. Identification by mass spectrometry and functional analysis of novel proteins of the yeast [U4/U6|U5] tri-snRNP. *EMBO J* **18**: 4535–4548.

Grainger RJ, Beggs JD. 2005. Prp8 protein: at the heart of the spliceosome. *RNA* **11**: 533–557.

Hilliker AK, Mefford MA, Staley JP. 2007. U2 toggles iteratively between the stem IIa and stem IIc conformations to promote pre-mRNA splicing. *Genes Dev* **21**: 821–834.

Krishnan R, Blanco MR, Kahlscheuer ML, Abelson J, Guthrie C, Walter NG. 2013. Biased Brownian ratcheting leads to pre-mRNA remodeling and capture prior to first-step splicing. *Nat Struct Mol Biol* **20**: 1450–1457.

Kuhn AN, Reichl EM, Brow DA. 2002. Distinct domains of splicing factor Prp8 mediate different aspects of spliceosome activation. *Proc Natl Acad Sci* **99**: 9145–9149.

Lacadie SA, Tardiff DF, Kadener S, Rosbash M. 2006. In vivo commitment to yeast cotranscriptional splicing is sensitive to transcription elongation mutants. *Genes Dev* **20**: 2055–2066.

Lardelli RM, Thompson JX, Yates JR 3rd, Stevens SW. 2010. Release of SF3 from the intron branchpoint activates the first step of pre-mRNA splicing. *RNA New York N* **16**: 516–528.

Li X, Zhang W, Xu T, Ramsey J, Zhang L, Hill R, Hansen KC, Hesselberth JR, Zhao R. 2013. Comprehensive in vivo RNA-binding site analyses reveal a role of Prp8 in spliceosomal assembly. *Nucleic Acids Res* **41**: 3805–3818.

Liu L, Query CC, Konarska MM. 2007. Opposing classes of prp8 alleles modulate the transition between the catalytic steps of pre-mRNA splicing. *Nat Struct Mol Biol* **14**: 519–526.

Mathew R, Hartmuth K, Möhlmann S, Urlaub H, Ficner R, Lührmann R. 2008. Phosphorylation of human PRP28 by SRPK2 is required for integration of the U4/U6-U5 tri-snRNP into the spliceosome. *Nat Struct Mol Biol* **15**: 435–443.

Moehle EA, Braberg H, Krogan NJ, Guthrie C. 2014. Adventures in time and space: splicing efficiency and RNA polymerase II elongation rate. *RNA Biol* **11**: 313–319.

Perriman RJ, Ares M Jr. 2007. Rearrangement of competing U2 RNA helices within the spliceosome promotes multiple steps in splicing. *Genes Dev* **21**: 811–820.

Price AM, Görnemann J, Guthrie C, Brow DA. 2014. An unanticipated early function of DEAD-box ATPase Prp28 during commitment to splicing is modulated by U5 snRNP protein Prp8. *RNA New York N* **20**: 46–60.

Query CC, Konarska MM. 2012. CEF1/CDC5 alleles modulate transitions between catalytic conformations of the spliceosome. *RNA* **18**: 1001–1013.

Query CC, Konarska MM. 2004. Suppression of multiple substrate mutations by spliceosomal prp8 alleles suggests functional correlations with ribosomal ambiguity mutants. *Mol Cell* **14**: 343–354.

Small EC, Leggett SR, Winans AA, Staley JP. 2006. The EF-G-like GTPase Snu114p regulates spliceosome dynamics mediated by Brr2p, a DExD/H box ATPase. *Mol Cell* **23**: 389–399.

Song EJ, Werner SL, Neubauer J, Stegmeier F, Aspden J, Rio D, Harper JW, Elledge SJ, Kirschner MW, Rape M. 2010. The Prp19 complex and the Usp4Sart3 deubiquitinating enzyme control reversible ubiquitination at the spliceosome. *Genes Dev* **24**: 1434–1447.

Staley JP, Guthrie C. 1999. An RNA switch at the 5′ splice site requires ATP and the DEAD box protein Prp28p. *Mol Cell* **3**: 55–64.

Stevens SW, Barta I, Ge HY, Moore RE, Young MK, Lee TD, Abelson J. 2001. Biochemical and genetic analyses of the U5, U6, and U4/U6 X U5 small nuclear ribonucleoproteins from Saccharomyces cerevisiae. *RNA* **7**: 1543–1553.

Tseng C-K, Liu H-L, Cheng S-C. 2011. DEAH-Box ATPase Prp16 has dual roles in remodeling of the spliceosome in catalytic steps. *RNA* **17**: 145–154.

Wiesner S, Stier G, Sattler M, Macias MJ. 2002. Solution Structure and Ligand Recognition of the WW Domain Pair of the Yeast Splicing Factor Prp40. *J Mol Biol* **324**: 807–822.

Wlodaver AM, Staley JP. 2014. The DExD/H-box ATPase Prp2p destabilizes and proofreads the catalytic RNA core of the spliceosome. *RNA New York N* **20**: 282–294.

Publishing Agreement

It is the policy of the University to encourage the distribution of all theses, dissertations, and manuscripts. Copies of all UCSF theses, dissertations, and manuscripts will be routed to the library via the Graduate Division. The library will make all theses, dissertations, and manuscripts accessible to the public and will preserve these to the best of their abilities, in perpetuity.

Please sign the following statement:

I hereby grant permission to the Graduate Division of the University of California, San Francisco to release copies of my thesis, dissertation, or manuscript to the Campus Library to provide access and preservation, in whole or in part, in perpetuity.

Argent McRae
Author Signature

12/19/2014
Date